Universitat Autònoma de Barcelona

Targeting astrocytes to prevent neurodegeneration in patients with multiple sclerosis

Clara Matute Blanch

Targeting astrocytes to prevent neurodegeneration in patients with multiple sclerosis

Clara Matute Blanch

PhD Thesis, 2021

Programa de Doctorado en Medicina, Departamento de Medicina, Universitat Autònoma de Barcelona.

Vall d'Hebron Barcelona Hospital Campus | Vall d'Hebron Institut de Recerca | Cemcat Centre d'Esclerosi Múltiple de Catalunya | UAB Universitat Autònoma de Barcelona

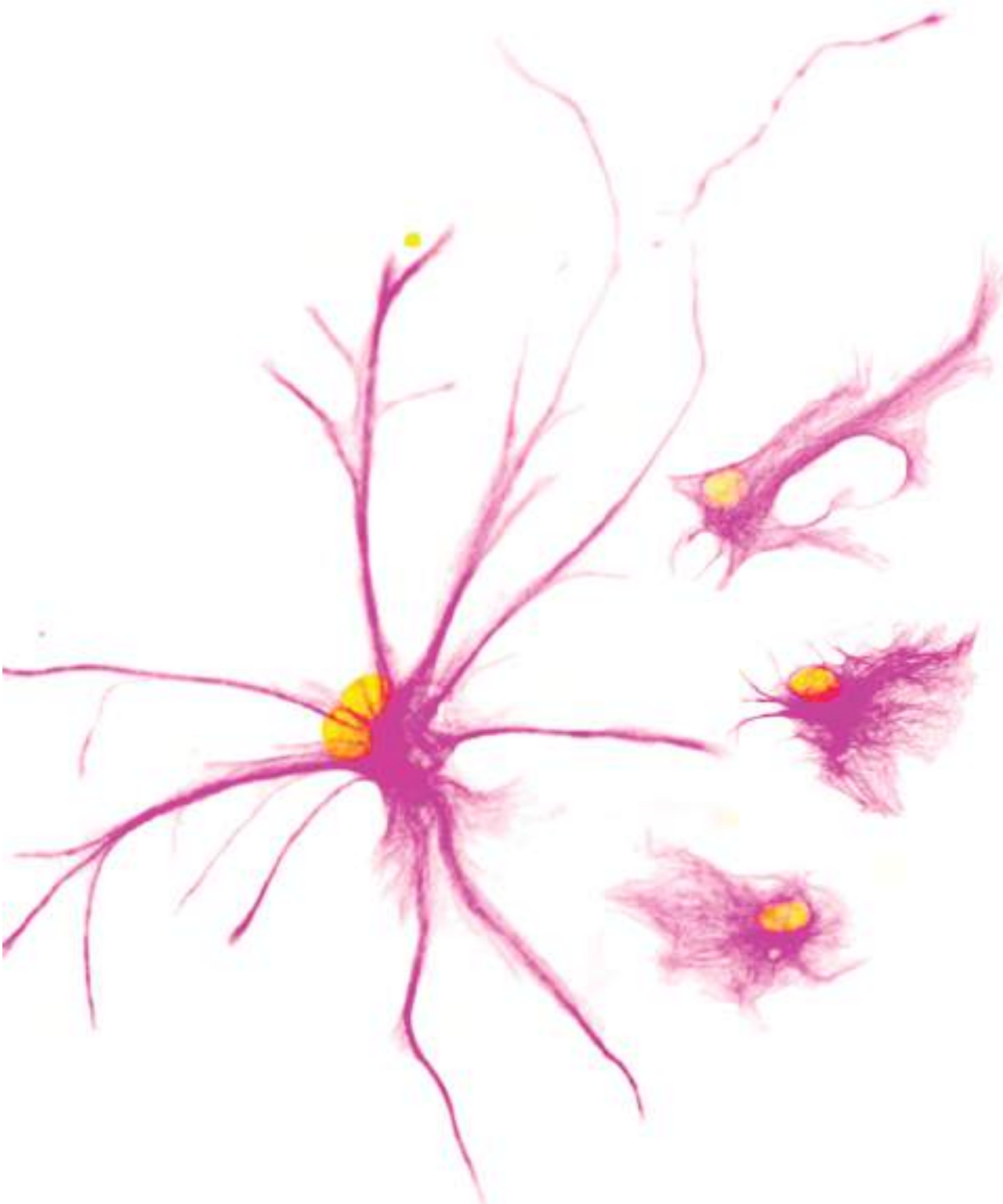

Programa de Doctorado en Medicina,
Departamento de Medicina,
Universitat Autònoma de Barcelona.

Targeting astrocytes to prevent neurodegeneration in patients with multiple sclerosis

Clara Matute Blanch

PhD Thesis, 2021

Supervisors:
Dr. Manuel Comabella López
Prof. Xavier Montalban Gairín

Tutor:
Dr. Albert Selva O'Callaghan

Barcelona, 2021.

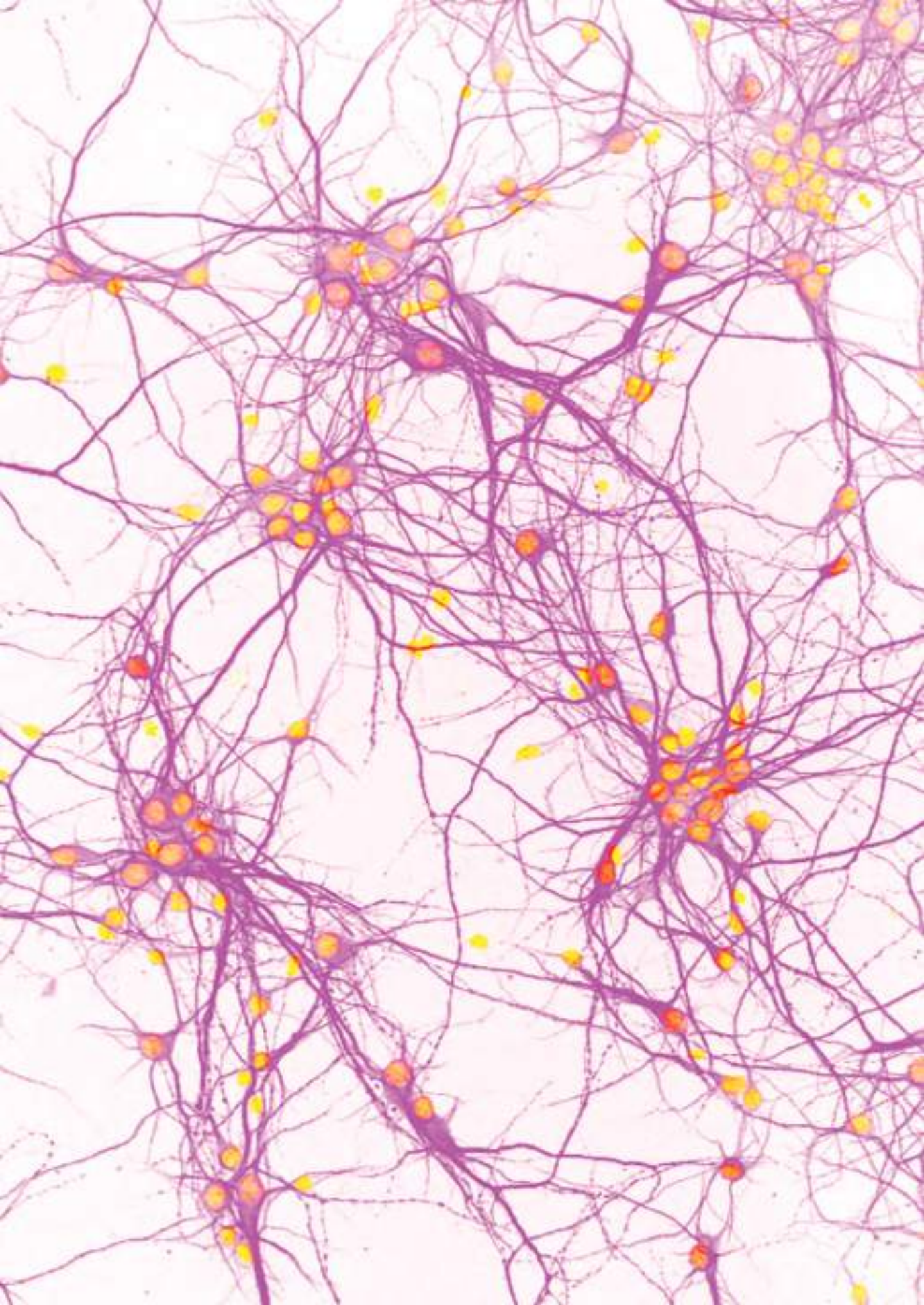

Nobody said it was easy.

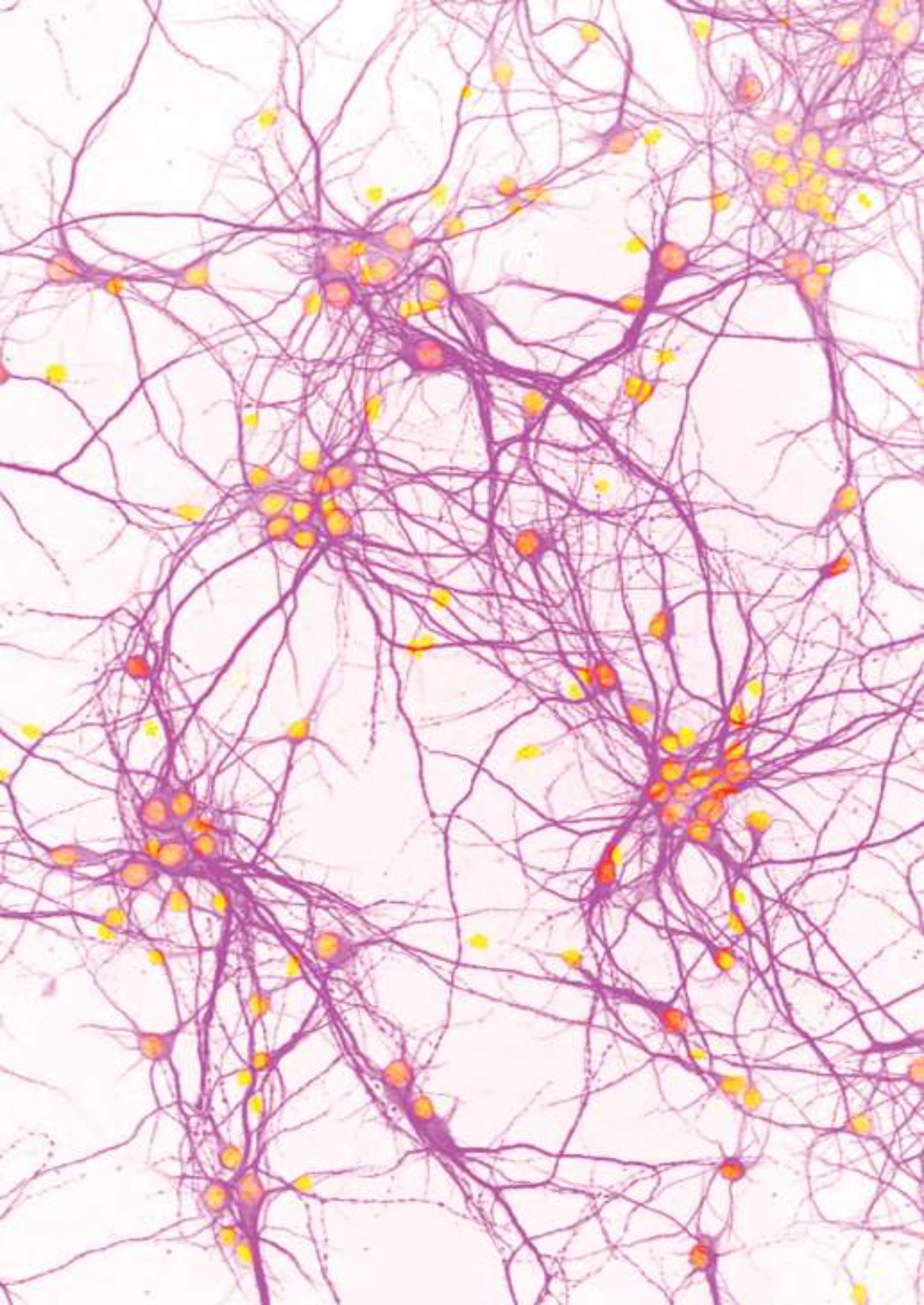

Acknowledgements

Más que llegar hoy aquí, es el camino lo que me llena de orgullo. Lo más bonito que me ha enseñado esta tesis es a vencer la desesperanza, seguir intentándolo una, otra, y otra vez más, reinventarme de todas las maneras posibles y a no darme nunca por vencida.

Pero llegar al otro lado del muro no habría sido posible sin todas las personas que me han acompañado durante este camino.

Quiero agradecer a mis directores de tesis, Manuel Comabella y Xavier Montalban, por brindarme la oportunidad de formar parte de este gran grupo. Gracias Manolo por poner en mis manos un proyecto tan bonito cargado de tantas nuevas ilusiones. Gracias por confiar en mí y no perder la esperanza que acabaría saliendo algo bueno. Gràcies Xavier, per la teva confiança i entusiasme en animar-nos a ser millors professionals cada dia.

A mis compañeros del lab por hacerme sentir como en casa y vivir conmigo esta montaña rusa. A nuestro querido argentino, agradecerle abrirme las puertas de esta casa. Nico, ha sido maravilloso verte “ablandarte” estos años. Gracias por tantos cafés y tantas buenas charlas. Mireia, sento que ens hem fet grans juntes. Gràcies per ser-hi sempre, i pels teus axuxons amb i sense pandemia. Ets l’ànima del lab. A mi compañera de tesis y de santuario, Laura. Ha sido una suerte vivir esta etapa contigo, gracias por compartir tanto conmigo. Equipo CER, gracias por dejarme empapar de vuestro orden y saber hacer, y ayudarme a vencer el caos. Carmen, ha sido una suerte inmensa tenerte cerca. Gracias por tener tu puerta abierta siempre que lo he necesitado. Herena, ets una todoterreno, gràcies per fer-me un lloc a la teva llibreta de projectes i ajudar-me en tot el que has pogut i més. A mi padawan que revolvió el lab con su llegada: Rucsanda, creo que al final hemos sabido hacer un buen equipo tú y yo juntas. Gracias por apretar cuando me quedaban menos fuerzas. A Sunny, Mercè y María por irradiar alegría por los pasillos. Mercè, gràcies per ajudar-me quan t’ha sigut possible. María, es una maravilla tenerte al ladito, eres todo luz. Al último en llegar, nuestro atracador de pasillos profesional, neurobiólogo

y mejor persona, Andrés. Gracias por llenarme de confianza y fuerzas en la última etapa de esta maratón. Gracias por valorar tanto mis ideas y mi trabajo y por hacerme creer que esto es sólo el principio.

A mis compañeros del Cemcat, en especial a Luciana Midaglia por realizar una excelente selección de los pacientes junto con Manuel Comabella. Gracias Luciana por tu interés e ilusión en mi trabajo, ha sido fantástico contar con tu ayuda. Agradecer a todo el personal del Cemcat, la excelente labor que hacen cada día atendiendo a los pacientes con cariño, respecto y profesionalidad.

A l'Anna Duarri i l'Agueda Martínez, les fantàstiques postdocs de la nostra sala de cultius per compartir amb mi la seva experiència, escoltar-me i aconsellar-me sempre que ho he necessitat i per mantenir l'esperit de "¡lo que pasa en cultivos, se queda en cultivos!".

Al huracán argentino que nos visitó allá el 2019, Vero, gracias por arrojar luz e ilusión cuando todo estaba tan oscuro. Gracias por hacer que trabajar con neuronas fuera un poquito menos traumático y, sobretodo, por transmitirme tu pasión por la ciencia. Gracias también por abrirme las puertas de la UB, que tan importante ha sido su contribución en este estudio. Agradecer a Sara Fernández García su empatía, buena disposición y su tiempo, en salvarme la vida ayudándome en esos dos últimos cultivos de neuronas que no había manera de que sobrevivieran. Por supuesto, agradecer al Dr. Jordi Alberch por facilitarme la ayuda de Sara. A l'Albert Giralt, agrir-li les seves idees tan enriquidores sempre que he tingut la sort de creunar-nos. Finalmente, quería agradecer a la Unidad de Microscopía Avanzada del Campus Clínic de la UB el excelente trabajo que hacen. En especial, agradecer a María Calvo y Gemma Martín el cariño con el que han tratado mi estudio buscando el mejor análisis posible.

A la Dra. Luisa María Villar del Hospital Universitario Ramón y Cajal por su vital contribución con las valiosas muestras de líquido cefalorraquídeo de los pacientes. Gracias May por tu comprensión y por gestionar de forma tan efectiva algunos envíos más urgentes que otros.

A Gerardo García Díaz Barriga agradecerle su contribución con los análisis bioinformáticos y los estudios morfológicos neuronales. ¡Gracias por enseñarme a manejarme en un mundo tan desconocido para mí, he intentado seguirte todo lo que he podido!

Uno de los grandes regalos que me ha dado la ciencia es Maite. Viure amb tu aquesta jungla ha sigut preciós. No puc estar més agraïda i orgullosa d'haver arribat fins aquí juntes. No ho creiem però, al final, tot arriba i qui lluita troba el seu camí. No tinc cap dubte que et menjaràs el món allà on vagis i serà preciós seguir al teu costat per celebrar la vida.

A la família que escullo cada dia, gràcies per fer-me sentir immensament estimada i valorada i per sentir els meus èxits i fracassos com si fossin vostres.

A la meva família, especialment, als meus pares per ajudar-me a ser qui soc ara, recolzar-me en totes les meves aventures i fer-me creure que tot és possible amb esforç, constància i amor.

Al Justo, per ser el millor company de vida que podia imaginar. Gràcies per ser al meu costat tots aquests anys.

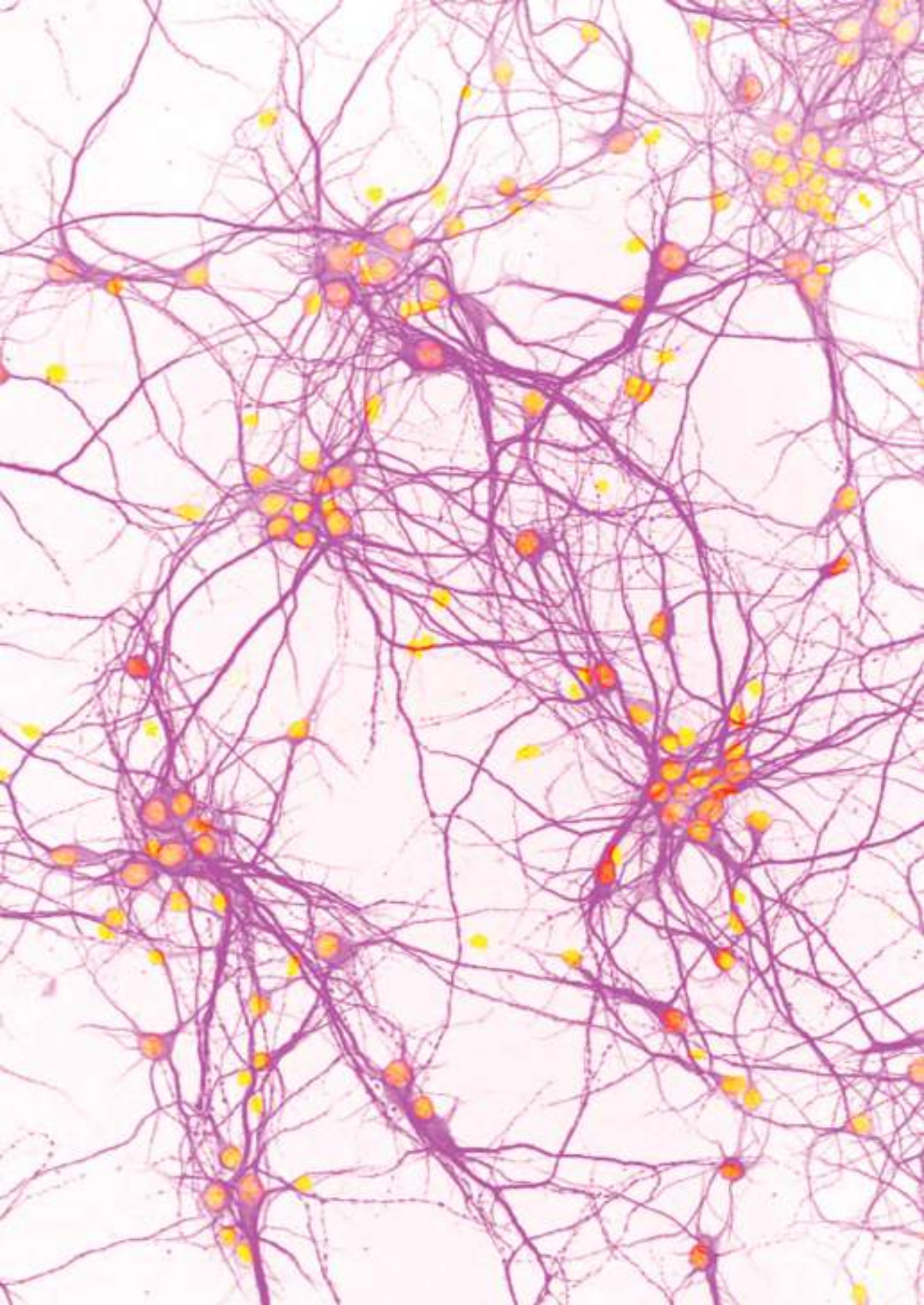

Presentation

The work presented in this thesis was performed in the laboratory of Clinical Neuroimmunology from the Centre d'Esclerosi Múltiple de Catalunya (Cemcat), located at the Vall d'Hebron Institut de Recerca (VHIR), Vall d'Hebron Barcelona Hospital Campus (Barcelona, Spain). This thesis was co-supervised by Dr. Manuel Comabella López, head of the laboratory, and Prof. Xavier Montalban Gairín, director of the Cemcat.

The Cemcat is a reference centre for multiple sclerosis (MS), and has the mission to improve the quality of life of people with neuroimmunological diseases, in particular MS. It has a multidisciplinary team comprised with more than 70 highly experienced professionals dedicated to clinical care, physical and cognitive rehabilitation, teaching, and research on MS. The latter is one of the key areas of excellence at the Cemcat. Clinical and basic research is focused on a better understanding of MS pathogenesis, with the ultimate goal of developing effective treatments for the disease that may improve the quality of life of patients. In particular, the group led by Dr. Manuel Comabella López has conducted an intense research based on the characterization of diagnostic, disease activity, and treatment response biomarkers in MS.

This project forms part of one of the main research lines conducted at the Cemcat: 'New therapeutic targets and/or approaches for MS'. Despite that our group has extensive experience on the immunopathogenesis of MS, this is the first project focused on targeting astrocytes and opens an interesting research line in neurobiology that aims to investigate the molecular bases of neurodegeneration and neuroprotection in the disease.

The results presented in this thesis have led to one scientific article which is currently under peer review for publication in an international journal.

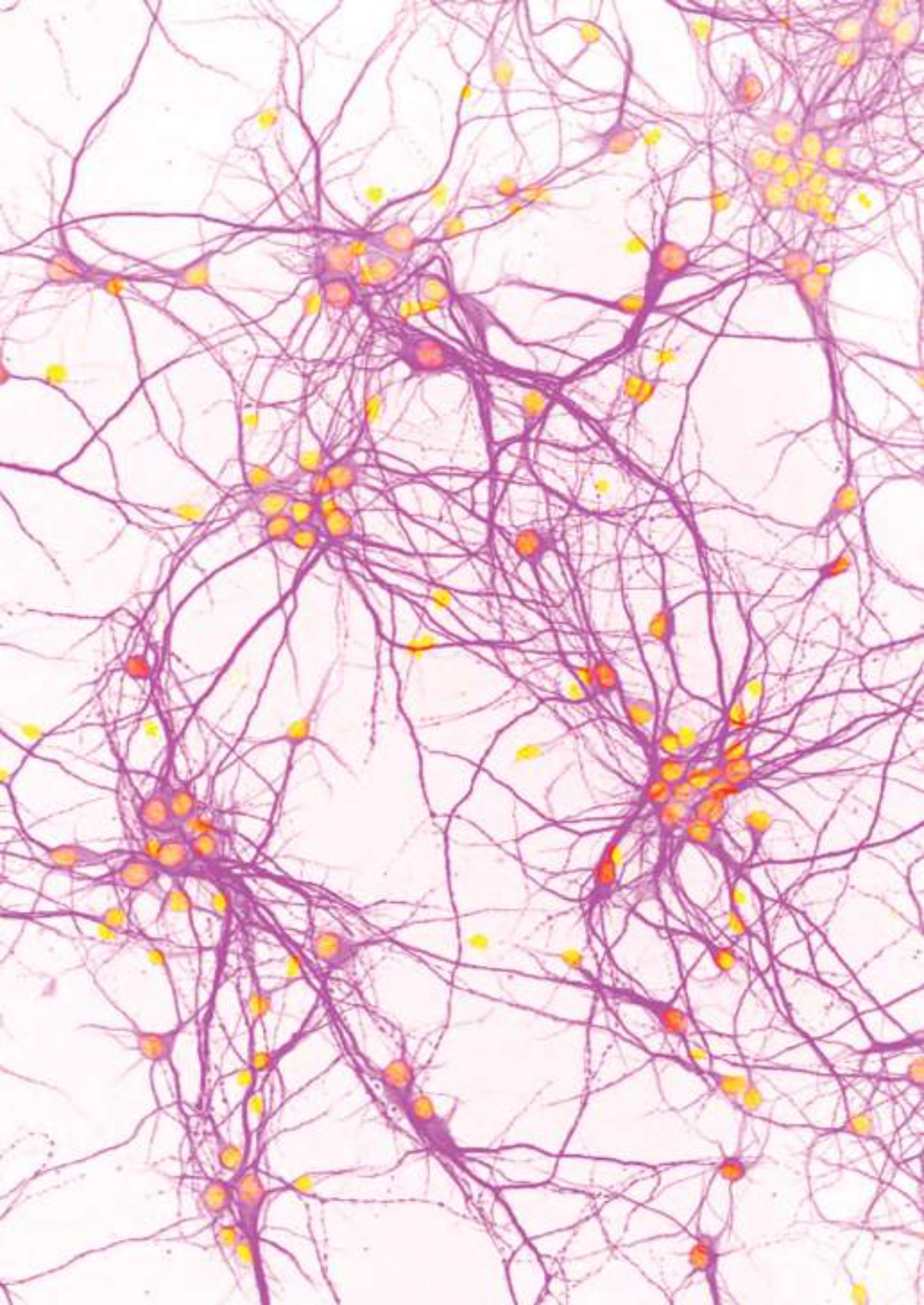

Abbreviations

AHR: aryl hydrocarbon receptor

AKT: protein kinase B

AMPA: α-amino-3-hydroxy-5-methyl-4-isoxazolepropionic acid

ANG-1: angiopoietin 1

APOE: apolipoprotein E

AQP4: water channel aquaporin 4

Arrdc3: arrestin domain containing 3

BAFF: B-cell-activating factor

BBB: blood-brain barrier

BDFN: brain-derived neurotrophic factor

bFGF: basic fibroblast growth factor

BRP-39: breast regression protein 39

C: complement component

CCL2: C-C motif chemokine 2

CCRL2: CC receptor-like 2

CDMS: clinically definite MS

CHI3L1: chitinase 3-like 1

CIS: clinically isolated syndrome

Cladribine: 2-chlorodeoxyadenosine

CNDP1: beta-Ala-His dipeptidase

CNS: central nervous system

CNTF: ciliary neurotrophic factor

CSF: cerebrospinal fluid

CSPG: sulfate groteoglycan

CTLA-4: cytotoxic T-lymphocyte protein 4

CX30: connexin 30

CX43: connexin 43

CXCL1: C–X–C motif chemokine 1

CXCL10: C–X–C motif chemokine 10

CXCL13: C–X–C motif chemokine 13
CXCRL2: CXC receptor-like 2
DAPI: 4',6-diamidino-2-phenylindole
DDA: data-dependent acquisition
DIS: dissemination in space
DIT: dissemination in time
DIV: days *in vitro*
DMT: disease-modifying treatment
EAAT: excitatory amino acid transporter
EAE: experimental autoimmune encephalomyelitis
EDSS: expanded disability status scale
Egr2: early growth response 2
ERK: mitogen-activated protein kinase
Fas: tumour necrosis factor receptor superfamily member 6
FBS: fetal bovine serum
FC: fold change
FDR: false discovery rate
FGF-21: fibroblast growth factor 21
FLAIR: fluid attenuated inversion recovery
FosB: proto-oncogene
GABA: γ-aminobutyric acid
GalC: galactocerebrosidase
Gapdh: glyceraldehyde-3-phosphate dehydrogenase
G-CSF: granulocyte colony-stimulating factor
GDF-15: growth/differentiation factor 15
GDNF: glial-derived neurotrophic factor
GFAP: glial fibrillary acidic protein
GM-CSF: granulocyte-macrophage colony-stimulating factor
GO: Gene Ontology
gp130: interleukin-6 receptor subunit beta
Gpc: glypican

HCD: high-energy collision dissociation

Iba1: ionized calcium-binding adaptor molecule 1

IFN: interferon

IL: interleukin

IL-6: interleukin-6

iPSC: induced pluripotent stem cells

JAK2: janus kinase 2

KEGG: Kyoto Encyclopedia of Gene and Genomes

Kir4.1: inwardly rectifying K^+ channel 4.1

Klf6: kruppel like factor 6

LC/MS: liquid chromatography and mass spectrometry

Lcn2: lipocalin 2

LIF: leukemia inhibitor factor

MACS: magnetic cell sorting

MAP2: microtubule-associated protein 2

Mapk: mitogen-activated protein kinase

M-CSF: macrophage colony-stimulating

Megf10: multiple epidermal growth factor-like domains protein 10

Mertk: tyrosine-protein kinase Mer

MHC-II: major histocompatibility complex class II

MMP: matrix metalloproteinase

MRI: magnetic resonance imaging

MS: multiple sclerosis

MS-High: high inflammatory multiple sclerosis

MS-Low: low inflammatory multiple sclerosis

NAWM: normal-appearing white matter

NeuN: neuronal nuclear antigen

Nfkb1: nuclear factor NF-kappa-B p105 subunit

NfL: neurofilament light chain

NF-κB: nuclear factor kappa B

NGS: normal goat serum

NIK: NF-κB-inducing kinase
NINC: non-inflammatory neurological controls
NMDA: N-methyl-D-aspartate
NO: nitric oxide
Nr4a1: nuclear receptor subfamily 4 group A member 1
NTC: no template control
OCB: oligoclonal band
OPC: oligodendrocyte precursor cells
PAI-1: plasminogen activator inhibitor 1
PCSK9: proprotein convertase 9
PD: proton density
PDGF-BB: platelet-derived growth factor subtype BB
PDL: poly-D-lysine
PLAU: urokinase-type plasminogen activator
PPMS: primary progressive multiple sclerosis
PSD-95: post-synaptic density protein 95
Ptgs2: prostaglandin-endoperoxide synthase 2
Rela: transcription factor p65
ROS: reactive oxygen species
RRMS: relapsing-remitting multiple sclerosis
S1P: sphingosine 1-phosphate
S1PR1: S1P receptor 1
SEM: standard error of the mean
SEMA7A: semaphorin-7A
SHH: Sonic hedgehog
SPARCL1: SPARC-like protein 1
SPMS: secondary progressive multiple sclerosis
STAT3: signal transducer and activator of transcription 3
TGF-β: transforming growth factor-β
TNF-α: tumour necrosis factor-α
tPA/PLAT: tissue-type plasminogen activator

Treg: regulatory T

TrkB: tropomyosin-related kinase B

Trp53: cellular tumour antigen p53

TSP: thrombospondins

Txnip: thioredoxin interacting protein

VEGFA: vascular endothelial growth factor A

VLA-4: very late antigen 4

ZO-1: zonula occludens 1

Index

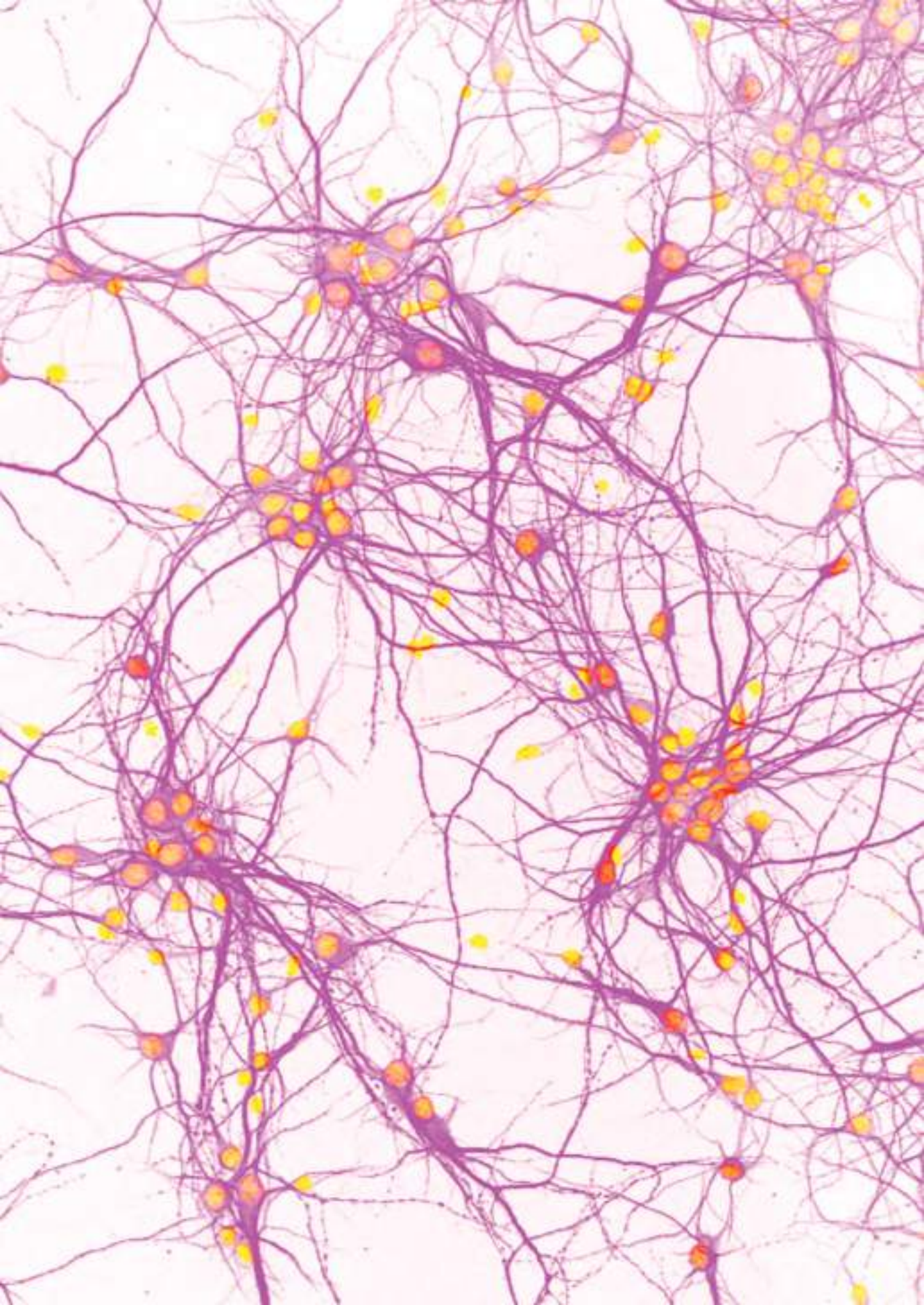

Abstract

Multiple sclerosis (MS) is a demyelinating autoimmune disease of the central nervous system (CNS). Most MS patients initially have an inflammatory phase characterized by periods of clinical relapses and remissions. Over time, a large proportion of patients will enter a progressive neurodegenerative phase of the disease characterized by sustained and irreversible neurological deterioration. Currently available therapies for MS patients are highly effective to suppress inflammation, but largely fail to prevent the neurodegenerative component that inevitably leads to disease progression (1-3).

Despite that reactive astrogliosis is now one of the pathological hallmarks in MS, astrocytes have always been considered as static bystander cells. However, astrocytes are involved in many important CNS functions, such as ion, pH and water homeostasis, maintenance of blood-brain barrier properties, control of energy supply to neurons, and regulation of function and formation of synapses (4). Furthermore, compelling evidence points to astrocytes as key contributors to the neurodegenerative component observed in MS. However, the mechanisms underlying the regulation of astrocytic responses remain unknown.

In the present study, we aimed to investigate how inflammation in MS induces astrocyte reactivity modulating the astrocytic response that leads to neuronal damage. We report an exhaustive molecular and functional characterization of astrocyte reactivity following exposure to cerebrospinal fluid (CSF) from MS patients classified according to the degree of inflammatory activity. We showed that mouse astrocytes exposed to CSF from patients with high inflammatory activity (MS-High) exhibited a specific pro-inflammatory reactive state that was characterized by enhanced nuclear factor kappa B (NF-κB) signalling. This reactive astrocyte state conferred an aberrant response through an altered pro-inflammatory secretome that drove neuronal dysfunction and impaired synaptic plasticity. SerpinE1 was identified as a potential downstream mediator of the non-cell-autonomous toxic effect on neuronal function based on its significant up-regulation in secretomes from

astrocytes exposed to CSF from MS-High patients. Furthermore, we identified chitinase 3-like 1 (CHI3L1) as a potential upstream modulator of astrocyte reactivity via activation of NF-kB signalling based on its significantly increased levels in the CSF from MS-High patients.

Taken together, our findings indicate that the inflammatory microenvironment in the CNS of MS patients can induce specific reactive astrocyte states that trigger neuronal degeneration and may ultimately contribute to disease progression.

Resumen

La esclerosis múltiple (EM) es una enfermedad autoinmune y desmielinizante del sistema nervioso central (SNC). La mayoría de los pacientes presentan una fase inicial inflamatoria que alterna períodos de exacerbaciones y remisiones. A lo largo del tiempo, una gran proporción de pacientes entrará en una fase de la enfermedad de neurodegeneración progresiva que se caracteriza por un deterioro neurológico mantenido e irreversible. Los tratamientos actualmente disponibles para los pacientes con EM son muy efectivos en la supresión de la inflamación, pero altamente ineficientes en la prevención del componente neurodegenerativo que inevitablemente conlleva a la progresión de la enfermedad (1-3).

A pesar de que la astrogliosis reactiva es ahora una de las características patológicas de la EM, los astrocitos siempre se han considerado como células estáticas de soporte. Sin embargo, los astrocitos están involucrados en muchas funciones importantes del SNC, como la homeostasis de iones, pH y agua, el mantenimiento de las propiedades de la barrera hemato-encefálica, el control del suministro energético a las neuronas, y la regulación de la función y formación de las sinapsis (4). Además, evidencias convincentes apuntan a los astrocitos como contribuyentes clave al componente neurodegenerativo observado en la EM. Sin embargo, los mecanismos subyacentes a la regulación de las respuestas astrocíticas siguen siendo desconocidos.

En el presente estudio, nos propusimos investigar cómo la inflamación en la EM induce astrogliosis reactiva, modulando la respuesta astrocítica que conduce al daño neuronal. Presentamos una caracterización molecular y funcional exhaustiva de la reactividad de los astrocitos tras la exposición al líquido cefalorraquídeo (LCR) de pacientes con EM clasificados según el grado de actividad inflamatoria. Demostramos que los astrocitos de ratón expuestos a LCR de pacientes con alta actividad inflamatoria (MS-High) exhibían un estado reactivo pro-inflamatorio específico caracterizado por una mayor señalización de *nuclear factor kappa B* (NF-kB). Este estado reactivo de los astrocitos confirió una respuesta aberrante a través de un secretoma alterado y pro-inflamatorio que conduce a la disfunción neuronal y

al deterioro de la plasticidad sináptica. SerpinE1 se identificó como un mediador potencial del efecto tóxico paracrino sobre la función neuronal en base a su expresión aumentada en el secretoma de los astrocitos expuestos a LCR de pacientes con MS-High. Además, identificamos la proteína *chitinase 3-like 1* (CHI3L1) como un posible modulador de la reactividad astrocítica a través de la activación de la señalización de NF-kB, en función de sus niveles significativamente aumentados en el LCR de pacientes con MS-High.

Conjuntamente, nuestros hallazgos indican que el microambiente inflamatorio en el SNC de los pacientes con EM puede inducir estados de reactividad astrocítica específicos que desencadenan la degeneración neuronal y, en última instancia, pueden contribuir a la progresión de la enfermedad.

Introduction

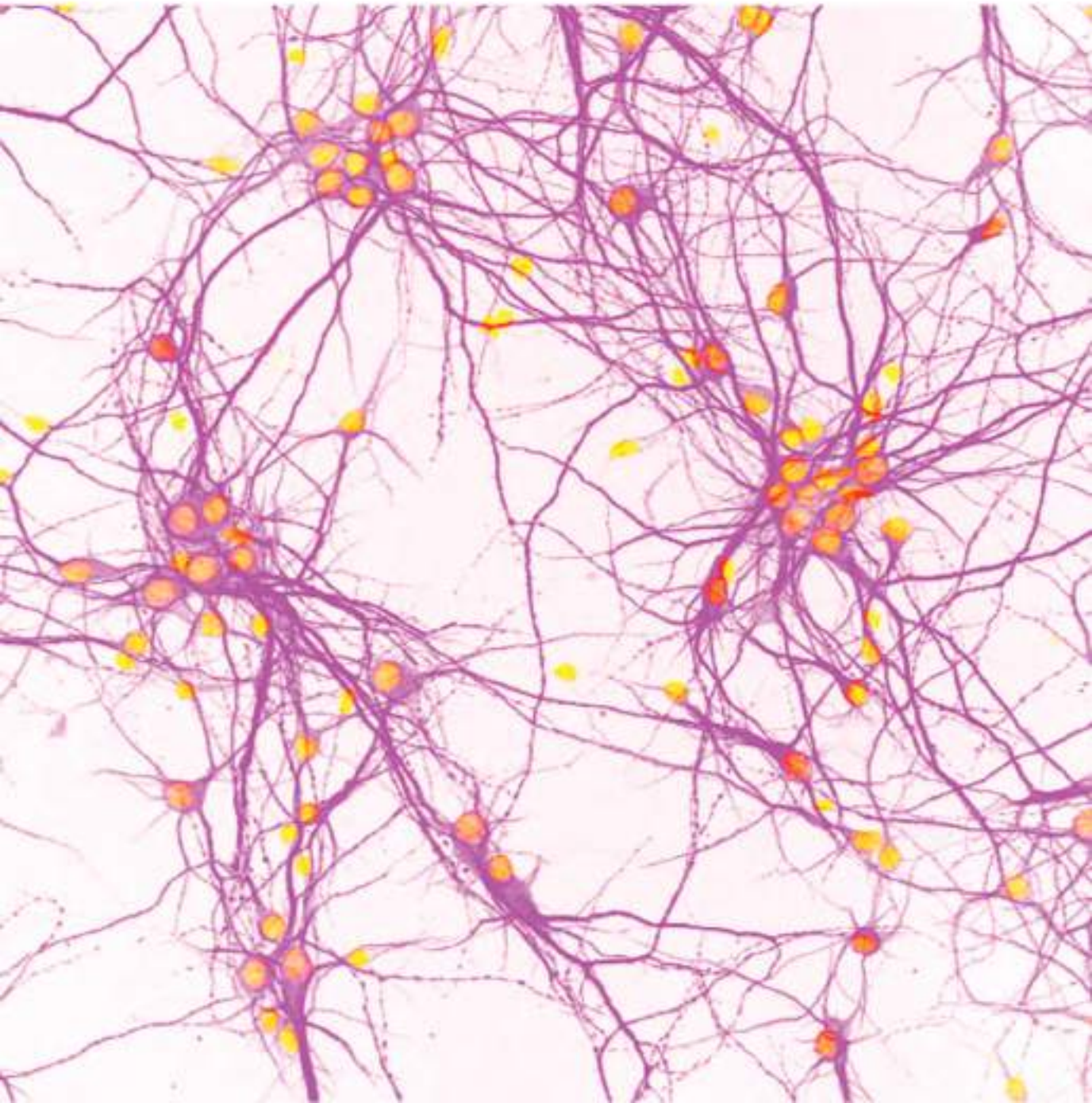

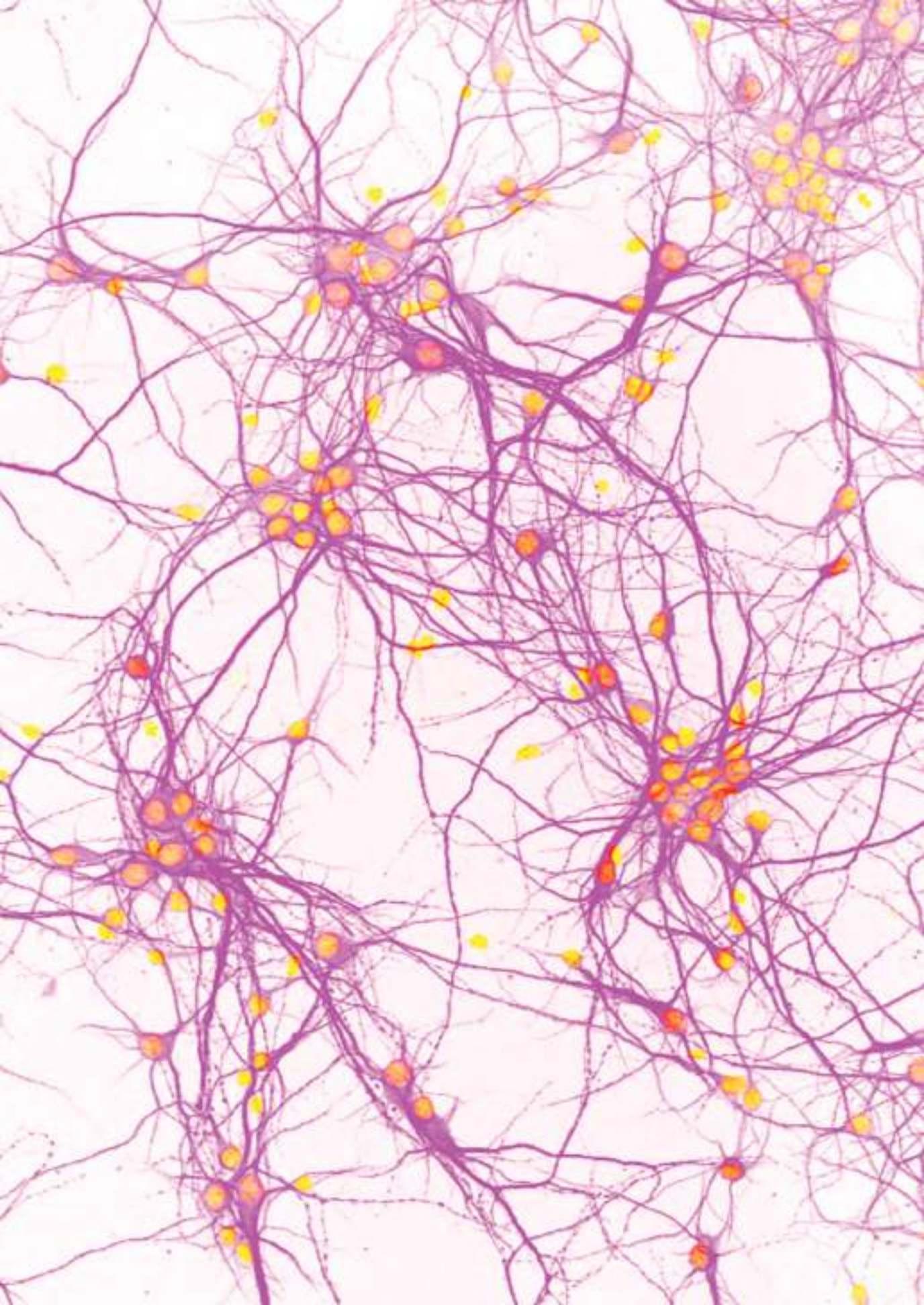

1. Introduction

1.1. Multiple sclerosis

Multiple sclerosis (MS) is a chronic, inflammatory, demyelinating, and neurodegenerative disease of the central nervous system (CNS). It represents one of the leading causes of non-traumatic disability among young adults, and has become the most common demyelinating disease worldwide, affecting 2.5 million people (5). This carries a significant social and economic impact.

MS onset typically occurs in young adults (20-40 years of age), although 5% of diagnosed patients experienced their first clinical symptoms during childhood and adolescence (6) or in late adulthood (>50 years of age) (7). It is more prevalent in women than in men (2.3-3.5:1) (8).

The MS aetiology remains unknown. However, decades of investigation suggest that disease predisposition and progression are influenced by both a complex multifactorial genetic background and environmental factors (9, 10). The main environmental factors linked to MS risk are Epstein-Barr virus, vitamin D deficiency, smoking, salt intake and adolescent obesity (11).

1.1.1. Pathology

The main pathological hallmarks of MS are inflammation, demyelination, reactive astrogliosis, oligodendrocyte loss and neurodegeneration (12, 13).

Focal areas of demyelination, known as plaques or lesions, occur both in the white and grey matter, and are typically observed in the brain, optic nerve, and spinal cord (14). The loss of myelin sheaths affects the saltatory conduction of the action potential that ultimately causes neurological symptoms. Moreover, acute demyelination compromises axonal cytoskeleton integrity and increases demyelinated axon vulnerability to persistent inflammation and axonal transection (15). Then, chronically demyelinated axons degenerate in consequence of the loss of glial support. Axonal and neuronal loss in acute and chronic demyelinated lesions

are considered the main contributors to neurological disability progression (13) (**Figure 1**).

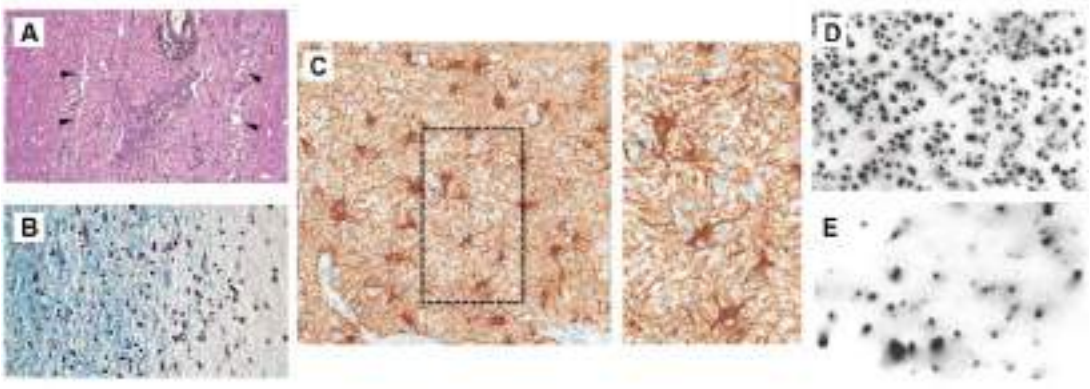

Figure 1. Main pathological hallmarks in MS lesions. Images represent the characteristic inflammation (A), demyelination (B), and reactive astrogliosis (C) in MS. Neurodegeneration is shown in panels D and E, when comparing axonal density in control tissue (D) and in MS lesion (E). Adapted from: Han MH, Hwang SI, Roy DB, Lundgren DH, Price JV, Ousman SS, Fernald GH, Gerlitz B, Robinson WH, Baranzini SE, Grinnell BW, Raine CS, Sobel RA, Han DK, Steinman L. Proteomic analysis of active multiple sclerosis lesions reveals therapeutic targets. Nature. 2008; 451(7182):1076-1081 (A, B); Sofroniew MV, Vinters HV. Astrocytes: biology and pathology. Acta Neuropathologica. 2010; 119:7-35 (C); and Trapp BD, Nave KA. Multiple sclerosis: an immune or neurodegenerative disorder? Annual Reviews Neuroscience. 2008; 31:247-69 (D, E).

1.1.2. Pathogenesis

MS has been traditionally considered a primary autoimmune disease in which dysregulated autoreactive T cells are primed in the periphery, cross into the CNS and lead to the formation of new inflammatory demyelinating lesions (outside-in model). Despite the overwhelming evidence of an inflammatory component in MS, questions have raised as to whether the immune system is the root of the disease. In this regard, an alternative model suggests an immunological convolution between an underlying primary degenerative disorder and an aberrant immune response (inside-out model) (16).

Early inflammatory phase

Autoreactive T and B cells as well as monocytes infiltrate into the CNS via the cerebrospinal fluid (CSF) compartment (17) or by crossing the CNS endothelium (18). Once in the CNS, T cells encounter myelin antigens presented by perivascular macrophages. Reactivated T cells secrete cytokines and chemokines that activate both microglia and astrocytes, as well as disturb oligodendrocyte homeostasis. The pro-inflammatory environment produced by reactive T cells, microglia, and astrocyte secretions promotes the breakdown of the blood-brain barrier (BBB) (19-21), thus allowing the recruitment of additional immune cells into the CNS, including plasma cells, which produce antibodies that directly affect myelin sheaths (22), neuronal axons (23, 24), and glial cells (25). The new wave of immune cell infiltration together with CNS-resident cell activation will perpetuate inflammation within the CNS parenchyma and will ultimately lead to demyelination and neuro-axonal injury (21).

The main effector immune cells involved in the immunopathogenesis of MS are: (i) phagocytic cells, which mediate myelin sheaths impairment; (ii) the Th1 $CD4^+$ T cell subset, which secretes pro-inflammatory cytokines such as interferon-γ (IFN-γ), interleukin (IL)-2, and tumour necrosis factor-α (TNF-α) (26-28); (iii) the Th17 $CD4^+$ T cell subset, which secretes a wider range of pro-inflammatory cytokines: granulocyte-macrophage colony-stimulating factor (GM-CSF), IL-6, IL-17, IL-21, IL-22 and TNF-α, and granzyme B (29-31); (iv) cytotoxic $CD8^+$ T cells, which express death effector ligands and release cytotoxic granules, TNF-α and IFN-γ (32), outnumber $CD4^+$ T cells (33) and correlate with the extent of axonal damage (34, 35) in MS lesions; and (v) B cells, which produce pathogenic antibodies targeting myelin antigens (36, 37) . In addition, an immunoregulatory subset of $CD4^+$ T cells, Th2 and regulatory T (reg) cells, secrete IL-4, IL-10 and transforming growth factor-β (TGF-β), respectively, and have been reported to ameliorate CNS autoimmunity (38-41) (**Figure 2**).

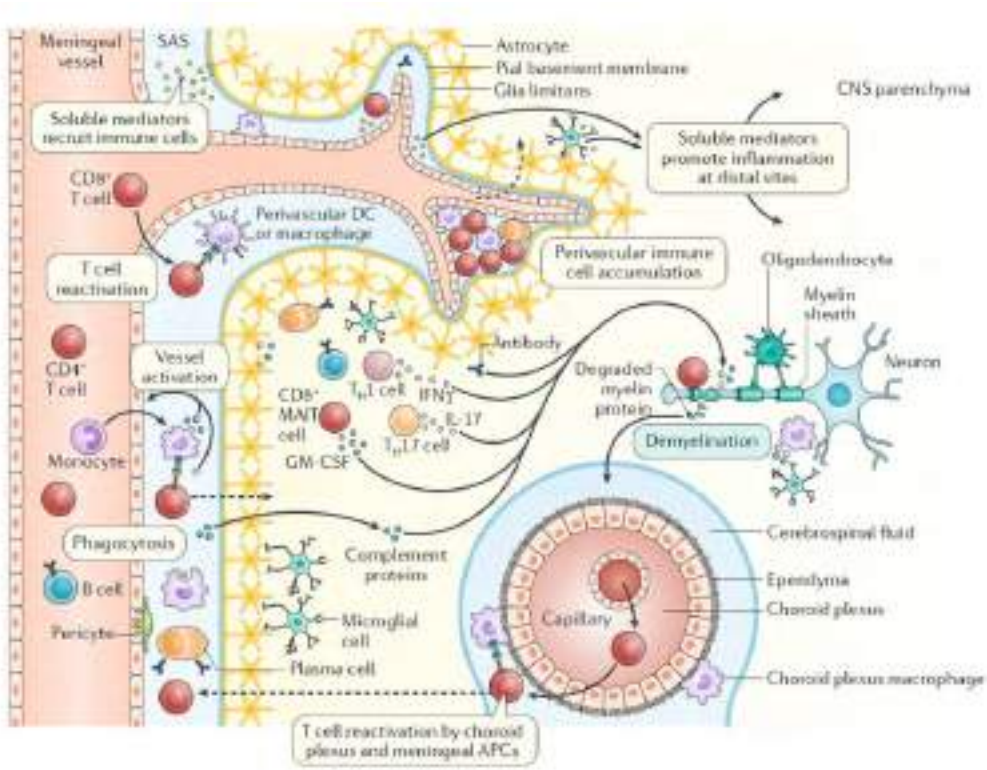

Figure 2. Early inflammatory phase of MS pathogenesis. Peripheral autoreactive immune cells infiltrate into the CNS parenchyma through the blood vessels directly crossing the blood-brain barrier, the subarachnoid space or choroid plexus (dashed arrows). Reactivated immune cells, along with reactive resident microglia and astrocytes, perpetuate CNS inflammation and promote demyelination as well as oligodendrocyte and neuronal damage, through the secretion of soluble factors (pro-inflammatory cytokines, antibodies) and direct cell contact-dependent mechanisms (phagocytosis). Abbreviations: APC: antigen-presenting cells; BBB: blood-brain barrier; GM-CSF: granulocyte–macrophage colony-stimulating factor; IFNγ: interferon-γ; IL: interleukin; Th: T helper. Adapted from: Filippi M, Bar-Or A, Piehl F, Preziosa P, Solari A, Vukusic S, Rocca MA. Multiple sclerosis. Nature Reviews Disease Primers. 2018; 4:43.

Progressive phase

Ongoing inflammation sustained by reactive CNS-resident microglia and astrocytes, through the release of a wide range of neurotoxic inflammatory mediators, culminates with a compartmentalized CNS chronic inflammation. The persistent exposure of neurons and oligodendrocytes to the existing inflammatory microenvironment promotes neuroaxonal injury that triggers chronic

neurodegenerative processes (42, 43). Thus, vulnerable demyelinated axons, due to the loss of myelin sheath and glia trophic support, will ultimately degenerate causing neuronal loss. Brain atrophy, as a consequence of neuronal death, can be assessed by magnetic resonance imaging (MRI) and represents the major cause of irreversible neurological disability observed in progressive MS (13, 44, 45).

There are several molecular mechanisms and factors underlying neurodegeneration mediated by both immunologic and neurobiological effectors, which eventually result in disease progression and chronic disability. The main neurodegenerative mechanisms induced by immunological processes are: (i) antigen-specific $CD8^+$ T lymphocyte-mediated cytotoxicity against myelin, oligodendrocytes, and neurons (34, 46-49); (ii) antibodies against myelin and non-myelin antigens (such as neurofascin, neurofilaments or glial inwardly rectifying K^+ channel 4.1 - Kir4.1) induce injury through activation of the complement cascade (24, 50-52); (iii) direct T cell-mediated neurotoxicity (53); (iv) the release of IFN-γ by $CD8^+$ T cells induces glutamate neurotoxicity and Ca^{2+} influx into neurons (54); (v) the release of TNF-α by $CD8^+$ T cells triggers neuronal death via the p55 receptor (55); (vi) the release of perforin and granzymes by $CD8^+$ T cells damages neuron cell membranes leading to Na^+ and Ca^{+2} influx as well as energy breakdown (56); (vii) reactive astrocytes secrete pro-inflammatory chemokines that attract immune cells and microglia to lesion sites (57); (viii) GM-CSF, macrophage colony-stimulating (M-CSF), and TGF-β released by reactive astrocytes regulate major histocompatibility complex class II (MHC-II) expression by microglia and its phagocytosis capacity (58); (ix) reactive astrocytes up-regulate B-cell-activating factor (BAFF) expression, which contribute to B-cell-dependent autoimmunity (59); (x) activated microglia can cause neuronal death by releasing harmful factors such as reactive oxygen species (ROS) (60), glutamate, and proteases (61); (xi) activated microglia secrete pro-inflammatory cytokines that induce mitochondrial injury both in neurons and glial cells (60, 62, 63); (xii) the uptake and release of Fe^{2+} by activated microglia increases the susceptibility to free radicals-driven demyelination and neurodegeneration (64); and (xiii) activated

microglia executes neuronal death by phagocytosis of stressed neurons (a process termed phagoptosis) (65).

On the other hand, the main neurobiological effectors causing oligodendroglial damage as well as axonal and neuronal degeneration are: (i) loss of glial trophic support (66, 67); (ii) mitochondrial dysfunction (62, 68, 69), (iii) excitotoxicity (70, 71); (iv) remyelination failure by both oligodendrocyte precursor cells (OPC) and oligodendrocytes (72, 73); (v) senescence transcriptomic changes in OPCs, which make them unable to differentiate into mature oligodendrocytes (74); and (vi) increased neuronal energy demand and alterations in ion channel homeostasis (75-77).

Growing evidence points to diffuse synaptic dysfunction and loss, known as synaptopathy, as a pathophysiological hallmark of MS independent of axonal transection and demyelination. Long-lasting alterations of synaptic homeostasis can be detrimental and lead to excitotoxic damage and neuronal death (78, 79). In this line, structural synaptic alterations have been observed in different CNS areas in the animal model of MS, the experimental autoimmune encephalomyelitis (EAE), including spinal cord, hippocampus, cerebellum, striatum, and cortex. In fact, in the spinal cord from EAE mice, a prominent retraction of both dendrites and synaptic terminals of motor neurons was observed during disease exacerbation and correlated with reactive astrogliosis (80-82). In addition, signs of apoptosis at the synaptic level have been detected in the acute phase of EAE in absence of neuronal loss (83), suggesting that synapses are early targets of the neurodegenerative component of the disease. Several studies have demonstrated that neuroinflammation can impair synaptic transmission at different levels, resulting in detrimental effects on synaptic excitability and, ultimately, neuronal function (84-86). In this regard, pro-inflammatory cytokines are known to affect the post-synaptic compartment and have been observed in both early and late phases of EAE (83, 87). By contrast, synaptic alterations triggered by axonal demyelination impair the pre-synaptic transmitter release and can be reversed in the chronic phase of EAE when a certain degree of remyelination occurs (87). Importantly, most of the synaptic

alterations have the potential to rapidly and spontaneously revert independently from the remyelination process (81).

The relevance of a synaptopathy in MS patients has been confirmed in several studies. Particularly, in a post-mortem histological study in patients with progressive MS, the demyelinated hippocampi showed minimal neuronal loss but significantly decreased levels of crucial proteins for synaptic maintenance, axonal transport, glutamate homeostasis and neurotransmission as well as synaptic plasticity (synaptophysin, synaptotagmin, and post-synaptic density protein 95 (PSD-95), among others) (88). Moreover, complement component (C)-1q and C3 proteins of the complement system were identified as mediators of the synapse elimination observed in hippocampus from MS patients (89).

Although the precise mechanisms underlying synaptic dysfunction in MS are not fully understood, recent studies demonstrated a causative effect mediated by $CD3^+$ T cells (83, 90-92), activated microglia (83, 93) as well as pro-inflammatory cytokines TNF-α (83, 91) and IL-1β (90, 93-96). Collectively, these evidences suggest a direct link between the inflammatory microenvironment in the CNS and a synaptopathy in MS, which can be independent from demyelination and neuronal loss. Likewise, it indicates that synaptic abnormalities could be the result of a combination of both diffuse and focal neuroinflammation as well as axonal demyelination (**Figure 3**).

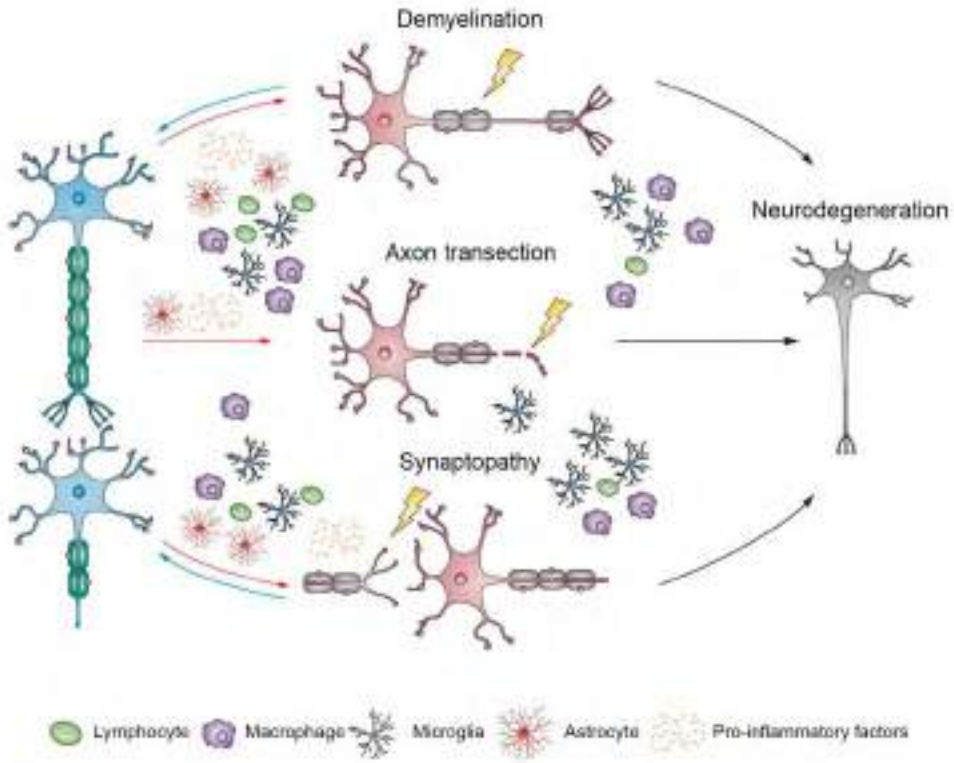

Figure 3. Demyelination, axonal loss and synaptopathy are pathophysiological hallmarks of MS. Inflammation driven by autoreactive lymphocytes triggers microglia, macrophage and astrocyte activation, which in turn, boosts inflammatory microenvironment through the release of soluble factors. Thus, inflammation (red arrows) in the CNS leads to demyelination, axon transection and synaptopathy. Chronic demyelinated axons undergo neurodegenerative processes such as mitochondrial dysfunction and ion channel alterations that promote neurodegeneration. Similarly, axonal loss is not reversible and results in neuronal death. Long-lasting synaptic dysfunction in chronic microglia activation can lead to neurodegeneration. Importantly, both demyelination and synaptic impairment are potentially reversible (blue arrows). Adapted from: Mandolesi G, Gentile A, Musella A, Fresegna D, De Vito F, Bullita S, Sepman H, Marfia GA and Centonze D. Synaptopathy connects inflammation and neurodegeneration in multiple sclerosis. Nature Reviews Neurology. 2015; 11, 711-724.

1.1.3. Clinical aspects

The symptomatohology of MS is highly heterogeneous between patients, but clinical manifestations normaly include visual, motor and sensory symptoms, as well as cognitive impairment (15). Neurological disability in patients is assessed by the Expanded Disability Status Scale (EDSS), which is used to monitor disability

progression over time (97). EDSS 3.0 indicates moderate disability, while EDSS above 5.5 indicates walking assistance.

The clinical course of MS is also heterogeneous and comprises several phenotypes defined considering the original clinical patterns (98) and new descriptors such as disease activity and clinical progression, which reflect ongoing inflammatory and neurodegenerative processes, respectively (99). Four different clinical courses have been described and can be categorized as relapsing or progressive: (i) clinically isolated syndrome (CIS); (ii) relapsing-remitting MS (RRMS); (iii) primary progressive MS (PPMS); and (iv) secondary progressive MS (SPMS) (99) (**Figure 4**).

Most patients (85-90%) initially present a first clinical attack (CIS) highly suggestive of demyelinating CNS disease but has yet to fulfil criteria for MS diagnosis (100). This first event is an unpredictable episode of neurological dysfunction due to demyelinating lesions typically affecting the optic nerve, brainstem or cerebellum, spinal cord, or cerebral hemispheres. Also, patients with a CIS may present cognitive impairment (100). RRMS is characterized by alternating periods of relapses with new neurological symptoms, followed by remissions with clinical stability. As the disease progresses, functional recovery from the acute episodes is incomplete and neurological disability accumulates. After approximately 19 years from a RRMS onset, most patients (65%) will eventually develop a progressive phase (SPMS). The SPMS course fluctuates in periods of progression with possible relapses in between, as well as periods of relatively stable disability. Finally, about 10-20% of MS patients develop a progressive course from disease onset (PPMS). Progression in PPMS is variable at the individual patient level, in which relapses and periods of relative disease stability throughout the course can occur. It is thought that the absence of an initial relapsing phase in PPMS patients may potentially be caused by clinically silent lesions (101, 102). In both progressive phenotypes, pathology is complex and involves neurodegeneration along with mild-to-moderate inflammation (103).

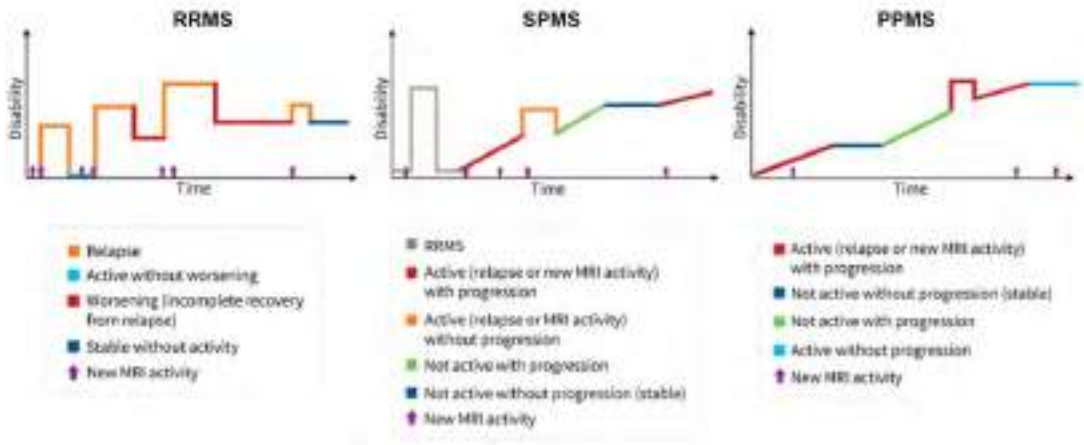

Figure 4. Clinical course of MS. Abbreviations: RRMS: relapsing-remitting multiple sclerosis; SPMS: secondary progressive multiple sclerosis; PPMS: primary progressive multiple sclerosis; MRI: magnetic magnetic resonance imaging. Illustration from: Klineova S, Lublin FD. Clinical course of multiple sclerosis. Cold Spring Harbor Perspectives in Medicine. 2018; 8(9):a028928.

1.1.4. Diagnosis and prognosis

There is a strong need for early MS diagnosis, since initiation of disease-modifying treatment (DMT) at early stages may significantly impact the disease evolution (104-106).

Current validated criteria for MS diagnosis are the 2017 McDonald criteria (107), which are fundamentally based on clinical criteria, MRI, and CSF findings. After a first clinical attack (CIS), clinically definite MS (CDMS) is confirmed when fulfilling clinical criteria for a second attack, or radiological criteria for dissemination in time (DIT) and space (DIS), or the combination of DIS with the presence of CSF-specific oligoclonal bands (OCB) (107).

MRI

MRI has been increasingly used over time and has become the most reliable paraclinical tool to support the diagnosis of MS. The conventional MRI techniques performed for diagnostic purposes are: T1-, T2-, and proton density (PD)-weighted imaging, and fluid attenuated inversion recovery (FLAIR) sequences.

Abnormal MRI with the presence of focal lesions is observed in almost all MS as well as CIS patients. MS lesions have features that facilitate the differential diagnosis from other CNS diseases resembling MS, such as signal intensity, localization, and morphology. Lesions commonly appear in periventricular, juxtacortical and infratentorial brain regions and in the spinal cord (**Figure 5A-E**).

In addition, the administration of gadolinium-based contrast agents when imaging, allows the identification of new active lesions and its discrimination from those inactive (**Figure 5F, G**). Signal enhancement occurs when there is an increase in BBB permeability, which represents ongoing inflammation.

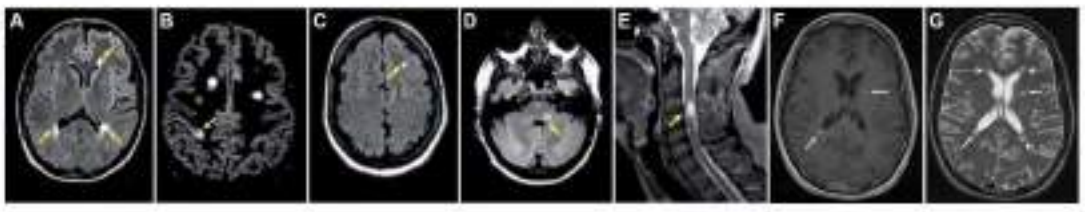

Figure 5. Typical MS lesions in MRI. DIS demonstration by different demyelinating lesions observed in the four typical areas of the CNS: periventricular (A), cortical (B), juxtacortical (C), infratentorial (D), and spinal cord (E) lesions. Yellow arrows highlight the corresponding lesions. DIT demonstration in T1- (F) and T2-weighted (G) imaging with the presence of gadolinium-enhanced (active, white arrows) and non-enhanced (inactive, white dashed arrows) lesions (F, G). Adapted from: Filippi M, Bar-Or A, Piehl F, Preziosa P, Solari A, Vukusic S, Rocca MA. Multiple Sclerosis. Nature Reviews Disease Primers. 2018; 4:43 (A-E); and Vigeveno RM, Wiebenga OT, Wattjes MP, Geurts JJG, Barkhof F. Shifting imaging targets in multiple sclerosis: from inflammation to neurodegeneration. Journal of Magnetic Resonance Imaging. 2012; 36:1-19 (F, G).

MRI has also been critical not only for MS diagnosis but also for monitoring disease activity and treatment response, as well as for MS prognosis. To date, brain MRI is still considered the most effective tool for prediction of MS conversion and disability accumulation. In this line, the number of brain lesions in CIS patients correlated with a higher risk for conversion to MS and disability progression, and are considered a high-impact prognostic factor (108-112).

Furthermore, MRI is for now the only tool that reliably allows assessing disease activity in MS (113). Also, it can be used to study the degree of inflammation, by the quantification of enhancing lesions, and the degree of neurodegeneration, through the analysis of brain and spinal cord atrophy. In this regard, it has been demonstrated a correlation between brain atrophy measures and the development of long-term disability in patients with MS (114).

OCB

The presence of CSF-restricted OCB allows the detection of an abnormal increase production of antibodies within the CNS. Original MS diagnostic criteria revision included CSF-specific IgG OCB findings supporting disease diagnosis (2), based on their high prevalence in MS patients (115) as well as their predictive role on CIS conversion to CDMS (116).

1.1.5. Disease modifying therapies (DMT)

Treatment strategy in MS aims to reduce the number of relapses in RRMS forms as well as to delay or prevent disability progression in patients. Currently available therapies are classified into: injectables, oral therapies, and monoclonal antibodies.

Injectables DMT include IFN-β and glatiramer acetate, which are first-line therapies for RRMS forms. The exact mechanism of action remains unknown but, overall, these drugs have anti-inflammatory and regulatory effects (117-119). Oral therapies are: fingolimod, teriflunomide, dimethyl fumarate, and cladribine. Fingolimod, an analogue of sphingosine 1-phosphate (S1P), prevents T cell migration from the secondary lymph organs, thus decreasing circulating T cells (120, 121). Teriflunomide is a metabolite that inhibits the proliferation of B and T cells (122, 123). Dimethyl fumarate has immunomodulatory effects by shifting from a pro-inflammatory (Th1) to an anti-inflammatory (Th2) cytokine profile (124). Cladribine (2-chlorodeoxyadenosine) is a synthetic deoxyadenosine analogue known to induce a cytotoxic effect on lymphocytes, leading to long-term depletion of T and B cells (125). Finally, several monoclonal antibodies are used to target immune responses in RRMS patients. Natalizumab, a humanized monoclonal antibody that binds to the

α-4 integrin of very late antigen 4 (VLA-4), prevents lymphocyte trafficking into the CNS (126, 127). Alemtuzumab, a humanized monoclonal antibody against CD52, targets T and B cells and induces their depletion and subsequent repopulation (128, 129). On the other hand, there are B-cell depleting monoclonal antibodies targeting CD20: rituximab (chimeric mouse-human), ocrelizumab and ofatunumab (both humanized), which deplete mature B cell populations (130, 131). Importantly, ocrelizumab is the first drug that have been approved for treatment PPMS (132).

Although the MS treatment pipeline has hugely evolved over the past 25 years since the approval of the first drug, available therapies are highly effective to suppress the predominantly inflammatory component observed in patients with RRMS. However, these therapies have proven to be largely ineffective in patients with progressive forms of the disease in whom the neurodegenerative component dominates (SPMS and PPMS). In this setting, a more in-depth understanding of the mechanisms of neurodegeneration occurring in the disease will certainly help in the identification of molecular targets that may set the rationale for the design of specific and effective therapeutic approaches to prevent neurodegeneration and hence stop progression in MS patients.

1.1.6. Biomarkers

Considering the high degree of disease heterogeneity, biomarkers are certainly necessary in MS. Biomarkers in MS may help in: (i) early disease diagnosis; (ii) prediction of CIS conversion to CDMS; (iii) stratification of disease phenotypes; (iv) prognosis of the disease course; and (v) prediction of treatment response at individual patient's level. To date, despite the efforts deposited, MS heterogeneity makes it challenging, and few biomarkers are implemented into the clinical practice: CSF IgG-OCB, IgG index, and MRI (reviewed in (133, 134). A promising biomarker that is gradually being implemented into MS clinical practice for therapy monitoring is the blood neurofilament light chain (NfL) (135).

Briefly, several CSF biomarkers candidates have shown promising results on early CIS conversion to MS: IgM OCB (136, 137), C–X–C motif chemokine 13 (CXCL13)

(138), chitinase 3-like 1 (CHI3L1) (139, 140), and NfL (141). In particular, CSF CHI3L1 levels have been also associated with early and rapid disability progression (140), and demonstrated a direct neurotoxic effect *in vitro* (142). However, there is still a need for validation of biological markers in order to be able to apply them into the clinical practice.

1.2. Astrocytes

1.2.1. Astrocytes in CNS homeostasis

Astrocytes are specialized glial cells originated from the neuroectoderm. They are the most abundant cell type in the CNS and represent a 70% of total cells in the brain and cover 20-50% of the brain volume. Worth noting, the ratio of astrocytes per neuron increases substantially among species when increases brain complexity and size, supporting an evolutionary advantage in greater number of astrocytes (143).

Astrocytes were first described in 1846 by Rudolf Virchow who defined a homogenous cell population that supports neurons. Later, Camilo Golgi and Ramón y Cajal identified diverse astrocyte morphologies in the human cerebellum (144). Since then, numerous astrocyte morphologies across different CNS regions have been described, but they are still classified into two main subtypes: protoplasmatic and fibrous. Protoplasmatic astrocytes are located throughout all grey matter and exhibit several stem branches that give rise to multiple finely branching processes in a uniform globoid distribution. Fibrous astrocytes are found throughout all white matter and exhibit a morphology characterized by many long fiber-like processes (4). Electron microscopy studies have revealed that protoplasmatic astrocyte processes envelop synapses while the processes of fibrous astrocytes contact to nodes of Ranvier. Also, both types of astrocytes showed gap junctions between neighbouring astrocytes through their processes (4).

Astrocyte physiology

Although astrocytes express almost the same set of ion channels and receptors as neurons and display evoked currents, they do not propagate action potentials along their processes (143, 145). Astrocyte excitability through regulated increases

in intracellular calcium concentration enables functional astrocyte-astrocyte as well as astrocyte-neuron intercellular communications. These Ca^{2+} intracellular fluctuations can be triggered by neurotransmitters released during neuronal activity or propagated to neighbouring astrocytes (146-151).

Among others, Kir4.1 is predominantly localized at distal astrocytic processes that envelop synapses or capillaries (152). Kir4.1 and water channel aquaporin 4 (AQP4) perform the maintenance of K^+ and water homeostasis in the CNS (153, 154). Excitatory amino acid transporter (EAAT)-1 and EAAT2 are glia-specific transporters responsible for glutamate uptake during synapses (155, 156). Also, astrocytes express glutamate receptors, such as N-methyl-D-aspartate (NMDA) and α-amino-3-hydroxy-5-methyl-4-isoxazolepropionic acid (AMPA) receptors, which are essential for excitatory glutamate synapses, as well as γ-aminobutyric acid (GABA) receptors that are crucial for inhibitory synapses (157).

Furthermore, astrocytes can interact with neighbouring astrocytes through gap junctions that give rise to multicellular networks, mainly formed by connexin 43 (CX43) and connexin 30 (CX30). These networks allow astrocytes to dissipate molecules, such as K^+ and glutamate, which are thought to prevent detrimental extracellular accumulation of these molecules (158).

Astrocyte functions

Despite the traditional view that long-considered astrocytes as static bystander cells involved in supporting neurons, it is now clear that astrocytes perform diverse and dynamic functions which essentially orchestrate CNS development and function (**Figure 6**).

Role in BBB

Astrocytes establish extensive contacts and bidirectional interactions with endothelial cells from blood vessels. This allows the regulation of local CNS blood flow according to changes in neuronal activity (159). It has been shown that they can

also modulate CNS blood vessel diameter as well as blood flow by the release of mediators such as prostaglandins, nitric oxide (NO), and arachidonic acid (160, 161).

Another major function of astrocytes is the regulation and maintenance of the BBB. Astrocytic endfeets almost completely cover all CNS capillaries, where they contribute to strength tight junctions and their expression of polarized transporters and enzymes allow the transport of metabolites(19, 162). Astrocytes express tight junction proteins, including occluding, claudin-5, and zonula occludens 1 (ZO-1), which correlate with the induction and maintenance of the BBB integrity (19). In addition, astrocytes secrete a wide range of molecules that have shown to be involved in BBB maintenance: (i) vascular endothelial growth factor A (VEGFA), which is an angiogenic factor that promotes endothelial cell activation and proliferation (163, 164); (ii) glial-derived neurotrophic factor (GDNF); (iii) basic fibroblast growth factor (bFGF); (iv) angiopoietin 1 (ANG-1), that influences endothelial function enhancing vascular stabilization and decreasing permeability by increasing tight junction protein expression (165); and (v) TFG-β, that tightens the BBB and reduces its permeability (19) (**Figure 6A**).

Energy and metabolic support

Astrocyte is an essential contributor to the CNS metabolism by contacting simultaneously through its processes with blood vessels, neuronal soma, nodes of Ranvier (axons) and synapses, which allow diffuse glucose and metabolites from blood to neuronal elements (4) (**Figure 6B-D**). Compelling findings evidence that astrocytes are the main storage sites of glycogen in the CNS, which is directly proportional to high synaptic density areas (166). Several reports indicate that in periods of hypoglucemia, astrocyte glycogen is transformed to lactate which is then transferred to adjacent synapses (grey matter) and axons (white matter) (167-169) .

Role in synapsis

Astrocytes play an essential role in synapse formation, functional maturation and refinement of synapses and circuits. The initiation of the synaptogenesis process during development coincides with astrocyte generation (170). Astrocytes mediate

synaptogenesis regulation by both contact-dependent and secreted signals to neurons. It is known that astrocytes contact immature neurons to make them competent for synapse formation and regulate their function and stabilization. At the end of the synaptogenic period, weak and immature synapses are eliminated by astrocytes and microglia (171). Among the astrocyte-secreted synaptogenic modifying factors identified are: (i) thrombospondins (TSP)-1 and TSP-2 (172) as well as SPARC-like protein 1 (SPARCL-1)/hevin (173), which induce the formation of structural glutamatergic silent synapses; (ii) glypican (Gpc)-4 and Gpc6, that induce functionally active synapses (174); (iii) SPARC, that negatively regulates synapse formation and function; (iv) cholesterol, that increases the pre-synaptic function; (v) TNF-α, which increases AMPA receptor levels enhancing neuronal activity (175); (vi) TGF-β, found to both induce excitatory (176) and inhibitory (177) synapse formation, as well as up-regulate C1q expression in neurons, leading to synapse elimination by microglial phagocytosis (178, 179); (vii) multiple epidermal growth factor-like domains protein 10 (Megf10) and tyrosine-protein kinase Mer (Mertk), which drive phagocytosis of synapses (180); and (viii) IL-33, which promotes synapse engulfment by microglia (181).

Furthermore, astrocytes play a direct role with neurons integrating synaptic information, controlling synaptic transmission and plasticity, as well as responding to synaptic activity. This process is encompassed in the term of ‘tripartite synapse’. Astrocytes influence synaptic function by both the regulated release of synaptic active molecules (glutamate, purines, GABA and D-serine) as well as the uptake of neurotransmitters via glutamate transporters (148, 150, 182) (**Figure 6B**).

Anti-inflammatory microenvironment

Importantly, during homeostasis in healthy CNS, astrocytes are known to contribute to the maintenance of an anti-inflammatory microenvironment by constitutively (i) secreting low levels of anti-inflammatory factors, such as TFG-β and IL-10 (183); (ii) expressing tumor necrosis factor receptor superfamily member 6 (Fas) ligand, which induces cell death in Fas receptor expressing cells (mainly

immune cells) (184, 185); and (iii) inducing up-regulated expression of the co-inhibitory cell surface receptor cytotoxic T-lymphocyte protein 4 (CTLA-4) on Th cells, which induces anergy (186).

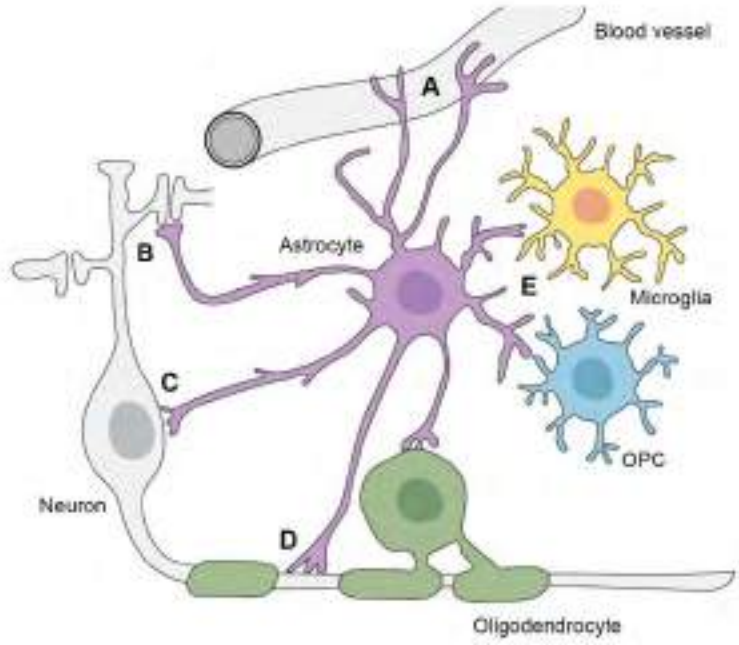

Figure 6. Astrocyte functions in CNS homeostasis. Astrocytes are involved in many essential roles for CNS homeostasis and function. Astrocytes have endfeets that ensheath CNS vasculature to regulate blood flow as well as maintaining BBB properties (A), regulate the formation, elimination, and function of synapses (B), contribute to energy and metabolic support as well as homeostatic function in synapse site (B), neuronal soma (C), and axons through nodes of Ranvier (D), and interact bidirectionally with microglia, OPC and oligodendrocytes (E). Adapted from: Allen NJ, Lyons DA. Glia as architects of central nervous system formation and function. Science. 2018; 362, 181-185.

Astrocyte heterogeneity

Astrocytes cover the entire CNS, in a well-organized non-overlapping manner, with no regions left devoid of astrocytes. The development of novel genomic technologies, such as bulk or single-cell RNA sequencing, and multiple potentially integrative approaches (e.g., mass spectrometry, electrophysiology, immunohistochemistry, electron microscopy, morphological reconstructions,

pharmacogenetics, etc.) have been crucial to the awareness of the complexity and the diversity of astrocyte subpopulations and activation states. Now the physiological diversity of astrocytes is indisputable, which is known to differ between specific brain circuits and regions, where individual astrocytes display distinct signalling pathways in subcellular compartments (4, 187, 188).

1.2.2. Astrocytes in MS

Reactive astrogliosis

Reactive astrogliosis has been recently redefined as 'the process whereby, in response to pathology, astrocytes engage in molecularly defined programs involving changes in transcriptional regulation, as well as biochemical, morphological, metabolic, and physiological remodelling, which ultimately results in gain of new function(s) or loss or upregulation of homeostatic one' (189). This phenomenon has been largely considered a hallmark in CNS disorders. Compelling evidence accumulated over years supports that reactive astrogliosis is a wide heterogenous spectrum of potential changes that are determined in a context-specific manner by diverse signalling events that differ with the nature and severity of the CNS insult (187, 189-192).

Astrocyte scar formation

As previously discussed, astrocytes become reactive at the early acute inflammatory phase of MS, as a result of CNS inflammation induced by immune cell infiltration (21). In MS active lesions, reactive astrocytes typically show a hypertrophic morphology with enlarged cell soma and reduced branching density of the process (190). Importantly, reactive astrocytes are not only present in the active margins of demyelinating lesions but into adjacent normal-appearing white matter (NAWM), suggesting their early contribution to lesion development (193, 194). This finding was supported by the observation of astrocytes in forming lesions before a significant immune cell infiltration occurred (195-197). Moreover, a recent study suggested that astrocytes could be an early contributor of lesion formation based on the observation of myelin debris uptake by astrocytes at the edge of active demyelinating MS lesions.

Investigators reported that myelin phagocytosis induced astrocytic nuclear factor kappa B (NF-κB) signalling and the secretion of immune cell-recruiting chemokines (194). Once reactive, astrocytes express cell adhesion molecules and secrete pro-inflammatory cytokines and chemokines associated to BBB breakdown, microglia activation as well as monocyte and lymphocyte recruitment into the parenchyma, which perpetuates CNS inflammation (19, 21). When chronic compartmentalized CNS inflammation occurs, reactive astrogliosis evolves from mild to moderate, and unless resolved, from moderate to severe, which ends up with the formation of a compact astrocyte scar-border (187, 190, 191). Despite years of a negative view of reactive astrogliosis as a pathogenic process that uniquely causes injury, astrocyte scar formation is now known to act as a functional barrier that isolate damaged, inflamed, and fibrotic tissue from surrounding viable neural tissue. Loss-of-function studies based on transgenic technology in EAE model allowed the unexpected demonstration of the essential function in the restriction of cytotoxic inflammation by reactive astrocytes (198-201). There, proliferative hypertrophic astrocytes display both contact-dependent and secretion-mediated mechanisms that limit lesion development and restrict the spread and persistent entry of inflammatory cells into the lesion site (187). In this line, several studies using transgenic models of reactive astrogliosis ablation or attenuation in EAE resulted in increased lesion size, neuronal loss, demyelination, and exacerbated disease severity (198-204). Compelling evidence has been reported relating to the beneficial effects of reactive astrogliosis scar formation, including: (i) BBB repair after traumatic injury is critically dependent on the presence of proliferating scar-forming astrocytes (198, 199); (ii) astrocyte-secreted Sonic hedgehog (SHH) promotes BBB repair (205, 206); (iii) astrocyte-derived apolipoprotein E (APOE) facilitates the maintenance of BBB integrity and protects against neuroinflammation (207); (iv) interleukin-6 receptor subunit beta (gp130)-Janus kinase 2 (JAK2)-signal transducer and activator of transcription 3 (STAT3) signalling in astrocytes is a crucial protective pathway that induce anti-inflammatory responses through the formation of astrocyte scar-border (208); (v) astrocyte secretion of TGF-β in response to IL-10 attenuates microglia activation *in vitro* (209) and induces resolution of inflammation in CNS neuroinflammation models

(210, 211); and (vi) astrocyte scar formation aids axon regeneration through the up-regulation of growth supportive molecules such as chondroitin sulfate groteoglycan (CSPG)-4, CSPG5 and laminins (212).

Astrocyte interactions with microglia

Astrocytes and microglia, as so their interactions, have extensively shown to modulate CNS physiology in homeostasis and disease (reviewed in (213-215)). Astrocyte-microglia communication through the release of multiple cytokines and inflammatory mediators modulates CNS inflammation. Several studies have reported that activated microglia controls astrocyte reactivity: (i) LPS-activated microglia by the secretion of IL-1α, TNF-α and C1q induced a neurotoxic phenotype in reactive astrocytes characterized by phagocytic activity and lack of neurotrophic support (216); (ii) aryl hydrocarbon receptor (AHR) signalling in microglia modulated the transcriptional program of astrocytes; microglial VEGF-B enhanced NF-κB signalling and astrocytes, worsening EAE; and microglial TGF-β induced the production of neuroprotective factors and limited EAE progression (217); (iii) microglia-secreted TNF-α induced astrocytic glutamate release which promoted neuron excitotoxicity (218); (iv) microglia-derived IL-10 induced astrocyte production of TGF-β, which in turn up-regulated the expression of anti-inflammatory genes in microglia (209); (v) astrocyte-derived GM-CSF is a known inducer of microglial activation involved in multiple pro-inflammatory processes essential for EAE development (204, 219-221); (vi) astrocyte production of IL-6 was involved in increased activation of microglia ; and (vii) IL-33 secreted by astrocytes modulated microglia synapse engulfment (181, 222).

Astrocyte interactions with neurons

As previously described, astrocytes are essential to the proper functioning of neuronal activity. Therefore, it is not surprising that astrocyte-neuron interactions are critical for the pathogenesis of many neurodegenerative diseases (reviewed in (223)). Multiple studies have described neurotoxic capabilities of reactive astrocytes in different contexts of CNS inflammation: (i) NF-κB signalling in reactive astrocytes

triggers the production of NO, which in excess is neurotoxic (224); (ii) increased levels of brain-derived neurotrophic factor (BDFN) and the up-regulation of its receptor (tropomyosin-related kinase B – TrkB) in reactive astrocytes resulted in NO-mediated neurotoxicity *in vitro*; also, astrocyte-specific ablation of TrkB reduced neurodegeneration and ameliorated EAE (225); (iii) dysregulation of neurotransmitter uptake and release in astrocytes can promote neuronal death (218, 226); and (iv) alterations in the metabolic support of astrocytes to neurons induce neurodegeneration (227).

Astrocyte interactions with oligodendrocytes

Oligodendrocytes express a wide variety of receptors that respond to stimuli secreted by astrocytes and vice versa (228, 229). Despite the precise mechanisms underlying astrocyte-oligodendrocyte interactions are largely uncovered, several studies have reported opposing outcomes: (i) reactive astrocytes promote oligodendrocyte apoptosis via TNF-α (230, 231), Fas ligand (232) and glutamate (218); (ii) the secretion of C–X–C motif chemokine 1 (CXCL1), IL-8 and C-C motif chemokine 2 (CCL2) induce the recruitment of OPCs to sites of inflammation (228, 229); (iii) astrocyte-derived ciliary neurotrophic factor (CNTF) promotes the differentiation of OPCs into mature myelinating oligodendrocytes, which has been associated to increased remyelinated areas (67); and (iv) oligodendrocyte secretion of IL-1β, CCL2, IL-17, and IL-6 induces NF-κB signalling in astrocytes which promotes pro-inflammatory responses (229, 233) .

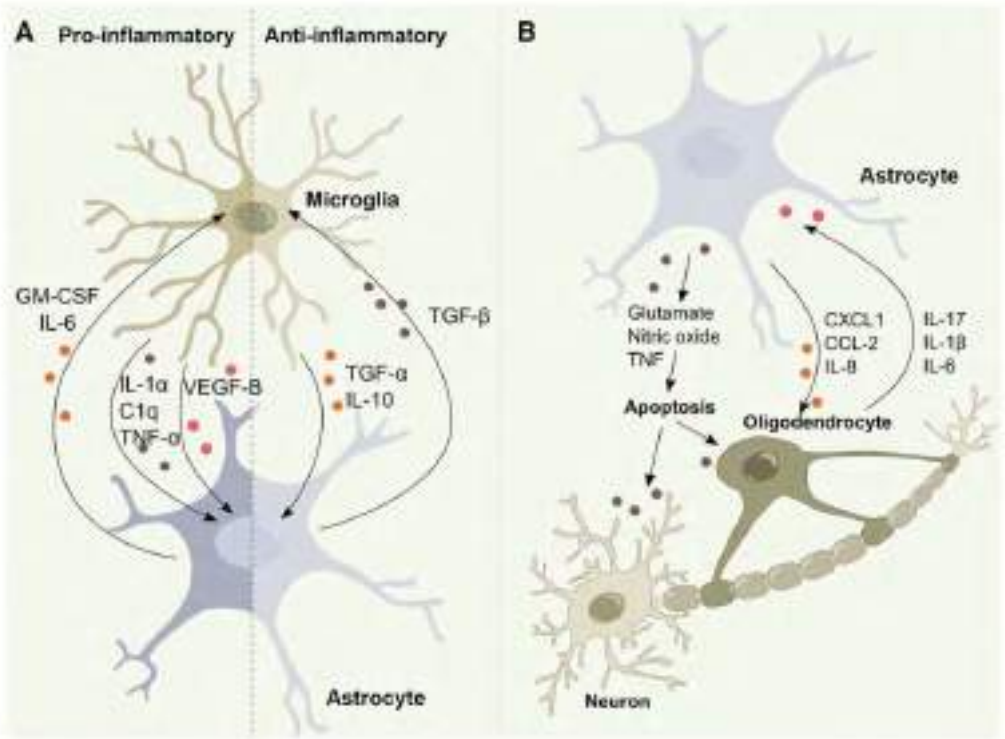

Figure 7. Astrocytes interactions with other CNS-resident cells in neuroinflammation. (A) Interactions between astrocytes and microglia promote their activation and regulate their responses in CNS inflammation. (B) Reactive astrocytes release neurotoxic factors that lead to neuronal and oligodendrocyte damage. Also, astrocytes secrete factors that attract oligodendrocyte, and respond to oligodendrocyte-secreted pro-inflammatory cytokines. Abbreviations: GM-CSF: granulocyte-macrophage colony-stimulating factor; IL: interleukin; C: complement component; TNF-α: tumour necrosis factor α; VEGF-B: vascular endothelial growth factor; TGF: transforming growth factor; CXCL: C–X–C motif chemokine; CCL: C-C motif chemokine. Illustration from: Linnerbauer M, Wheeler MA, Quintana FJ. Astrocyte crosstalk in CNS inflammation. Neuron. 2020; 108(4):608-622.

Hypotheses and objectives

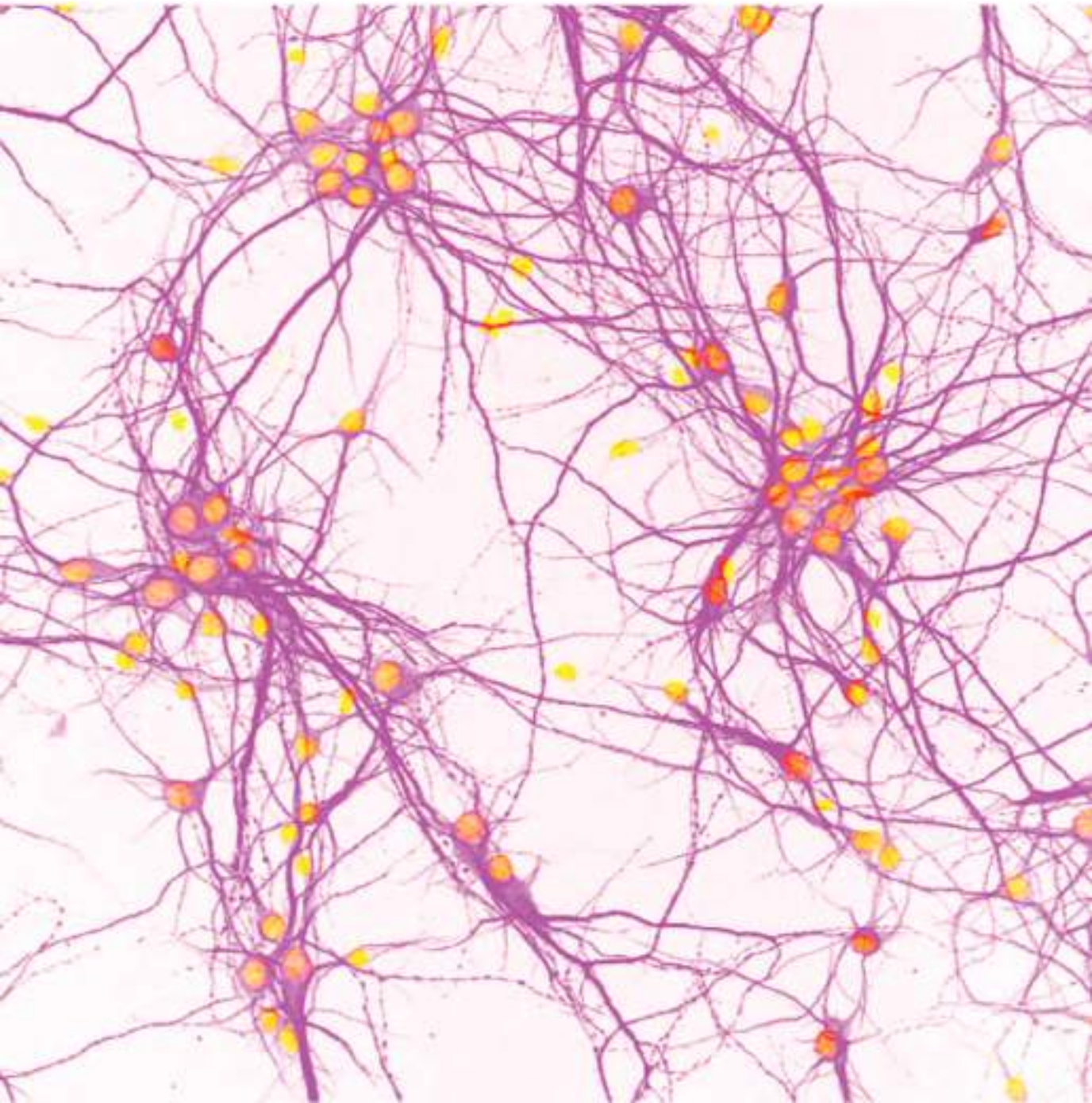

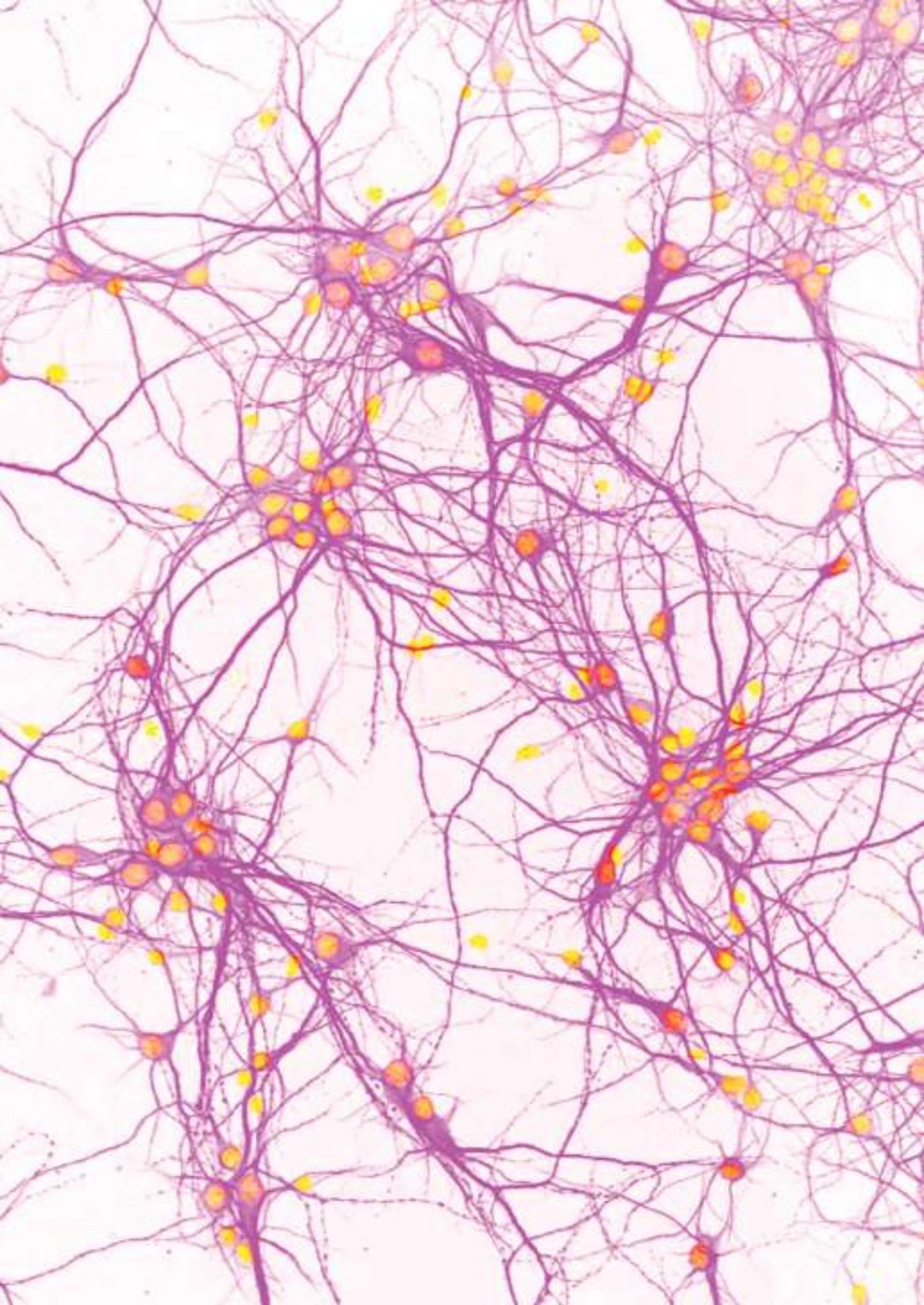

Astrocytes have emerged as key contributors to the pathogenesis of MS. Compelling evidence has reported both beneficial and detrimental effects driven by reactive astrocytes in CNS inflammation. Despite decades of extensive research in the field, the mechanisms underlying maladaptive astrocytic responses in a context of neuroinflammation are still largely unknown. Consequently, there are no therapies designed to specifically target reactive astrocyte signalling or astrocyte-derived mediators.

We were interested in deciphering the mechanisms involved in astrocyte reactivity in a context of MS-specific inflammatory microenvironment. The present study pursues the identification of the reactive astrocyte signalling that triggers the neuronal damage associated to the neurodegenerative component observed in MS.

2. Hypotheses and objectives

2.1. Hypotheses

Astrocytes are actively involved in the neurodegenerative process of MS by secreting soluble factors. The investigation of reactive astrocyte neurotoxic signatures will contribute to the identification of potential therapeutic targets that modulate maladaptive astrocyte responses and could ultimately aid to prevent neurodegeneration in MS. Since the CSF is the closest body fluid to the CNS that can be examined, we believe the CSF will reliably reflect the pathological microenvironment occurring in the CNS of MS patients and will be responsible for the astrocyte reactivity occurring in the disease.

2.2. Objectives

The **general objective** is to dissect how inflammation in MS induces astrocyte reactivity, modulates astrocyte function, and leads to neuronal damage.

To this end, we propose the following **specific objectives**:

1. To induce astrocyte reactivity through the exposure of mouse primary astrocytes to the CSF from MS patients with different degrees of inflammatory activity.

2. To evaluate the effect of CSF-exposed astrocyte secretomes on neuronal branching and synaptic plasticity.

3. To carry out a molecular characterization of reactive astrocytes, secretomes, and CSF from MS patients with different degrees of inflammatory activity using omics technology.

Methods

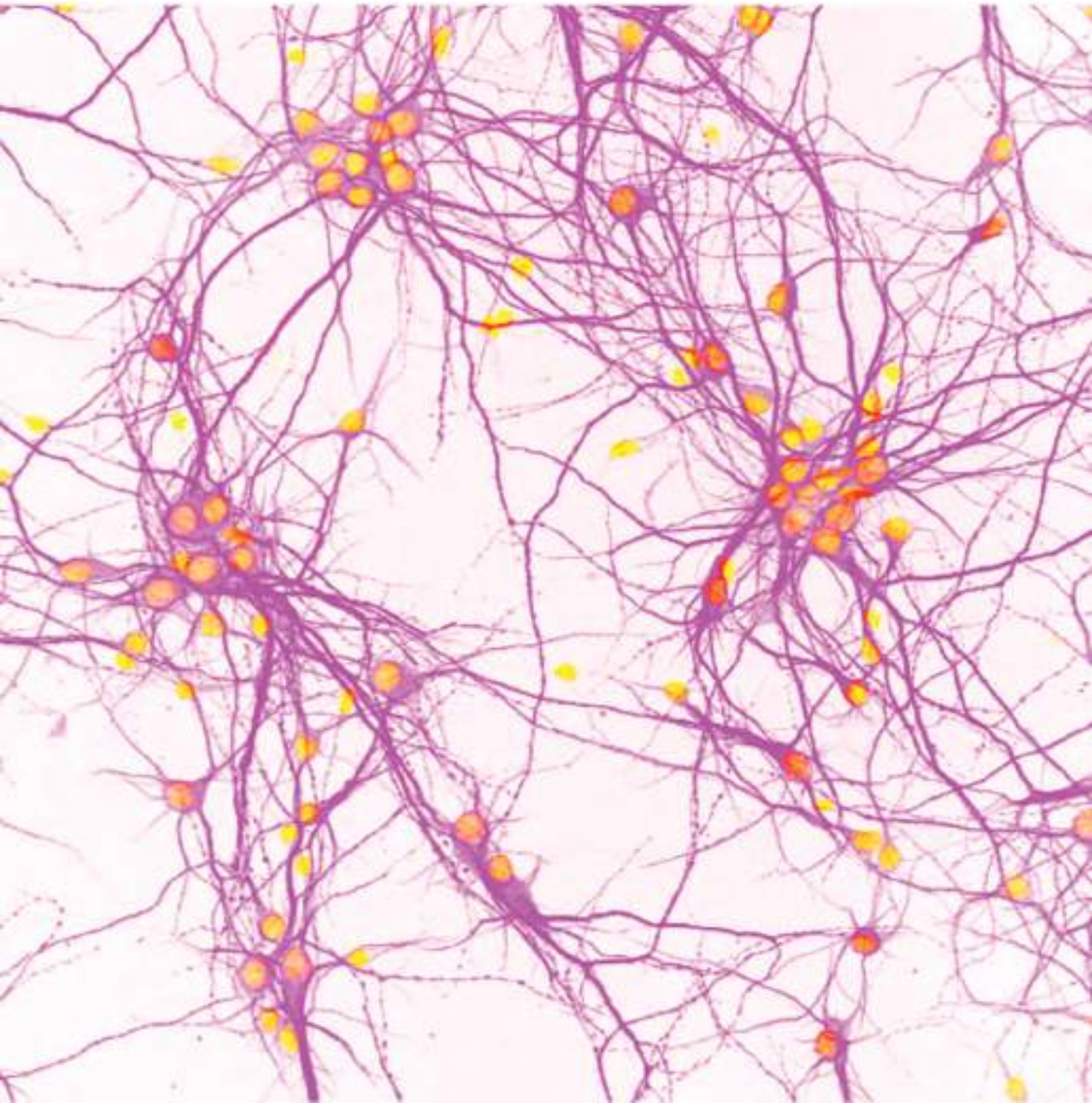

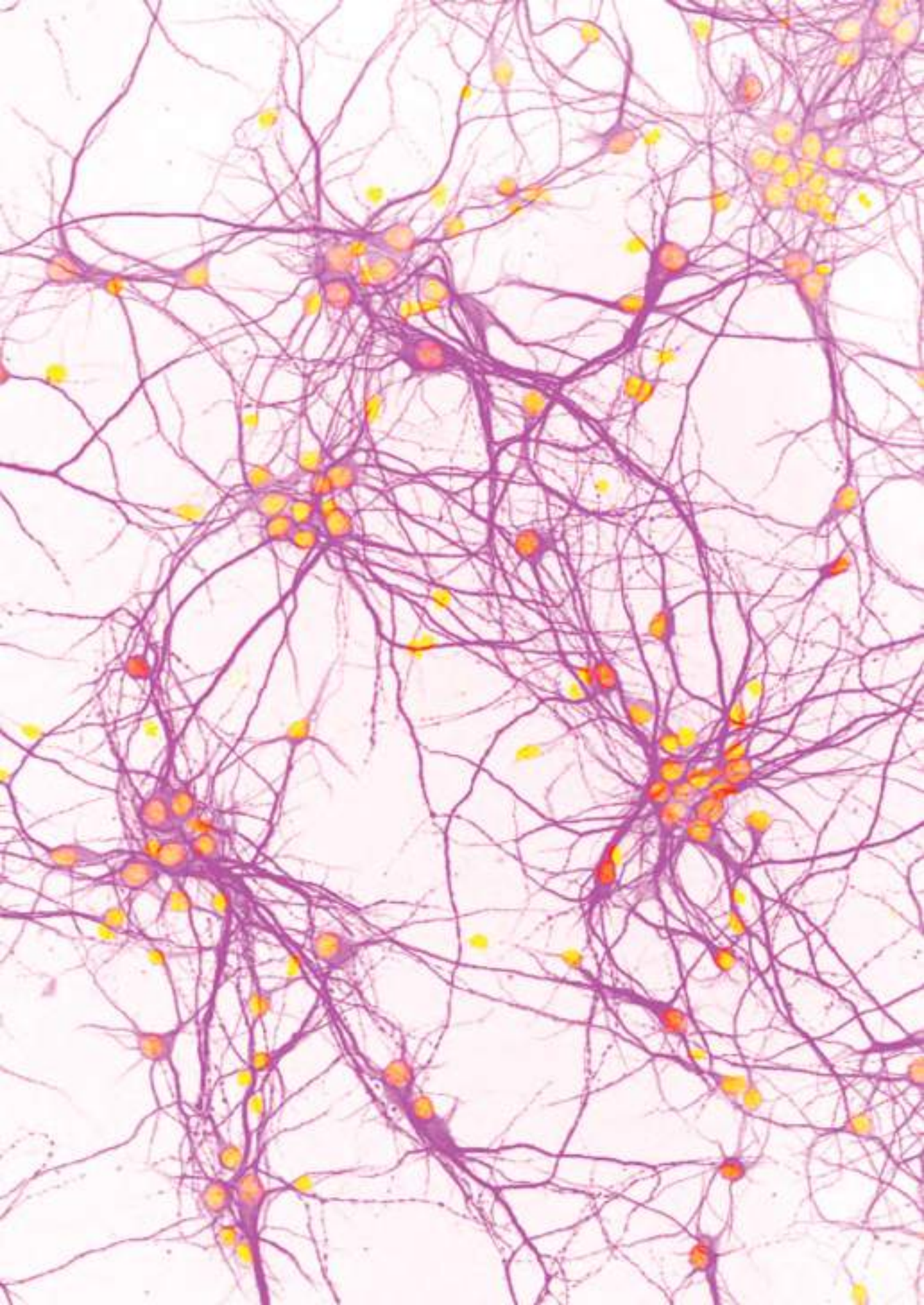

3. Methods

3.1. Mice

C57BL6/J 6–10-week-old pregnant mice, E17 C57BL6/J mouse embryos and P0-2 postnatal C57BL6/J mouse pups purchased from Charles River Laboratories (Saint Germain Nuelles, France) were used for primary cultures. All procedures were conducted in strict accordance with the guidelines established by the Ethical Committee for the Use of Laboratory Animals in Spain (Real Decreto 53/2013; Generalitat de Catalunya Decret 214/97) and the European Ethical Committee (Directive 2010/63/UE). The Ethics Committee on Animal Experimentation of the Vall d'Hebron Research Institute approved all experimental procedures described in this study (protocol number: 10/16 CEEA).

3.2. Mouse primary cultures

3.2.1. Astrocyte cultures

Primary mixed glial cultures were prepared from P0-2 cortices of C57BL6/J mouse pups. Mice were decapitated and brains were immediately dissected out. Meninges, choroid plexus, and hippocampus were removed, and the cerebral cortices were transferred into plates with warm HBSS without Mg^{+2} and Ca^{+2} (Gibco™, Carlsbad, CA, USA). Next, cortices were enzymatically and mechanically disrupted in the presence of papain (Worthington Biochemical Corporation, Lakewood, NJ, USA) and DNase I at 0.1 mg/ml (Sigma-Aldrich, St. Louis, MA, USA) for 10 min at 37ºC. Cell suspensions were filtered through a 70-µm nylon cell strainer, centrifuged at 500 x g for 5 min and resuspended in Advanced DMEM (Gibco™) supplemented with 10% of fetal bovine serum (FBS, Sigma), 20U/ml penicillin and 20µg/ml streptomycin (Gibco™). Cells were plated on coverslips precoated with 0.1 mg/ml poly-D-lysine (PDL) (Sigma-Aldrich) in 24-well plates and seeded at 25,000 cells/cm^2. Cultures were maintained at 37ºC in a humidified atmosphere containing 5% CO_2, and the medium was changed every 3 days.

3.2.2. Purification of astrocyte cultures

With the purpose of obtaining pure astrocyte primary cultures and eliminate microglia cells from mixed glial cultures, we tested two different methods of purification.

Shaking

We first tried classical shaking method (adapted from (234)) in order to eliminate microglia from mixed glial cultures. For shaking purification primary mixed glial cultures, obtained as detailed above, were plated on T-75 flask precoated with 0.05 mg/ml PDL (Sigma-Aldrich) and seeded at 60,000 cells/cm^2. When cultures reached 80-90% confluency, normally after 7-10 DIV, we shaked them for 15h at 200 rpm and the last 1h at 250 rpm. After shaking, cells were washed, trypsinized and plated on coverslips precoated with 0.1 mg/ml PDL (Sigma-Aldrich) in 24-well plates and seeded at 37,500 cells/cm^2. Cells were maintained at 37ºC in a humidified atmosphere containing 5% CO_2, and the medium was changed every 3 days. Cultures were used for characterization when reached 70% confluency, after 2-3 DIV.

Magnetic cell sorting (MACS)

Magnetic cell isolation purification of mixed glial cultures was performed using an approach based on MACS® Technology. The purification strategy was based on a negative selection of the cells of interest, isolating microglia by means of a positive selection with MicroBeads conjugated to specific antibodies for CD11b (Miltenyi Biotech, Bergisch Gladbach, Germany). This sorting strategy allowed us to purify astrocytes avoiding their manipulation and that of their surface antigens. The cell separation protocol was carried out at the time of culture generation, as detailed below.

Purified primary astrocyte cultures were prepared from P0-2 cortices of C57BL6/J mouse pups. Cell suspensions obtained as detailed before were filtered through a 70-µm nylon cell strainer, centrifuged at 500 x g for 5 min, stained by Trypan Blue exclusion and counted in a Neubauer chamber. Following the manufacturer's

instructions, 10^7 cells were resuspended in 90 µl of separation buffer and 10 µl of CD11b MicroBeads (MicroBeads conjugated to monoclonal rat anti-mouse CD11b antibody, Miltenyi Biotech). MicroBeads were incubated for 15 min at 4ºC to bind specifically to cells expressing CD11b (microglia). After washing and centrifuging, cells were resuspended in separation buffer and flowed through a MS cell separator column (Miltenyi Biotech) fitted into a MidiMACS™ cell separator (Miltenyi Biotech). The eluted volume, corresponding to the negative fraction not bound to the MicroBeads, was collected. Finally, the cell suspension of interest was centrifuged at 500 x g for 5 min and resuspended in Advanced DMEM (Gibco™) supplemented with 10% FBS (Sigma-Aldrich), 20U/ml penicillin and 20µg/ml streptomycin (Gibco™). Astrocytes were plated on coverslips precoated with 0.1 mg/ml PDL (Sigma-Aldrich) in 24-well plates or 12-well plates precoated with 0.1 mg/ml PDL (Sigma-Aldrich), seeded at 25,000 cells/cm^2. Cultures were maintained at 37ºC in a humidified atmosphere containing 5% CO_2, and the medium was changed every 3 days.

3.2.3. Primary neuronal cultures

Primary neuronal cultures were prepared from E17 cortices of C57BL6/J mouse embryos. Isolated brains were placed in warm Neurobasal medium (Gibco™) and cortices were transferred into Falcon tubes containing warm Neurobasal medium supplemented with 2% B27 supplement, 1% GlutaMAX, 20U/ml penicillin and 20µg/ml streptomycin (all from Gibco™). Cortices were gently dissociated with a fire-polished glass Pasteur pipettes and neuronal cell suspensions were plated on coverslips precoated with 0.1 mg/ml PDL (Sigma-Aldrich) in 24-well plates. Neurons were seeded at 40,000 cells/cm^2 with supplemented Neurobasal medium, grown in serum-free conditions. Cultures were maintained at 37ºC in 5% CO_2 and the medium was partially changed at 11 days *in vitro* (DIV) with fresh supplemented Neurobasal medium.

3.3. Characterization of primary cultures

Primary mouse cultures were characterized by immunofluorescence staining in order to determine the presence of different cell types and thus assess the purity of

each culture. Mixed glial cultures were characterized at 10 DIV, shaking-purified cultures at 13 DIV, MACS-purified cultures at 7 DIV, and neuronal cultures at 18 DIV.

Cells were washed twice with PBS and fixed in cold 4% paraformaldehyde for 20 min at room temperature, permeabilized in 0.1% Triton X-100 in PBS for 15 min and blocked with 5% Normal Goat Serum (NGS, Millipore, Burlington, Massachusetts, USA) in PBS for 1h in gentle shaking. Then, cells were incubated with primary antibodies (**Table 1**) diluted in PBS with 1% NGS at 4ºC overnight. After washing, cells were incubated with the corresponding fluorescent secondary antibodies goat anti-rabbit Alexa Fluor-488 (Invitrogen, Carlsbad, CA, USA) and goat anti-mouse Alexa Fluor-594 (Invitrogen), in the blocking solution for 1h at room temperature with gentle shaking. Finally, cell nuclei were stained with DAPI (4',6-diamidino-2-phenylindole, Sigma-Aldrich) and coverslips were mounted with Fluoromount-G (Invitrogen).

Table 1. Primary antibodies used for culture characterization immunofluorescences.

Primary antibody	Dilution	Target
Rabbit polyclonal anti-GFAP	1:500	Astrocytes
Mouse monoclonal anti-GFAP	1:500	Astrocytes
Rabbit polyclonal anti-Iba1	1:500	Microglia
Mouse monoclonal anti-NeuN	1:500	Neurons
Mouse monoclonal anti-MAP2	1:500	Neurons
Rabbit polyclonal anti-GalC	1:500	Oligodendrocytes

Cell markers used to identify different cell populations in cell cultures. Abbreviations: GFAP: anti-glial fibrillary protein; Iba1: ionized calcium-binding adaptor molecule 1; NeuN: neuronal nuclear antigen; MAP2: microtubule-associated protein 2; GalC: galactocerebrosidase.

Images were acquired using a Leica DFC550 fluorescence microscope (Leica Microsystems, Wetzlar, Germany) and LAS V4.5 visualization software (Leica Microsystems) with a x20 objective. Alternatively, neuronal cultures images were acquired using a Zeiss LSM980 confocal microscope (ZEISS, Oberkochen,

Germany) and ZEN visualization software (ZEISS) with a x25 objective and a 0.8 digital zoom.

Randomized fields were imaged and counted using FIJI-ImageJ (NIH, Wayne Rasband, USA). Astrocytes were labelled with anti-glial fibrillary acidic protein (GFAP); microglia by ionized calcium-binding adaptor molecule 1 (Iba1); neurons by neuronal nuclear antigen (NeuN) and microtubule-associated protein 2 (MAP2); and oligodendroglial lineage by galactocerebrosidase (GalC). The quantification of the presence of each cell type in cultures was expressed as the percentage of the mean total number of $GFAP^+$ (astrocytes), $Iba1^+$ (micrglia), $NeuN^+$ or $MAP2^+$ (neurons), and $GalC^+$ (oligodendrocytes) cells respect to the number of total cells ($DAPI^+$). For each cell culture, five random fields for cell marker were imaged and quantified in duplicate, and a total of 3 independent cultures were characterized. Antibody references are detailed in the **Annex 2 (Table A1)**.

3.4. Astrocyte exposure to CSF from MS patients

3.4.1. Patients and samples

Inclusion criteria

MS patients

MS patients fulfilling the 2017 McDonald criteria (107) were classified into high and low inflammatory activity phenotypes at the time of the first demyelinating event. Patients with high inflammatory activity (MS-High, N=13) were characterized by: (i) the presence of moderate-high lesion load (>50 T2 lesions) and at least 5 T1 contrast enhancing lesions in the brain baseline MRI; (ii) an EDSS of ≥4.0 in less than 10 years after the first demyelinating event; and (iii) positive CSF IgG OCB. Patients with low inflammatory activity (MS-Low, N=9) were characterized by: (i) the presence of minimal lesion load (≤9 T2 lesions) and without T1 contrast enhancing lesions in the brain baseline MRI; (ii) an EDSS of ≤3.0 after a follow-up longer than 10 years from the first demyelinating event; and (iii) positive CSF IgG OCB.

Controls

Patients with headache in whom an inflammatory condition was ruled out (normal brain MRI, normal CSF biochemistry, and negative CSF IgG oligoclonal bands) were also included as non-inflammatory neurological disease controls for comparison purposes (NINC, N=9). Two independent cohorts of MS-High patients, screening, and validation were recruited, the latter including also MS-Low patients and non-inflammatory controls.

Patients and controls were recruited both at the Centre d'Esclerosi Múltiple de Catalunya (Cemcat, Barcelona) and the Hospital Ramón y Cajal (Madrid). The study was approved by the corresponding Hospital Ethics Committees, and all patients gave their informed consent.

CSF sampling

CSF samples were collected by lumbar puncture for diagnosis purpose, centrifuged to remove cells, and stored frozen at -80ºC until used. None of the patients included were receiving corticosteroid treatment at the time of CSF collection. Due to the large volume required for the CSF stimulation experiments, we generated CSF pools from each of group of patients. For the screening cohort we created 2 pools, each pool containing CSF samples from 2 different patients. For the validation cohort, we generated 3 pools, each pool containing CSF samples from 3 different patients. **Table 2** summarizes the pool-based demographic data from patients included in the study.

Table 2. Demographic data of the MS patients and controls included in the study.

	Age (years)	Female/male (% females)
Screening cohort		
MS-High	**25.6 (4.0)**	**4/0 (100.0)**
Pool-1	22.0 (2.3)	2/0 (100.0)
Pool-2	29.1 (8.0)	2/0 (100.0)
Validation cohort		
MS-High	**29.3 (2.0)**	**7/2 (77.8)**
Pool-1	24.7 (2.7)	2/1 (66.7)
Pool-2	27.3 (2.6)	2/1 (66.7)
Pool-3	36.0 (1.1)	3/0 (100.0)
MS-Low	**35.4 (2.6)**	**6/3 (66.7)**
Pool-1	43.3 (4.9)	2/1 (66.7)
Pool-2	34.0 (2.6)	2/1 (66.7)
Pool-3	29.0 (1.0)	2/1 (66.7)
NINC	**42.0 (3.9)**	**8/1 (88.9)**
Pool-1	30.0 (6.0)	3/0 (100.0)
Pool-2	52.0 (4.0)	3/0 (100.0)
Pool-3	44.0 (2.6)	2/1 (66.7)

Age is expressed as mean (standard error of the mean, SEM). Numbers in bold represent the mean values of all the pools included in each group of patients and controls. Abbreviations: MS-High: high inflammatory multiple sclerosis; MS-Low: low inflammatory multiple sclerosis; NINC: non-inflammatory neurological controls.

3.4.2. CSF stimulation and secretome generation

Astrocyte exposure to CSF samples from MS patients and controls were carried out in MACS-purified astrocyte primary cultures at 7 DIV. First, cultures were deprived from FBS for 24h and extensively washed with non-supplemented medium (Advanced DMEM, Gibco™). Then, astrocytes were exposed to medium (Basal) or CSF pools from each group of patients at 50% in non-supplemented media for 6 and 12h. After extensively washing to completely remove the remaining CSF, fresh Neurobasal medium (non-supplemented, Gibco™) was added and secretomes were

collected after 12 and 18h. Finally, secretomes were centrifuged (1500rpm, 5 min) to discard cellular debris, aliquoted and stored at -80ºC until used for experiments. Astrocyte cultures were returned to the incubator in non-supplemented Advanced DMEM medium (Gibco™) until used for following procedures.

For screening experiments, 2 independent astrocyte cultures were stimulated, generating a unique secretome pool per condition. For validation experiments, 3 independent cultures were stimulated, generating a total of 3 different secretome pools per condition.

In addition, in order to evaluate an accurate astrocytic stimulation, extra wells of astrocytes stimulated with a combination of IL-1β and TNF-α at 20 ng/ml each (PeproTech, Rocky Hill, NJ, USA) were included as positive control of stimulation and were manipulated under the same experimental conditions.

3.5. Functional study of the effects of astrocyte secretomes on neurons

The effects of secretomes derived from pre-exposed astrocytes to CSF from patients and controls were assessed on mouse primary cortical neurons at 18 DIV. Secretomes were previously supplemented with 2% B27 supplement (Gibco), 1% GlutaMAX (100X) (Gibco), 2U/ml penicillin and 2µg/ml streptomycin (Gibco). Then, neurons were treated for 3 DIV with medium (-) or secretomes derived from non-stimulated astrocytes (Basal) or pre-exposed to CSF from each group of patients.

3.5.1. Effects on neuronal morphology

The effects on neuronal morphology were evaluated by immunofluorescence and neurons were stained with chicken polyclonal MAP2 (1:5000, Abcam, Cambridge, UK), goat anti-chicken Alexa Fluor-647 (Invitrogen) and DAPI (Sigma-Aldrich). The immunofluorescence protocol is detailed in section 3.1 and antibody references in the **Annex 2 (Table A1)**.

Images were acquired using a Leica Confocal SP5-II with a x40 oil-immersion objective. Confocal z-stacks were taken at 1,024x1,024 pixel resolution every 2 µm. Conditions such as pinhole size (1 AU) and frame averaging (four frames per z-step)

were held constant throughout the study. An automated acquisition of 5 randomized fields per replicate using the multiposition mode was performed. For each experiment, two replicates per condition were analyzed from two-three independent experiments.

Automated quantification of branching and dendrite length was performed in DAPI and MAP2 max z-projection images processed using a custom-made pipeline in Cell Profiler v4 software (Cambridge, Massachusetts, USA) as previously reported (235). All images were background corrected to enhance the neuronal body applying a threshold module. The intensity of the threshold determined whether each pixel was treated as a region of interest or background. Nuclei were detected from the DAPI channel with the "IdentifyPrimaryObjects" module. An adaptive threshold mask was set to obtain MAP2-positive staining. After filtering for nuclei inside the MAP2 mask, "IdentifySecondaryObjects" with nuclei as seed and a watershed gradient through the MAP2 mask was used to define neuronal soma and dendrites. The "MorphologicalSkeleton" and "MeasureSkeleton" modules were then applied to obtain measurements of the number of trunks and branches for each neuron per image. Also, the skeletonized images were used to measure the dendritic trunks that have their origin in the neuronal soma and the branches along the dendrites per cell per image.

3.5.2. Effects on synaptic plasticity

The effects of astrocytic secretomes on synaptic plasticity were assessed by immunofluorescence and neurons were stained with chicken polyclonal MAP2 (1:5000, Abcam), mouse monoclonal PSD-95 (1:250, Abcam), rabbit monoclonal Synaptophysin (1:500, Abcam), and DAPI (Sigma-Aldrich). The corresponding fluorescent secondary antibodies used were goat anti-chicken Alexa Fluor-647, goat anti-mouse Alexa Fluor-568, and goat anti-rabbit Alexa Fluor-488 (1:500, Invitrogen). The immunofluorescence protocol is detailed in section 3.1 and antibody references in the **Annex 2 (Table A1)**.

Neurons were imaged using a Leica Confocal SP5-II with a x63 oil-immersion objective and a digital zoom of 4. Confocal z-stacks were taken at 1,024x1,024 pixel resolution every 0.5 µm. Conditions such as pinhole size (1 AU) and frame averaging (four frames per z-step) were held constant throughout the study. An automated acquisition of 10 randomized fields per replica using the multiposition mode was performed. Each position corresponded to a single neuron (n=10 neurons per replica) and contained 1-3 secondary dendrites thereof. The number of dendrites analyzed was >20 dendrites for replicate. For each experiment, two replicates per condition were analyzed from two-three independent experiments.

Images obtained were analyzed using FIJI-ImageJ (NIH) and a custom-programmed macro (Advanced Optic Microscopy Unit, Hospital Clínic-CCITUB, Barcelona, Spain) designed to automatically analyze all images from experiments. Dendrite regions of interest were determined after intensity thresholding, binarization and filtering strategies to exclude small segments. Dendrite volume from each section was obtained by the product of dendrite area by voxel depth, and total dendrite volume per image was obtained by the addition of all the dendrite volumes from all sections. The number of positive PSD-95, Synaptophysin and PSD-95/Synaptophysin puncta was counted per dendrite volume (MAP2 staining). PSD-95/Synaptophysin colocalization puncta was quantified using the Colocalization Highlighter Plugin (Pierre Bourdoncle, Institut Jacques Monod, Service Imagerie, Paris, France). Two points were considered to colocalize when: (i) their respective fluorescence intensities were strictly higher than the threshold of their channels (determined by the automatic Triangle threshold); and (ii) their fluorescence intensity ratio was strictly higher than the ratio setting value (50% of a 0-100% ratio).

3.6. Molecular characterization of astrocyte signature

A comprehensive molecular characterization of the astrocyte reactive signature was performed using omics technologies at 3 different levels: (i) CSF-stimulated astrocytic secretomes (proteome array); (ii) Basal and CSF-stimulated astrocytes

(transcriptomic and proteomic analyses); and (iii) CSF from MS patients and controls (proteomic analysis).

3.6.1. Secretome characterization

Proteome Profiler Array

Secretome samples from astrocytes exposed to CSF from MS patients and controls were assessed using a proteome profiler array: Mouse XL Cytokine Array Kit (ARY028; R&D Systems, UK), which detects 111 mouse proteins simultaneously. Protein detection was performed using a streptavidin-HRP and chemiluminescent system, revealed with CP-BU (AGFA, Mortsel, Belgium) films, which produce a signal at each capture spot corresponding to the amount of protein bound. Pixel intensities on developed films from each spot were collected using a transmission-mode scanner and analyzed with FIJI-ImageJ (NIH). An average signal of pixel density was determined of the pair of duplicate spots representing each analyte and averaged background were subtracted. Relative changes per analyte were obtained comparing MS-High samples to MS-Low and NINC.

A total of 3 different secretome pools from each condition (MS-High, MS-Low and NINC) were analyzed (n=3 biological replicates, from 3 different stimulated astrocyte cultures). Secretome samples from different exposure conditions generated in the same astrocyte culture were assessed simultaneously with the proteome array in order to minimize the variability.

SerpinE1 validation by ELISA

Protein levels of Serpin E1/PAI-1 were validated by ELISA (DY3828, R&D Systems). Non-diluted secretome samples were measured in duplicate, following the indications provided by the manufacturers. The intra-assay coefficient of variation was 8.9%. A total of 3 different secretome pools from each condition (Basal, NINC, MS-Low and MS-High) were analyzed (n=3 biological replicates, from 3 different stimulated astrocyte cultures).

3.6.2. Transcriptomic study

After collecting secretomes, non-stimulated (Basal) and CSF pre-exposed astrocyte cultures were trypsinized for cell pellet collection and stored at -80ºC until used. Total RNA was isolated from Basal and CSF pre-exposed astrocyte pellets using the RNeasy Mini Kit (Qiagen, Hilden, Germany) with on-column DNase digestion (Qiagen) in order to remove any genomic DNA trace according to the manufacturer's instructions. RNA quality was analyzed by capillary electrophoresis (Bioanalyzer 2100, Agilent Technologies, Santa Clara, CA, USA). All samples included in the study had RIN values >9.5 (range 9.5-10) and rRNA ratio (28s/18s) >1.7 (range 1.7-2.1). Then, sense ssDNA suitable for labelling was generated from total RNA with the GeneChip WT Plus Reagent Kit (Affymetrix, UK), fragmented, labelled, and hybridized to the arrays with the GeneChip WT Terminal Labelling and Hybridization Kit (Affymetrix, UK). Subsequently, Clariom S Pico Assay HT mouse arrays were scanned according to the manufacturer's instructions in a GeneTitan™ Multi-Channel instrument (Affymetrix, UK).

Different types of quality controls were performed to confirm that all arrays were suitable for normalisation and then, that were appropriated for differentially expression analysis. Because batch (pool) effects were detected, batch factor was included in the linear model used for differential expression analysis. In order to increase statistical power and reduce unnecessary noise, those genes whose standard deviation was below the 65 percentile of all standard deviations were removed. Finally, a list of 7,104 genes were included in the analysis. A linear model with empirical Bayes moderation of the variance (236) adjusted by pool effect was used to identify differentially expressed genes between non-stimulated (Basal) and CSF pre-exposed astrocytes. P-values were adjusted to obtain a strong control over the false discovery rate (FDR) using the Benjamini-Hochberg method. Genes with adjusted p-values <0.05 were considered significantly differentially expressed.

3.6.3. Proteomic study

Astrocyte intracellular protein and CSF pools content were determined using liquid chromatography and mass spectrometry (LC/MS) analysis.

Sample preparation

Pellets from 1-1.25 million astrocytes were resuspended in 6M urea, 200mM ammonium bicarbonate. A total of 3 different pellet samples from each condition obtained from astrocytes exposed to medium (Basal) and CSF pools were analyzed.

Pooled CSF samples (25 µl from each of 3 patients, 75 µl total volume) were precipitated with 6 volumes of cold acetone and the pellet was dissolved in 80 µl of 6M urea, 200mM ammonium bicarbonate. A total of 3 different CSF pool samples from MS patients and controls were analyzed.

Samples (pellets and pooled CSF) were reduced with dithiothreitol (90 nmol, 37 ºC, 60 min) and alkylated in the dark with iodoacetamide (180 nmol, 25 ºC, 30 min). The resulting protein extract was first diluted to 2M urea with 200 mM ammonium bicarbonate for digestion with endoproteinase LysC (1:10 w:w, 37ºC, o/n; #129-02541, Wako, FUJIFILM Wako Pure Chemical Corporation, Osaka, Japan), and then diluted 2-fold with 200 mM ammonium bicarbonate for trypsin digestion (1:10 w:w, 37ºC, 8h; #V5113, Promega, Madison, Wisconsin, USA). After digestion, the peptide mixture was acidified with formic acid and desalted with a MicroSpin C18 column (The Nest Group Inc, Ipswich, Massachusetts, USA) prior to LC-MS/MS analysis.

Chromatographic and mass spectrometric analysis

Samples were analyzed using an LTQ-Orbitrap Fusion Lumos mass spectrometer (Thermo Fisher Scientific, San Jose, CA, USA) coupled to an EASY-nLC 1200 (Proxeon; Thermo Fisher Scientific, Odense, Denmark). Peptides were loaded directly onto the analytical column and were separated by reversed-phase chromatography using a 50 cm column with an inner diameter of 75 µm, packed with 2 µm C18 particles spectrometer (Thermo Scientific, San Jose, CA, USA). Chromatographic gradients started at 95% buffer A and 5% buffer B with a flow rate

of 300 nl/min for 5 minutes and gradually increased to 25% buffer B and 75% A in 79 min and then to 40% buffer B and 60% A in 11 min. After each analysis, the column was washed for 10 min with 10% buffer A and 90% buffer B.

The mass spectrometer was operated in positive ionization mode with nanospray voltage set at 2.4 kV and source temperature at 275ºC. The acquisition was performed in data-dependent acquisition (DDA) mode, and full MS scans with 1 micro scans at resolution of 120,000 were used over a mass range of 350-1400 m/z with detection in the Orbitrap mass analyzer. In each cycle of data-dependent acquisition analysis, following each survey scan, the most intense ions above a threshold ion count of 10,000 were selected for fragmentation. The number of selected precursor ions for fragmentation was determined by the “Top Speed” acquisition algorithm and a dynamic exclusion of 60 seconds. Fragment ion spectra were produced via high-energy collision dissociation (HCD) at normalized collision energy of 28% and they were acquired in the ion trap mass analyzer. AGC was set to 2E4, and an isolation window of 0.7 m/z and a maximum injection times of 12 ms were used.

Digested bovine serum albumin (New England Biolabs, Ipswich, Massachusetts, USA) was analyzed between each sample to avoid sample carryover and to assure stability of the instrument, and QCloud (237) was used to control instrument longitudinal performance during the study.

Mass Spectrometry Data Analysis

Acquired spectra were analyzed using the Proteome Discoverer software suite (v2.0; Thermo Fisher Scientific) and the Mascot search engine (v2.6; Matrix Science (238)). Astrocyte data was searched against Swiss-Prot Mouse database (February 2020), and CSF data against Swiss-Prot Human database (February 2020), plus a list (239) of common contaminants and all the corresponding decoy entries. For peptide identification, a precursor ion mass tolerance of 7 ppm was used for MS1 level, trypsin was chosen as enzyme, and up to three missed cleavages were allowed. The fragment ion mass tolerance was set to 0.5 Da for MS2 spectra. Oxidation of methionine and N-terminal protein acetylation were used as variable

modifications whereas carbamidomethylation on cysteines was set as a fixed modification. FDR for peptide identification was set to a maximum of 5%.

Peptide quantification data were retrieved from the “Precursor ion area detector” node from Proteome Discoverer (v2.0) using 2 ppm mass tolerance for the peptide extracted ion current (XIC). The obtained values were used to calculate protein fold-changes and their corresponding adjusted p-values. Protein changes were considered significant when adjusted p-values were below 0.05.

The raw proteomics data have been deposited to the PRIDE (240) repository with the dataset identifier PXD027152.

3.6.4. Reverse transcription quantitative PCR (RT-qPCR) studies

RNA samples from all conditions and experiments were obtained from resting (Basal) or stimulated astrocyte pellets using the RNeasy Mini Kit (Qiagen) with on-column DNase digestion (Qiagen). For qPCR studies, complementary DNA (cDNA) was synthesized using the High-Capacity cDNA Archive Kit (Applied Biosystems™, Foster City, CA, USA) following the manufacturer’s instructions.

Astrocyte reactivity to CSF exposure in the screening experiments was assessed by lipocalin 2 (*Lcn2*) (Mm01324470_m1), C–X–C motif chemokine 10 (*Cxcl10*) (Mm00445235_m1) and interleukin-6 (*Il6*) (Mm00446190_m1). We also determined *Lcn2* (Mm01324470_m1) expression as positive control of astrocyte stimulation evaluation.

Top differentially expressed genes between MS-High and MS-Low CSF pre-exposed astrocytes obtained in the microarrays study were validated by qPCR using the same RNA samples, and reverse transcribed to cDNA as above-mentioned. All primers and probes were from Applied Biosystems: prostaglandin-endoperoxide synthase 2 (*Ptgs2*) (Mm00478374_m1), FosB proto-oncogene (*Fosb*) (Mm00500401_m1), nuclear receptor subfamily 4 group A member 1 (*Nr4a1*) (Mm01300401_m1), early growth response 2 (*Egr2*) (Mm00456650_m1), Kruppel

like factor 6 (*Klf6*) (Mm00516186_g1), arrestin domain containing 3 (*Arrdc3*) (Mm00626887_m1) and thioredoxin interacting protein (*Txnip*) (Mm00452393_m1).

All qPCR studies were performed using the housekeeping gene glyceraldehyde-3-phosphate dehydrogenase (*Gapdh*, Mm99999915_g1) as well as the TaqMan Gene Expression Master Mix (Applied Biosystems). Assays were run on the ABI PRISM® 7900HT system (Applied Biosystems) and obtained Ct values from all experiments were normalized to the expression of the housekeeping gene (*Gapdh*). The relative level of gene expression was calculated with the $2^{-\Delta\Delta Ct}$ method (241, 242). Results were expressed as fold change (FC) in gene expression in stimulated astrocytes compared to Basal astrocytes, which were used as calibrators. No template control (NTC) samples were included in qPCR studies. Finally, analyses were performed with SDS 2.4 software (Applied Biosystems) and any sample with a quantification cycle value of greater than 35 was considered as non-amplified (243).

3.6.5. Astrocyte stimulation with CHI3L1

Purified astrocyte primary cultures at 7 DIV were deprived from FBS for 24h and stimulated with PBS (Vehicle) or 300 and 600 ng/ml of mouse recombinant CHI3L1 (2649-CH; R&D Systems) for 6h. After extensively washing, Neurobasal medium (non-supplemented, Gibco) was added, and RNA was isolated after 18h as above-mentioned. The potential of CHI3L1 to reproduce the astrocyte gene expression signature obtained from the microarrays study was evaluated by qPCR studies as previously described.

3.6.6. Bioinformatic analysis

The analysis of the biological significance was performed using Metascape (https://metascape.org) (244) to identify overrepresented pathways and ontologies based on annotation databases: the Gene Ontology (GO) and the Kyoto Encyclopedia of Gene and Genomes (KEGG). After mouse-human gene ID harmonization with Metascape's annotation tool, astrocyte-secreted proteins (proteome array), astrocyte differentially expressed genes (microarrays), astrocyte intracellular proteins (LC/MS), and human CSF proteins (LC/MS) compliant with p-

value <0.01 and absolute FC >0.5 were uploaded and analyzed using default settings ("Expression analysis"). The TRRUST database (https://www.grnpedia.org/trrust) (245) was used to identify transcriptional factors regulatory networks. Finally, network diagrams for protein-protein interactions were obtained and graphed through the web portal of the STRING Interactome database (https://string-db.org) with a confidence score cut-off of 400.

3.7. Statistical analysis

Statistical details for each experiment are described in the corresponding figure legends. Statistical analysis was performed using SAS® 9.4 (SAS Institute Inc., Cary, NC, USA), except for microarrays data that were analyzed using R (R version 3.6.1, Copyright© 2018 The R Project for Statistical Computing). Data were analyzed assuming a normal or lognormal distribution according to the residual distributions. For comparisons, least square means were contrasted applying a mixed model approach, where the experimental condition was treated as a fixed factor, and experiment and pool as random factors. Different methods to control the effect of multiple comparisons on the type I error level were used. First, Dunnet's adjustment was used when multiple comparisons were done against a "control" experimental condition. Second, Tukey's adjustment was applied when all pairwise comparisons were of interest. Third, when only several selected comparisons were considered then Bonferroni adjustment was used. Finally, FDR with the Benjamini-Hochberg method was applied when analyzing data from microarrays, LC/MS proteomics and proteome array. P-values<0.05 were considered statistically significant.

Dot-scatter bar graphs used for data representation were performed using GraphPad Prism 8.0 software (GraphPad Software, San Diego, CA, USA).

Results

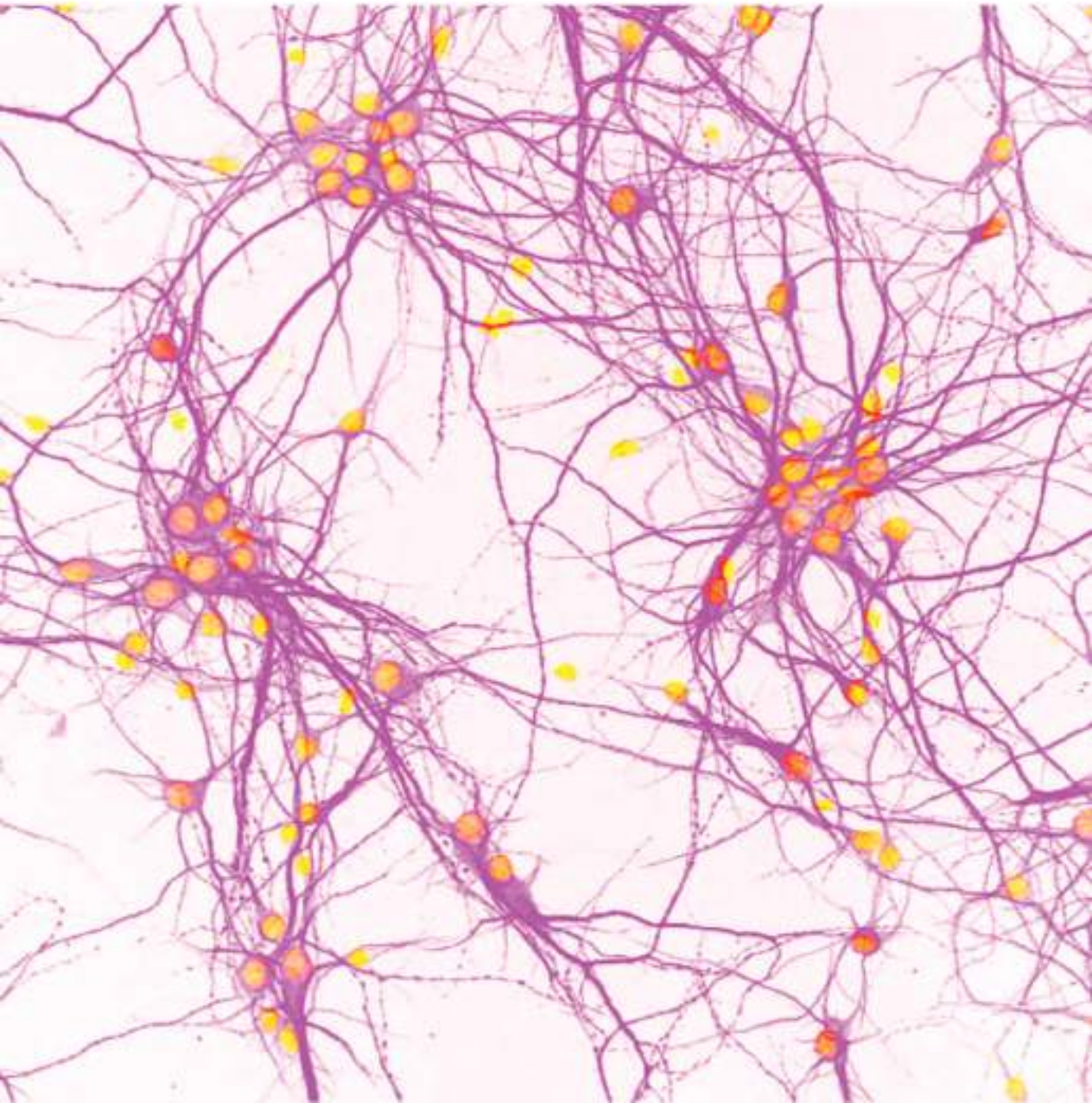

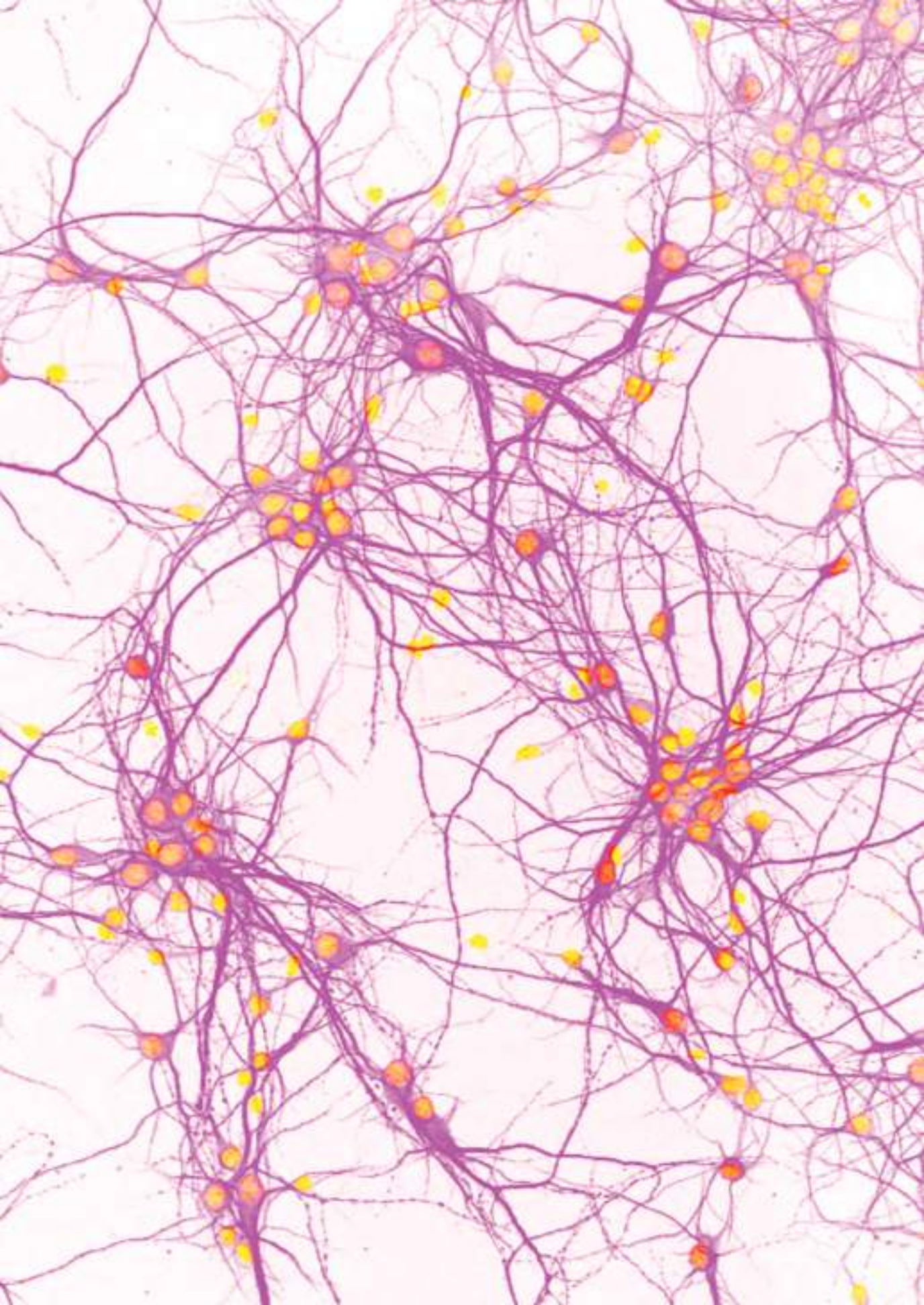

4. Results

4.1. Purification of astrocyte cultures

We first optimized the generation of primary mouse astrocyte cultures. With the purpose of obtaining pure astrocyte cultures that allowed us to specifically study the astrocytic response in a MS context, we tested two different methods of purification and assessed them by immunofluorescence. Mixed glial cultures showed a considerable presence of microglial cells (9.8 ± 0.5%) and both shaking (1.5, ± 0.6%, $p<0.0001$) and MACS-based (0.0 ± 0.0%, $p<0.0001$) purification methods significantly reduced the contamination of microglia (**Figure 8**). Indeed, MACS cell sorting applied at the time of culture generation completely removed microglia from cell cultures (**Figure 8A**). Therefore, mouse MACS-purified primary astrocyte cultures were used for experiments.

4.2. Characterization of primary cultures

Cell cultures used for further experiments were characterized by immunofluorescence. Our mouse cortical MACS-purified primary astrocyte cultures presented a high percentage of astrocytes identified with the intermediate filament marker GFAP (89.9 ± 3.4%) with a minimal contamination of neurons labelled with the neuronal nuclear marker NeuN (2.1 ± 1.2%). As expected, no presence of contaminating microglial cells were observed (Iba1; 0.0 ± 0.0%), as well as oligodendrocytes (GalC; 0.0 ± 0.0%) (**Figure 9**).

Cortical neuronal primary cultures showed a high percentage of neurons (MAP2; 91.0 ± 0.8%) with presence of astrocytes (GFAP; 10.7 ± 0.7%) (**Figure 10**). Neither microglia nor oligodendrocytes were observed in neuronal cultures (data not shown).

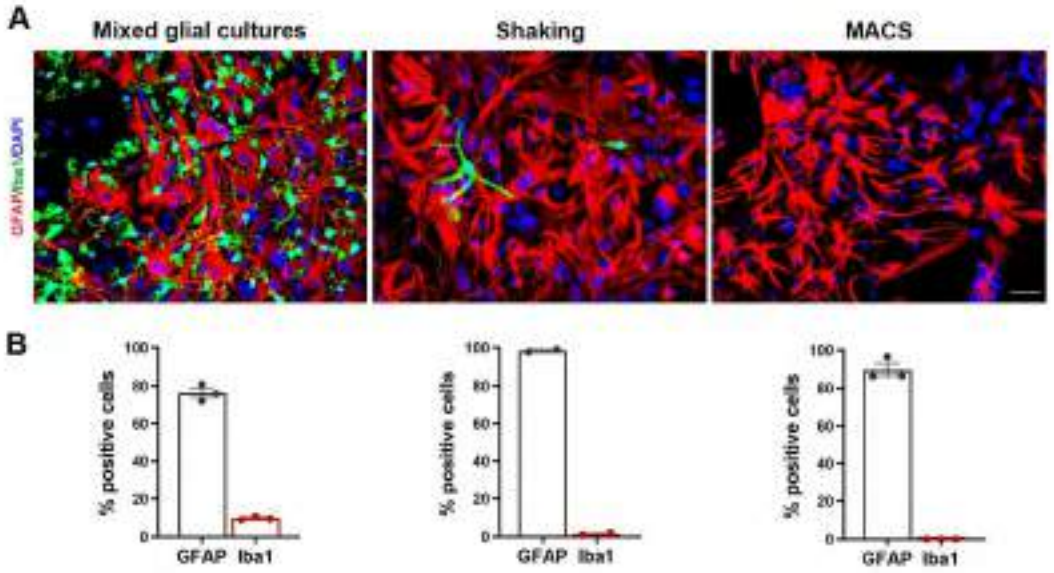

Figure 8. Evaluation of astrocyte cultures purification. (A) Illustrative fluorescent microscopy images of non-purified mixed glial cultures and purified by shaking and MACS technology. Cultures were immunostained with GFAP to label astrocytes (red), Iba1 for microglia (green) and DAPI for cell nuclei (blue). (B) Graphs represent the quantification of the percentage of the mean total number of astrocytes ($GFAP^+$) and microglial (Iba^+) cells respect to the number of total cells ($DAPI^+$) in mixed glial (n=3), shaking-purified mixed glial (n=2) and MACS-purified astrocyte (n=3) cultures. Data are shown as mean (SEM). Scale bar: 40 μm. Abbreviations: MACS: magnetic cell sorting; GFAP: glial fibrillary acid protein; Iba1: ionized calcium-binding adaptor molecule 1; DAPI: 4',6-diamidino-2-phenylindole.

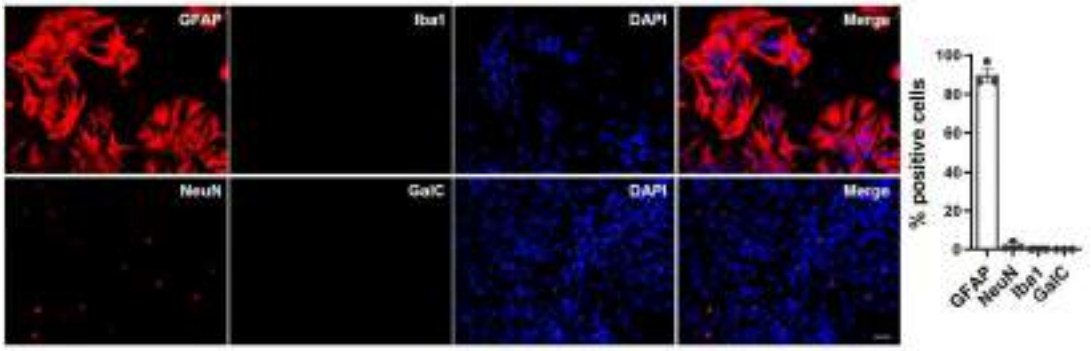

Figure 9. Characterization of MACS-purified primary astrocyte cultures. Illustrative fluorescent microscopy images showing cultures stained with GFAP to label astrocytes (red, above), Iba1 for microglia (green, above), NeuN for neurons (red, below), GalC for oligodendrocytes (green, below), DAPI for cell nuclei (blue), and the merge for the three channels of each group. On the right side, the quantification of the percentage of the mean total number of positive cells in the cultures respect to the number of total cells (DAPI). n=3 independent cultures. Data are shown as mean (SEM). Scale bar: 40 μm. Abbreviations: GFAP: glial fibrillary acid protein; Iba1: ionized calcium-binding adaptor molecule 1; NeuN: neuronal nuclear antigen; GalC: galactocerebrosidase; DAPI: 4',6-diamidino-2-phenylindole.

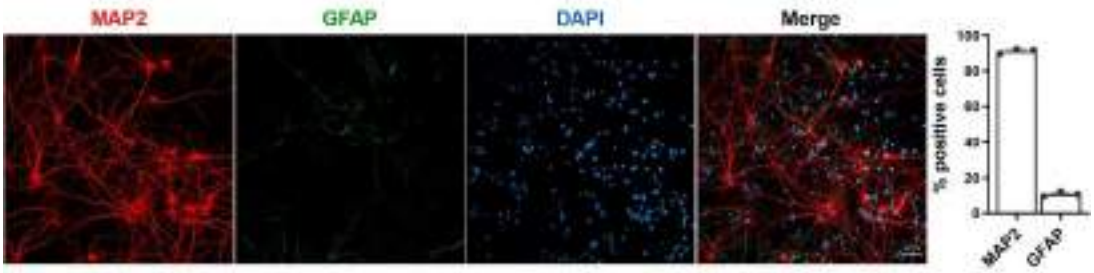

Figure 10. Characterization of primary neuronal cultures. Illustrative confocal microscopy images showing cultures stained with MAP2 to label neurons (red), GFAP for astrocytes (green), DAPI for cell nuclei (blue), and the merge for the three channels. On the right side, the quantification of the percentage of the mean total number of neurons and astrocytes in the cultures respect to the number of total cells (DAPI). n=3 independent cultures. Data are shown as mean (SEM). Scale bar: 40 μm. Abbreviations: MAP2: microtubule-associated protein 2; GFAP: glial fibrillary acid protein; DAPI: 4',6-diamidino-2-phenylindole.

4.3. Functional study of the effects of astrocyte secretomes on neurons

Astrocytes exposed to a highly inflammatory MS microenvironment induce neuronal dysfunction

To investigate whether astrocytes are essential contributors to neuronal damage in a MS-specific inflammatory microenvironment, we cultured primary mouse purified astrocytes in the presence of CSF from MS patients with high inflammatory activity at the time of the first demyelinating event (MS-High, **Table 2**). As astrocyte-secreted factors are known to provide trophic support for neurons that regulate the formation and function of synapses (172, 174), we focused our study on the astrocyte contribution through the release of soluble factors. We first conducted a screening assay in which two different CSF-exposure (6 and 12 h) and secretome-collection (6 and 18h) times were compared based on astrocyte reactivity induced and the effect of secretomes on mouse primary cortical neurons at 18 DIV (**Figure 11**).

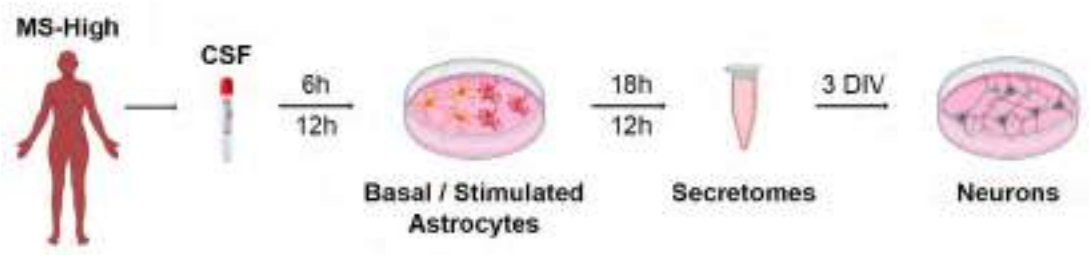

Figure 11. Functional screening assay of the effect of MS-High-exposed astrocyte secretomes on neurons. Illustration depicting CSF collection from a screening cohort of MS patients with high inflammatory activity (MS-High; N=4), followed by the exposure of astrocytes to the CSF *in vitro*, secretome collection and co-culture with neurons. Abbreviations: MS-High: high inflammatory multiple sclerosis; CSF: cerebrospinal fluid; DIV: days *in vitro*.

Astrocyte reactivity to CSF exposure was assessed by the expression of the neuroinflammation-associated reactive astrocyte marker LCN2 (216, 246), CXCL10 (214) and IL-6 (247). While astrocytes exposed to CSF at 6+18h showed 10.4-fold increased *Lcn2* expression (FC: 10.4 ± 4.4, p=0.026) compared to non-stimulated cells, 12+12h-exposure failed to induce significant *Lcn2*-associated astrocyte

reactivity (FC: 2.0 ± 0.1, p=0.503). *Cxcl10* and *Il6* expression was not modified in any of the CSF exposure conditions (**Figure 12**).

The accurate stimulation of astrocyte cultures was confirmed by determining *Lcn2* expression in cells stimulated with positive control of activation (IL-1β + TNF-α; 6+18h FC: 211.9 ± 26.0 versus Basal; 12+12h FC: 428.8 ± 61.2 versus Basal).

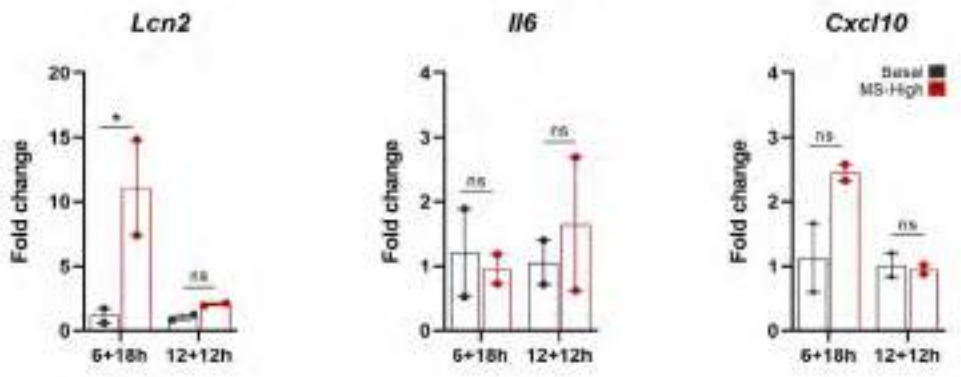

Figure 12. Astrocytes exposed to MS-High CSF at 6+18h condition became reactive. qPCR for the astrocyte reactive markers LCN2, IL-6 and CXCL10 of primary astrocytes exposed for 6 and 12h to medium (Basal) or CSF. Individual data values represent fold change = $2^{-(\text{average } \Delta\Delta Ct)}$ in mRNAs of CSF-exposed astrocytes relative to non-stimulated astrocytes (Basal). One-way ANOVA and Tukey's test for multiple comparisons; n=2 independent experiments. Data are shown as mean (SEM). *p<0.05. Abbreviations: Lcn2: lipocalin-2; IL-6: interleukin-6; CXCL10: C-X-C motif chemokine 10; MS-High: high inflammatory multiple sclerosis; CSF: cerebrospinal fluid; ns: non-significant.

Neurons treated with secretomes from astrocytes pre-exposed to CSF from MS-High patients in the 6+18h culture condition showed significant morphological alterations characterized by decreased neuronal arborization (**Figure 13A**). We found a significant decrease in the neuronal area (32.5%, p=0.001), the total dendrite tree length (38.3%, p=0.0004) and the number of dendrite segments (38.3%, p=0.0026) compared to neurons treated with basal secretomes (**Figure 13B**). In contrast, secretomes from MS-High in the 12+12h exposure condition had no significant effects on neuronal complexity (**Figure 13B**).

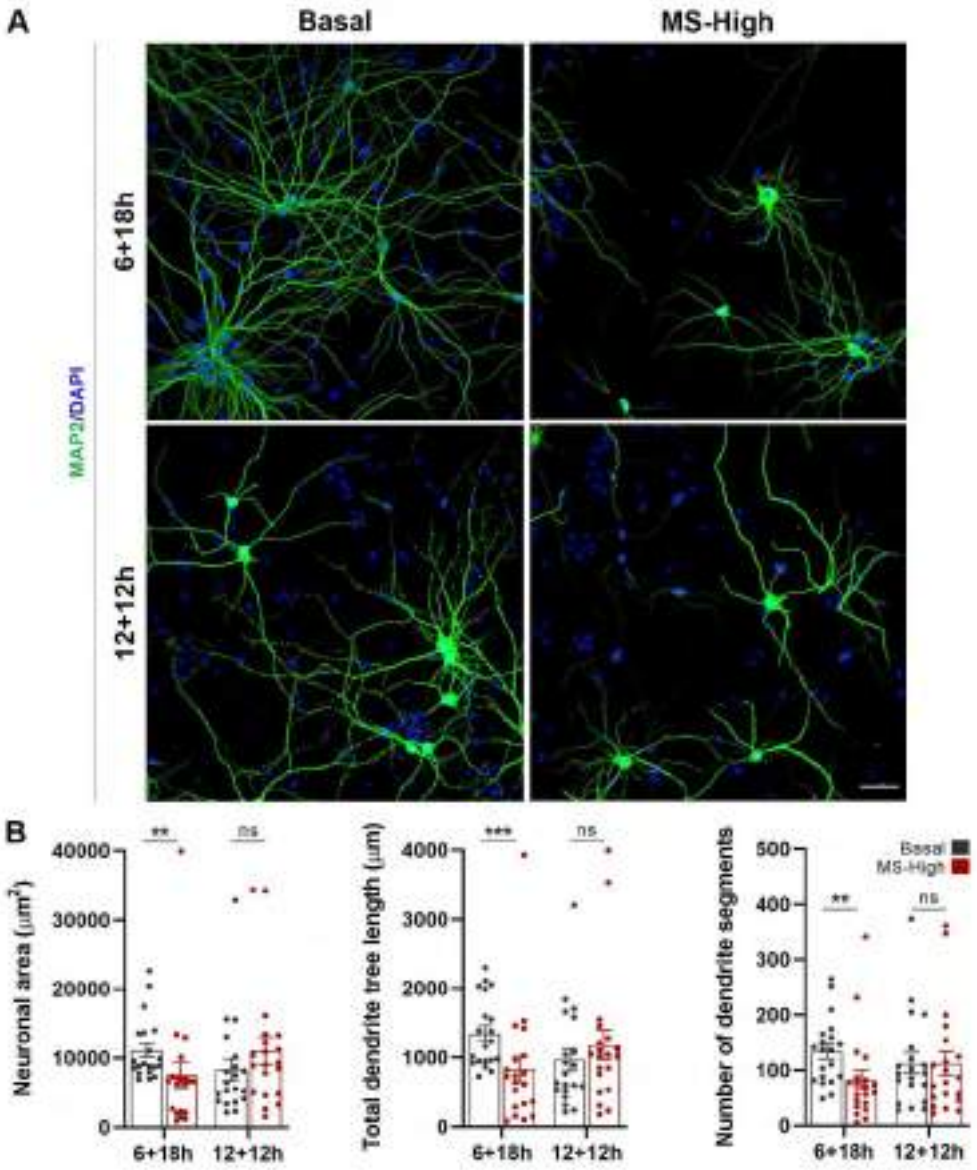

Figure 13. Astrocytes pre-exposed to CSF from MS patients with high inflammatory activity induce morphological alterations. (A) Illustrative confocal images of neurons treated with Basal or MS-High-exposed astrocyte secretomes. Neurons were immunostained with MAP2 (green) and DAPI (blue). (B) Graphs represent individual data of neuronal area, total dendrite tree length and number of dendrite segment per neuron. Least Squares Means Estimates and Bonferroni test for multiple comparisons, n=2 replicates per condition, n=2 independent experiments. Data are shown as mean (SEM). **p<0.01, ***p<0.001. Scale bar: 40 µm. Abbreviations: MS-High: high inflammatory multiple sclerosis; MAP2: microtubule-associated protein 2; DAPI: 4',6-diamidino-2-phenylindole; ns: non-significant.

We next asked whether the abnormalities observed in dendritic arborization in 6+18h exposure condition were accompanied by alterations in synaptic plasticity. Neurons treated with astrocytic secretomes stimulated with CSF from MS-High patients exhibited significant reductions in the density of both PSD-95 (29.4%, $p=0.008$) and Synaptophysin (25.8%, $p=0.011$) puncta, as well as in the number of active synapses (36.9%, $p<0.0001$), compared to neurons treated with basal secretomes (**Figure 14**). These results indicate that the 6+18h combination is more suitable to induce astrocyte reactivity that is associated with neuronal dysfunction, reason why it was selected for further experiments.

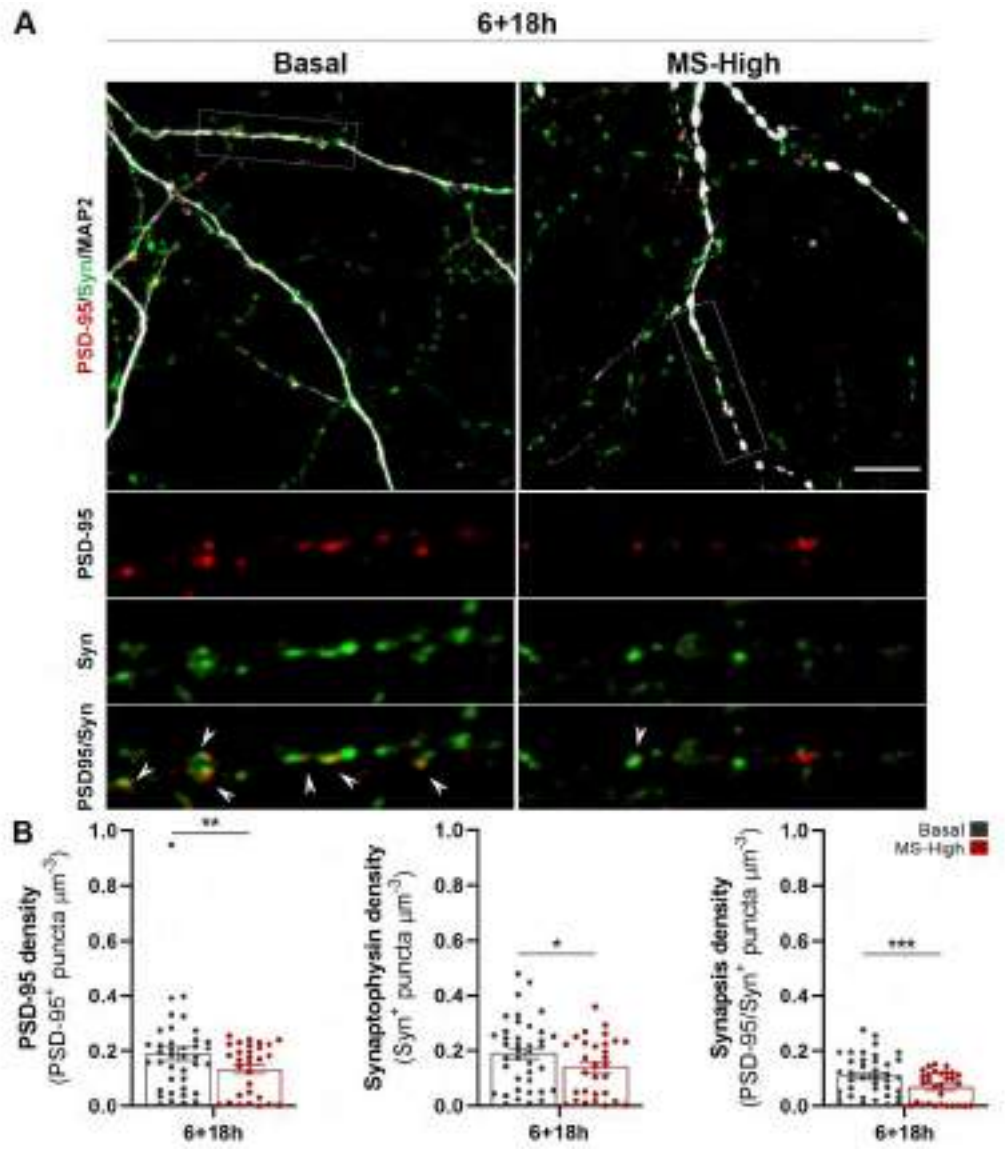

Figure 14. Astrocytes pre-exposed to CSF from MS patients with high inflammatory activity induce synaptic plasticity impairment. (A) Illustrative confocal images of neurons treated with Basal or MS-High-exposed astrocyte secretomes. Neurons were immunostained with MAP2 (white), the pre-synaptic marker synaptophysin (green) and the post-synaptic marker PSD-95 (red). Arrows in high-magnification insets point to co-localization of synaptophysin and PSD-95 (synapses). (B) Graphs represent individual data of the density of PSD-95, synaptophysin and PSD-95/synaptophysin double-positive puncta. Least Squares Means Estimates test; n=40 neurons per condition, n=2-3 dendrites per neuron, n=2 independent experiments. Data are shown as mean (SEM). *p<0.05, **p<0.01, ***p<0.001. Scale bar: 10 µm. Abbreviations: MS-High: high inflammatory multiple sclerosis; MAP2: microtubule-associated protein 2; PSD-95: post-synaptic density protein 95; Syn: synaptophysin.

A high inflammatory activity, based on high lesion load on brain MRI scans, at the time of the first demyelination event has been associated with an increased risk for development of neurological disability (112). This led us to investigate whether neuronal dysfunction was influenced by the degree of inflammatory activity present in the CNS of MS patients. To this aim, we cultured astrocytes in the presence of CSF from a new cohort of: (i) MS-High patients, (ii) MS-Low patients, and (iii) non-inflammatory controls (NINC), the latter included as MS-specificity controls (validation cohort; **Table 2**). We generated 3 different secretome pools per group from 3 stimulated astrocyte cultures. As in the screening assay, we first confirmed accurate astrocyte stimulation by evaluating *Lcn2* expression after control positive activation (IL-1β + TNF-α; Pool-1 FC: 239.8 ± 19.0; Pool-2 FC: 321.6 ± 55.5; Pool-3 FC: 218.1 ± 5.3; versus Basal). We then examined the effect of secretomes derived from CSF pre-exposed astrocytes on mouse primary cortical neurons at 18 DIV (**Figure 15**).

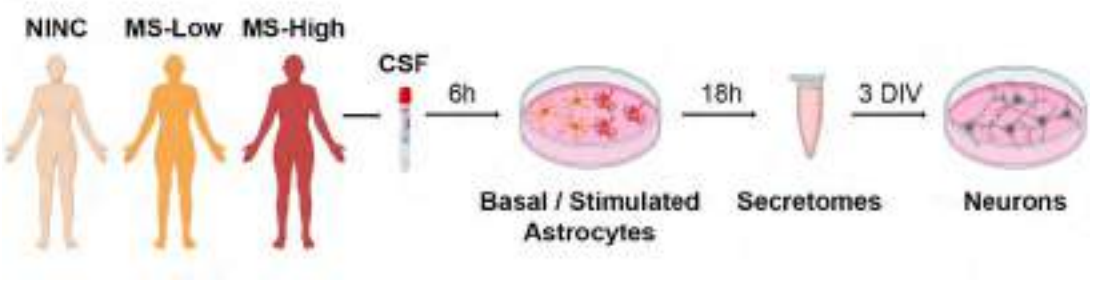

Figure 15. Flowchart of the functional validation assay of the effect of CSF-exposed astrocyte secretomes on neurons. Illustration depicting CSF collection from a validation cohort of MS patients with high inflammatory activity (MS-High, N=9), MS patients with low inflammatory activity (MS-Low, N=9) and non-inflammatory neurological controls (NINC, N=9) followed by the exposure of astrocytes to the CSF *in vitro*, secretome collection and co-culture with neurons. Abbreviations: NINC: non-inflammatory neurological controls; MS-Low: low inflammatory multiple sclerosis; MS-High: high inflammatory multiple sclerosis; CSF: cerebrospinal fluid; DIV: days *in vitro*.

Secretomes from resting astrocytes (Basal) markedly increased both PSD-95 (48.7%, p<0.0001) and Synaptophysin (23.5%, p=0.002) puncta, particularly enhancing the density of active synapses (83.1%, p<0.0001) compared to non-treated neurons (**Figure 16**). Interestingly, the degree of inflammatory activity influenced the degree of synaptic plasticity impairment. Neurons treated with secretomes from astrocytes pre-exposed to CSF from MS-High patients exhibited 16.9% and 20.8% less PSD-95 densities compared to secretomes from MS-Low patients and non-inflammatory controls (p=0.01 and p=0.0003 respectively, **Figure 16**). A similar trend was found for active synapsis density, with a 16.7% decrease in the MS-High versus the MS-Low groups (p=0.04, **Figure 16**).

Remarkably, neurons treated with secretomes from astrocytes pre-exposed to CSF from MS-High patients also showed morphological alterations typically observed in neurodegenerative processes such as decreased arborization (**Figure 17**). Particularly, MS-High astrocytic secretomes treated neurons exhibited a 39.3% reduction in neuronal area (p=0.020), 44.3% less complex dendritic tree (p=0.022), and a 43.8% decrease on the number of dendrite segments (p=0.039), compared to neurons treated with secretomes from MS-Low exposed astrocytes (**Figure 17B**).

Figure 16. Astrocyte-mediated synaptic plasticity impairment correlates with the degree of inflammatory activity in MS patients. (A) Illustrative confocal images of neurons treated with secretomes from astrocytes exposed to medium (Basal) or CSF. Neurons were immunostained with MAP2 (white), the pre-synaptic marker synaptophysin (green) and the post-synaptic marker PSD-95 (red). Arrows in high-magnification insets point to co-localization of synaptophysin and PSD-95 (synapses). (B) Graphs represent individual relative numbers of PSD-95, synaptophysin and PSD-95/synaptophysin double-positive puncta density normalized to untreated neurons (-). Least Squares Means Estimates test, Tukey-Kramer multiple comparisons test; n=3 independent secretome samples per group, n=180 neurons per condition (n=60 for non-treated group), n=2-3 dendrites per neuron, n=2 replicates per condition, n=3 independent experiments. Data are shown as mean (SEM). *p<0.05, **p<0.01, ***p<0.001. Scale bar: 10 µm. Abbreviations: NINC: non-inflammatory neurological controls; MS-Low: low inflammatory multiple sclerosis; MS-High: high inflammatory multiple sclerosis; MAP2: microtubule-associated protein 2; PSD-95: post-synaptic density protein 95; Syn: synaptophysin.

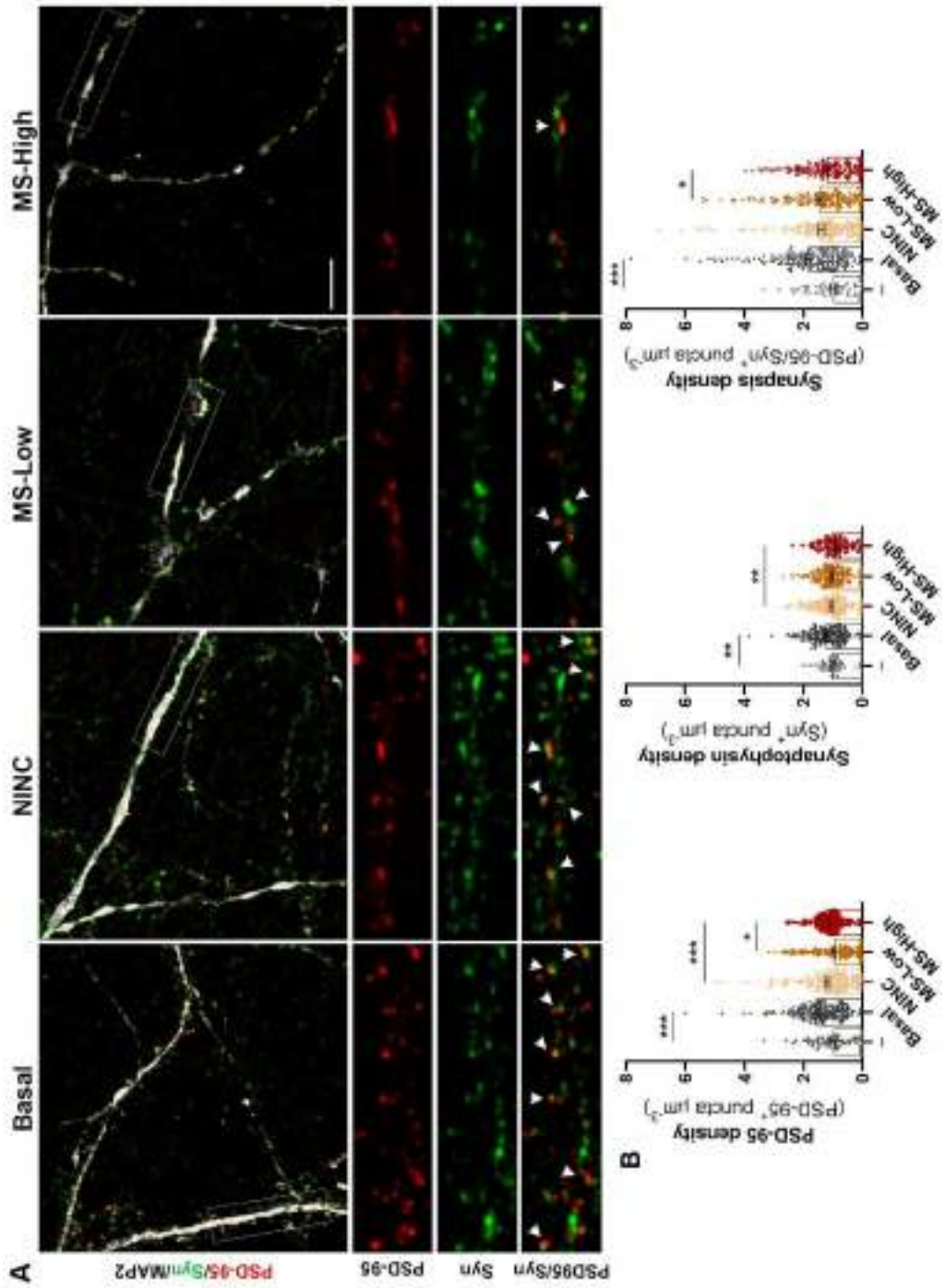
A
Basal
NINC
MS-Low
MS-High
PSD95/Syn
Syn
PSD-95
PSD-95/Syn/MAP2
B
PSD-95 density
(PSD-95+ puncta µm-3)
Synaptophysin density
(Syn+ puncta µm-3)
Synapsis density
(PSD-95/Syn+ puncta µm-3)
Basal
NINC
MS-Low
MS-High

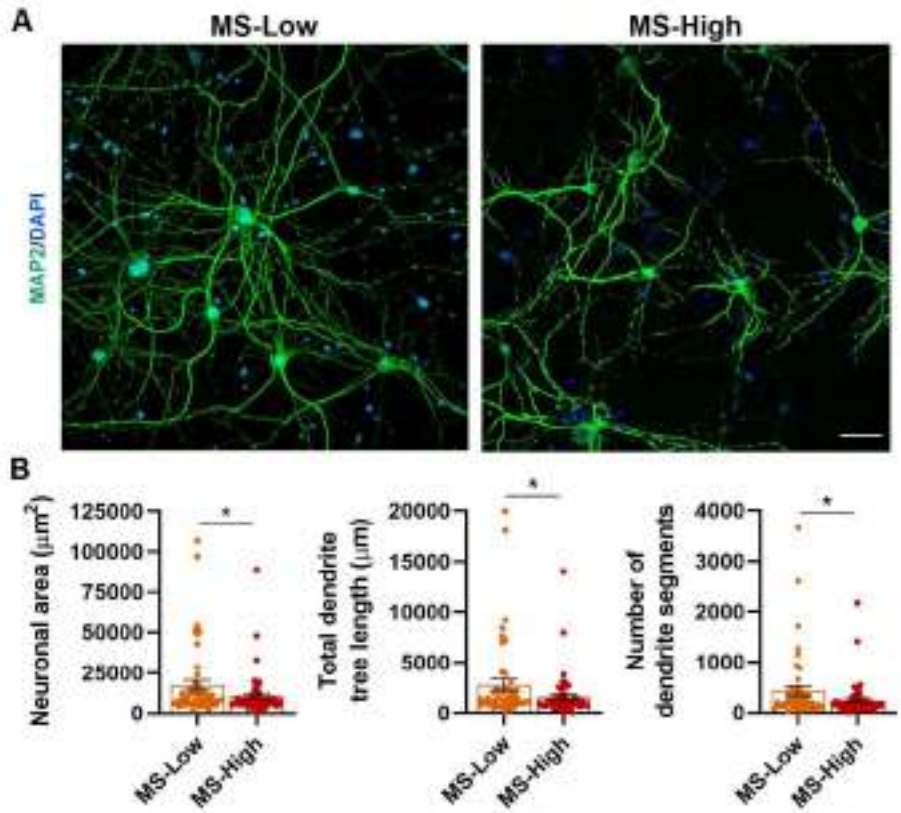

Figure 17. Astrocyte-mediated neuronal morphological alterations correlate with the degree of inflammatory activity in MS patients. (A) Illustrative confocal images of neurons treated with MS-High- and MS-Low-exposed astrocyte secretomes. Neurons were immunostained with MAP2 (green) and DAPI (blue). (B) Graphs represent individual data of neuronal area, total dendrite tree length and the number of dendrite segments per neuron. Least Squares Means Estimates test; n=3 independent secretome samples per group, n=2 replicates per condition, n=2 independent experiments. Data are shown as mean (SEM). *p<0.05. Scale bar: 40 µm. Abbreviations: MS-Low: low inflammatory multiple sclerosis; MS-High: high inflammatory multiple sclerosis; MAP2: microtubule-associated protein 2; DAPI: 4',6-diamidino-2-phenylindole.

These findings reveal that astrocytes pre-exposed to CSF from MS patients with high inflammatory activity exert a detrimental non-cell-autonomous effect on neuronal function and plasticity.

4.4. Molecular characterization of astrocyte signature

Secretomes from astrocytes exposed to a highly inflammatory MS microenvironment have an altered pro-inflammatory profile

We next investigated whether the detrimental effect of secretomes from MS patients with high inflammatory activity on neuronal function and synaptic plasticity could be due to the release of astrocyte-derived toxic mediators. For that purpose, astrocytic secretomes obtained following CSF exposure were characterized using a proteome profiling array. A total of 23 molecules were found up-regulated in secretomes derived from astrocytes pre-exposed to CSF from the different groups of patients and controls (**Figure 18** and **Table 3**). Among them, 12 molecules were significantly increased in secretomes from MS-High patients compared to those from MS-Low patients, and 20 when compared to non-inflammatory controls (FDR<0.05, **Figure 18B** and **Table 3**).

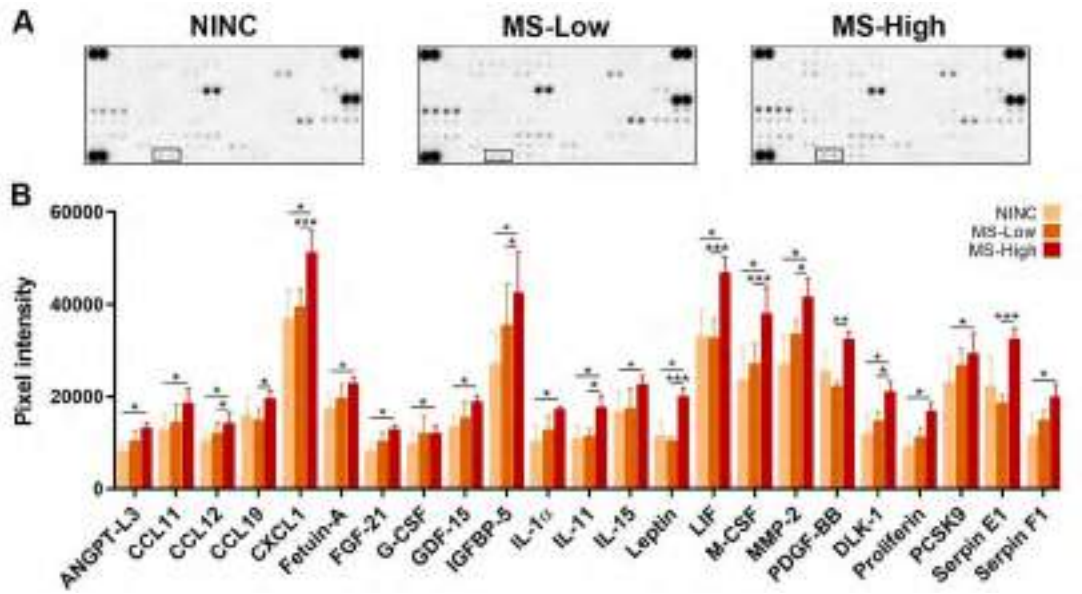

Figure 18. Astrocytes pre-exposed to CSF from MS patients with high inflammatory activity exhibit an altered secretome. (A) Proteome profiling array representative membranes of secretomes from CSF-exposed primary astrocytes. (B) Pixel intensity quantification showing 23 identified molecules up-regulated in the MS-High condition. Note that insets delimit SerpinE1 dots. FDR analysis. n=3 independent secretome samples per group, n=3 independent experiments. Data are shown as mean (SEM). *p<0.05, **p<0.01, ***p<0.001. Abbreviations: NINC: non-inflammatory neurological controls; MS-Low: low inflammatory multiple sclerosis; MS-High: high inflammatory multiple sclerosis; ANGPTL3: angiopoietin-like 3; CCL: C-C motif chemokine; CXCL: C-X-C motif chemokine; FGF-21: fibroblast growth factor 21; G-CSF: granulocyte colony-stimulating factor; GDF-15: growth/differentiation factor 15; GFBP-5: insulin-like growth factor-binding protein 5; IL: interleukin; LIF: leukemia inhibitor factor; M-CSF: macrophage colony-stimulating factor 1; MMP-2: matrix metalloproteinase-2; PDGF-BB: platelet-derived growth factor subunit B; DLK-1: protein delta homolog 1; PCSK9: proprotein convertase 9.

Astrocyte-secreted factors identified from astrocytes exposed to the MS-High condition compared to both the MS-Low (12 proteins) and NINC (20 proteins) using a proteome profiling array. Proteins are classified according to their adjusted p-value. Abbreviations: NINC: non-inflammatory neurological controls; MS-Low: low inflammatory multiple sclerosis; MS-High: high inflammatory multiple sclerosis; M-CSF: macrophage colony-stimulating factor 1; CXCL: C-X-C motif chemokine; LIF: leukemia inhibitor factor; PDGF-BB: platelet-derived growth factor subunit B; IGFBP-5: insulin-like growth factor-binding protein 5; MMP-2: matrix metalloproteinase-2; CCL: C-C motif chemokine; IL: interleukin; DLK-1: protein delta homolog 1; ANGPTL3: angiopoietin-like 3; PCSK9: proprotein convertase 9; GDF-15: growth/differentiation factor 15; G-CSF: granulocyte colony-stimulating factor; FGF-21: fibroblast growth factor 21.

Table 3. Astrocyte-secreted factors identified in the proteome profiling array.

Protein	Fold change	p-value	Adjusted p-value
MS-High vs. MS-Low			
Leptin	1.9	<.0001	<.0001
M-CSF	1.4	<.0001	<.0001
CXCL1	1.3	<.0001	<.0001
SerpinE1	1.7	<.0001	0.0002
LIF	1.4	<.0001	0.0008
PDGF-BB	1.4	0.0002	0.001
IGFBP-5	1.2	0.002	0.01
MMP-2	1.2	0.002	0.01
CCL19	1.3	0.002	0.01
IL-11	1.5	0.008	0.03
DLK-1	1.4	0.007	0.03
CCL12	1.2	0.007	0.03
MS-High vs. NINC			
ANGPTL3	1.6	0.001	0.01
MMP-2	1.5	0.001	0.01
CXCL1	1.4	0.0008	0.01
M-CSF	1.6	0.002	0.02
LIF	1.4	0.002	0.02
PCSK9	1.2	0.002	0.02
CCL12	1.3	0.003	0.02
GDF-15	1.4	0.004	0.02
Proliferin	1.8	0.005	0.02
DLK-1	1.7	0.005	0.02
IGFPB-5	1.5	0.006	0.03
Leptin	1.7	0.008	0.03
IL-1α	1.6	0.01	0.03
Serpin F1	1.7	0.01	0.04
IL-11	1.6	0.01	0.04
IL-15	1.3	0.01	0.04
G-CSF	1.6	0.02	0.04
FGF-21	1.5	0.02	0.04
CCL11	1.4	0.02	0.04
Fetuin-A	1.3	0.02	0.04

The 23 astrocyte-secreted factors identified were inflammatory-related molecules, mainly cytokines, chemokines, and growth factors. Functional annotation enrichment and interactome analysis using Gene Ontology and KEGG (Kyoto Encyclopedia of Gene and Genomes) revealed that these astrocyte-secreted factors are mainly involved in a set of pro-inflammatory pathways (**Table 4**).

When comparing the degree of inflammatory exposure to astrocytes, functional enrichment analysis of the 12 molecules up-regulated in astrocytes exposed to high compared to low inflammation confirmed the predominance of pathways involved in inflammation, like myeloid leukocyte migration ($p=1.9 \times 10^{-10}$), TNF signalling ($p=9.9 \times 10^{-8}$) and inflammatory response ($p=3.5 \times 10^{-7}$) (**Figure 19A**). In addition, important pathways known to be involved in synaptic plasticity homeostasis as tissue remodelling ($p=7.0 \times 10^{-7}$) and extracellular matrix organization ($p=0.0005$) were identified as the most significantly enriched (**Figure 19A**). Consistently, when studying the 20 secreted factors up-regulated in high compared to non-inflammatory condition, we also found mostly enriched pro-inflammatory pathways and, surprisingly, neuron death signalling ($p=1.2 \times 10^{-6}$) and programmed cell death ($p=0.0002$) (**Figure 19B**). Importantly, nuclear factor NF-kappa-B p105 subunit (*Nfkb1*) was identified as the main regulatory transcription factor among the astrocyte-secreted factors ($FDR=1.9 \times 10^{-8}$) as well as cellular tumour antigen p53 (*Trp53*) ($FDR=9.4 \times 10^{-5}$) (**Figure 19C**), which is known to induce NF-κB activation (248).

Functional annotation enrichment of the 23 astrocyte-secreted factors identified from astrocytes exposed to the MS-High condition compared to both the MS-Low and NINC. Pathways are classified according to their adjusted p-value. Mouse gene ID symbols are shown. Abbreviations: Csf1: M-CSF; Csf3: G-CSF; Cxcl: C-X-C motif chemokine; Il: interleukin; Lep: leptin; Lif: leukemia inhibitor factor; Pdgfb: platelet-derived growth factor subunit B; Ccl: C-C motif chemokine; Igfbp5: insulin-like growth factor-binding protein 5; Mmp-2: matrix metalloproteinase-2; Prl2c2: proliferin; Angptl3: angiopoietin-like 3; Ahsg: fetuin-A; Gdf15: growth/differentiation factor 15; Fgf21: fibroblast growth factor 21; Dlk1: protein delta homolog 1; Pcsk9: proprotein convertase 9.

Table 4. GO and KEGG functional analysis for the 23 astrocyte-secreted factors.

Pathways	Adjusted p-value	Genes
Cytokine-cytokine receptor interaction	1.5×10^{-17}	*Csf1, Csf3, Cxcl1, Il11, Il15, Il1a, Lep, Lif, Pdgfb, Ccl11, Ccl12, Ccl19*
Positive regulation of cell migration	5.8×10^{-12}	*Csf1, Igfbp5, Il1a, Mmp2, Pdgfb, Serpine1, Prl2c2, Ccl11, Ccl12, Ccl19, Angptl3, Cxcl1, Lep, Ahsg, Serpinf1, Csf3*
Myeloid leukocyte migration	6.5×10^{-11}	*Csf1, Cxcl1, Il1a, Pdgfb, Serpine1, Ccl11, Ccl12, Ccl19*
Positive regulation of MAPK cascade	7.9×10^{-11}	*Il11, Il1a, Lep, Lif, Pdgfb, Ccl11, Ccl12, Gdf15, Ccl19, Fgf21, Angptl3*
Tissue remodeling	1.5×10^{-9}	*Ahsg, Dlk1, Igfbp5, Il1a, Lep, Lif, Mmp2, Csf1, Gdf15, Il15*
Inflammatory response	2.1×10^{-9}	*Ahsg, Csf1, Cxcl1, Il1a, Lep, Serpine1, Ccl11, Ccl12, Serpinf1, Ccl19*
Leukocyte and monocyte chemotaxis	3.1×10^{-9}	*Pdgfb, Serpine1, Ccl11, Ccl12, Ccl19, Igfbp5, Serpinf1, Fgf21, Lep, Prl2c2, Gdf15*
Regulation of cell adhesion	4.6×10^{-8}	*Csf1, Il15, Il1a, Lep, Lif, Mmp2, Pdgfb, Serpine1, Ccl19, Ccl12, Ahsg, Dlk1, Fgf21, Cxcl1*
Positive regulation of peptidyl-tyrosine phosphorylation	5.8×10^{-8}	*Csf3, Il11, Il15, Lep, Lif, Pdgfb, Prl2c2, Il1a, Pcsk9, Fgf21*
Protein kinase B signaling	8.0×10^{-8}	*Csf3, Igfbp5, Lep, Ccl12, Gdf15, Ccl19, Csf1, Pdgfb, Il15*
Positive regulation of myeloid cell differentiation	1.1×10^{-7}	*Csf1, Csf3, Dlk1, Lep, Lif, Cxcl1, Il15, Ccl12, Ccl19, Il1a, Pdgfb*
TNF signaling pathway	1.1×10^{-7}	*Csf1, Cxcl1, Il15, Lif, Ccl12*
Positive regulation of ion transport	6.5×10^{-7}	*Cxcl1, Il1a, Lep, Lif, Pdgfb, Serpine1, Ccl12, Fgf21, Mmp2, Ahsg*
Jak-STAT signaling pathway	7.2×10^{-7}	*Csf3, Il11, Il15, Lep, Lif*
Transmembrane receptor protein tyrosine kinase signaling pathway	2.3×10^{-6}	*Ahsg, Csf1, Igfbp5, Lep, Pdgfb, Gdf15, Fgf21, Pcsk9, Serpine1*
Regulation of neuron death	3.0×10^{-6}	*Csf1, Csf3, Ccl12, Serpinf1, Fgf21, Pcsk9, Lif, Pdgfb*

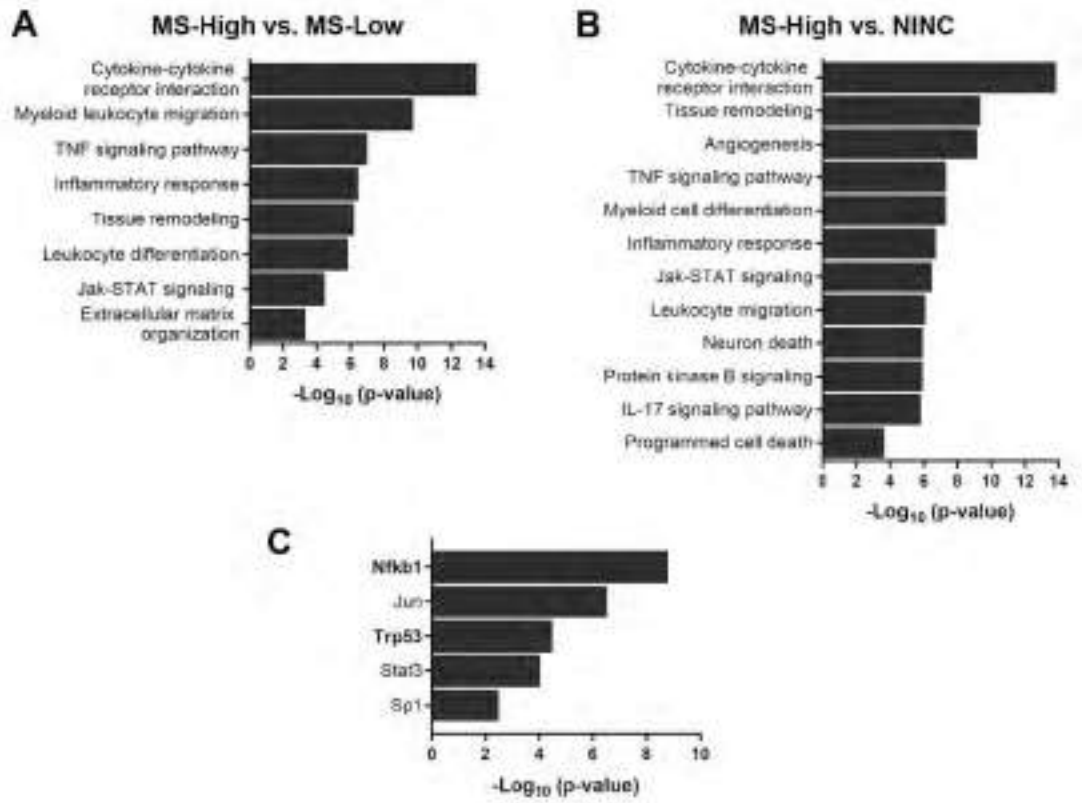

Figure 19. Astrocyte-secreted factors after MS-High CSF exposure are predominantly involved in inflammatory signalling. Plots showing GO and KEGG functional analysis for the MS-High condition compared to the MS-Low (A) and non-inflammatory control (NINC) (B) conditions. (C) TRRUST enrichment analysis of transcription factor candidates that regulate the expression of the 23-identified astrocyte-secreted factors in the MS-High condition. Abbreviations: MS-High: high inflammatory multiple sclerosis; MS-Low: low inflammatory multiple sclerosis; NINC: non-inflammatory neurological controls; TNF: tumor necrosis factor; Jak: janus kinase; STAT: signal transducer and activator of transcription; IL: interleukin; Nfkb1: nuclear factor-kappa-B p105 subunit; Jun: transcription factor AP-1; Trp53: cellular tumour antigen p53; Stat3: signal transducer and activator of transcription 3; Sp1: transcription factor Sp1.

An interesting finding among astrocyte-derived differentially secreted pro-inflammatory mediators was SerpinE1, a protein that has been shown to be regulated by NF-kB in neuroinflammatory conditions (249, 250), to inhibit neurite outgrowth after an ischemic insult (251), and to exacerbate axonal damage and demyelination in MS animal models (252, 253). SerpinE1 was particularly increased by 1.7-fold in secretomes from MS-High compared to those from MS-Low patients (p=0.0002, **Figure 18** and **Table 3**), and was found to be significantly enriched in the extracellular matrix organization pathway (p=0.0005, **Figure 19A** and **Table 5**).

Table 5. Serpin E1 representation in MS-High-derived astrocyte secretome functional analysis.

Pathways	Adjusted p-value	Genes
Cytokine-cytokine receptor interaction	3.1×10^{-14}	*Csf1, Cxcl1, Il11, Lep, Lif, Pdgfb, Ccl2, Ccl19,* ***Serpine1****, Igfbp5, Mmmp2*
Myeloid leukocyte migration	1.9×10^{-10}	*Csf1, Cxcl1,* ***Serpine1****, Pdgfb, Ccl12, Ccl19, Lep, Igfbp5*
Inflammatory response	3.5×10^{-7}	*Csf1, Cxcl1, Lep,* ***Serpine1****, Ccl12, Ccl19*
Extracellular matrix organization	0.0005	*Mmp2,* ***Serpine1****, Pdgfb*

Functional annotation enrichment of astrocytic secretome data set of MS-High compared to MS-Low condition. Serpin E1 is highlighted in bold. Mouse gene ID symbols are shown. Abbreviations: Csf1: M-CSF; Cxcl: C-X-C motif chemokine; Il: interleukin; Lep: leptin; Lif: leukemia inhibitor factor; Pdgfb: platelet-derived growth factor subunit B; Ccl: C-C motif chemokine; Igfbp5: insulin-like growth factor-binding protein 5; Mmp-2: matrix metalloproteinase-2.

Considering its potential as neurotoxic mediator, SerpinE1 levels were also measured by ELISA in order to validate protein array findings. Levels were again found to be significantly increased in secretomes from astrocytes pre-exposed to CSF from MS-High compared to those from MS-Low patients (2.2-fold, p=0.01) and unstimulated astrocytes (2.8-fold, p=0.0008, **Figure 20**).

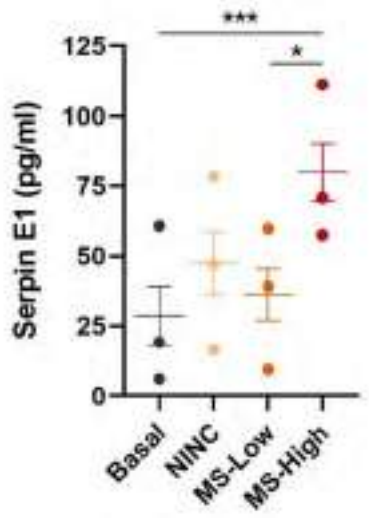

Figure 20. SerpinE1 is increased in secretomes from astrocytes exposed to CSF from MS patients with high inflammatory activity. Dot plot showing SerpinE1 levels determined by ELISA in astrocyte-derived secretomes. Least Squares Means Estimates test and Tukey-Kramer multiple comparisons test; n=3 independent secretome samples per group. Data are shown as mean (SEM). *p<0.05, ***p<0.001. Abbreviations: NINC: non-inflammatory neurological controls; MS-Low: low inflammatory multiple sclerosis; MS-High: high inflammatory multiple sclerosis.

Altogether, these results indicate that secretomes from astrocytes pre-exposed to CSF from MS patients with high inflammatory activity have a pro-inflammatory content that seems to be regulated by astrocytic NF-kB signalling. In addition, SerpinE1 may be one of the toxic mediators of the paracrine effect of astrocytes on neuronal function and plasticity.

Astrocytes exposed to a highly inflammatory MS microenvironment are characterized by a specific pro-inflammatory reactive state

As a next step, we investigated whether the pro-inflammatory secretomes that mediate neuronal dysfunction and synaptic plasticity impairment are associated with a specific reactive astrocyte state in MS patients with high inflammatory activity. To this aim, gene expression microarrays and liquid chromatography/mass spectrometry (LC/MS) analysis were carried out on RNA and intracellular protein samples isolated from non-stimulated and CSF pre-exposed astrocytes.

Astrocytes stimulated with CSF from MS-High patients exhibited a gene (**Figure 21A**) and protein (**Figure 21B**) expression profile that differed from the expression pattern observed following astrocyte exposure to CSF from MS-Low patients, non-inflammatory controls, and the unstimulated condition.

Further dissection of the gene expression profiling revealed a specific signature in astrocytes exposed to CSF from MS-High patients that was characterized by 7 differentially expressed genes (2 up-regulated and 5 down-regulated) when compared with the MS-Low condition (**Figure 22** and **Table 6**), and 23 differentially expressed genes (4 up-regulated and 19 down-regulated) when compared with the non-inflammatory control condition (adjusted p-values <0.05, **Figure 22** and **Table 7**). In contrast, no statistically significant differentially expressed genes were found between the MS-Low and the non-inflammatory control conditions (**Figure 22**), further supporting the specificity of the identified gene expression signature, which seems to be only present when the MS-High group is compared.

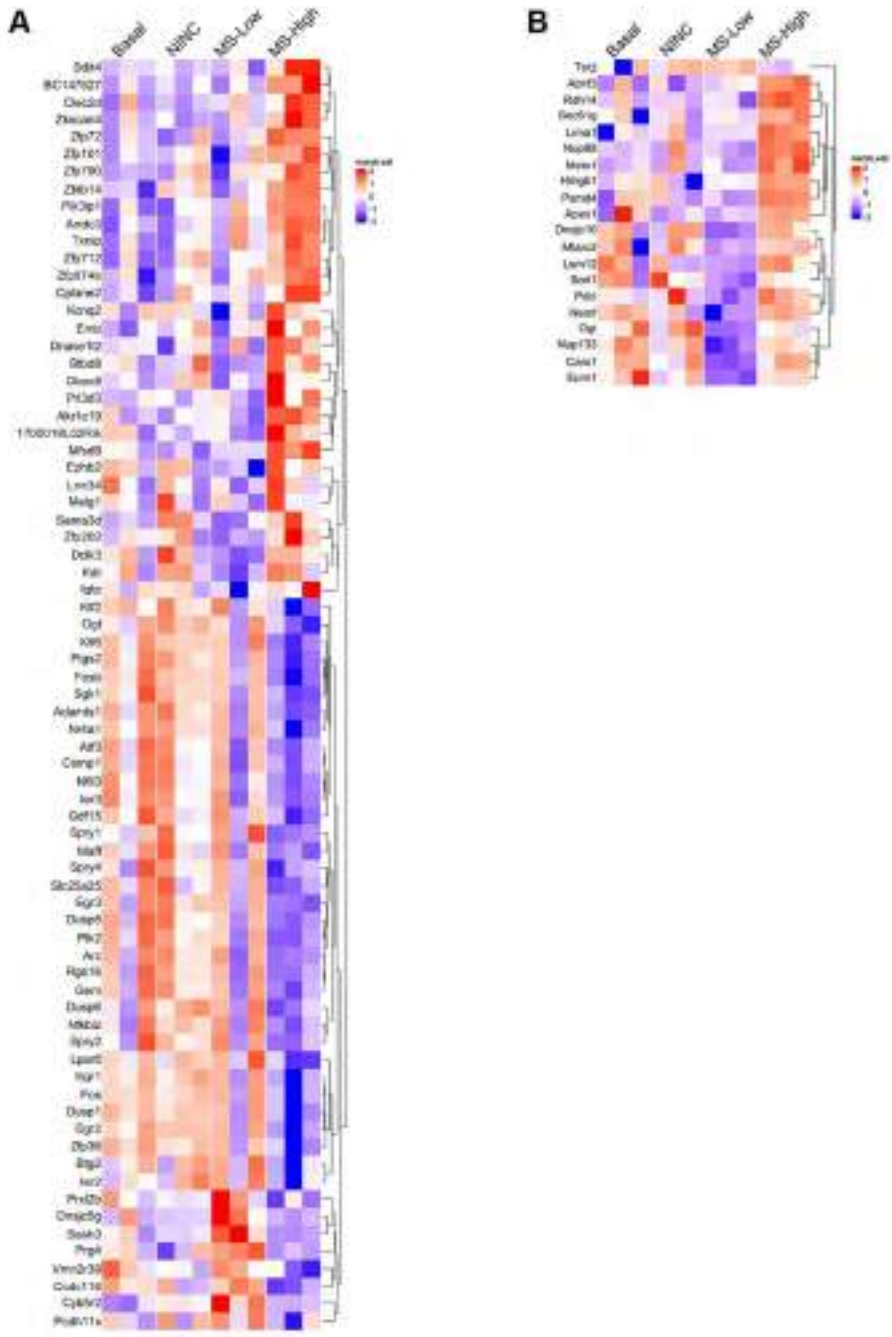

Figure 21. Astrocytes exposed to CSF from MS patients with high inflammatory activity show a specific gene and protein expression profile. Heatmaps showing normalized Log_2 gene (A) and protein (B) expression satisfying p-value <0.01 and absolute fold change >0.5. FDR analysis; n=3 independent biological samples per group. Abbreviations: NINC: non-inflammatory neurological controls; MS-Low: low inflammatory multiple sclerosis; MS-High: high inflammatory multiple sclerosis.

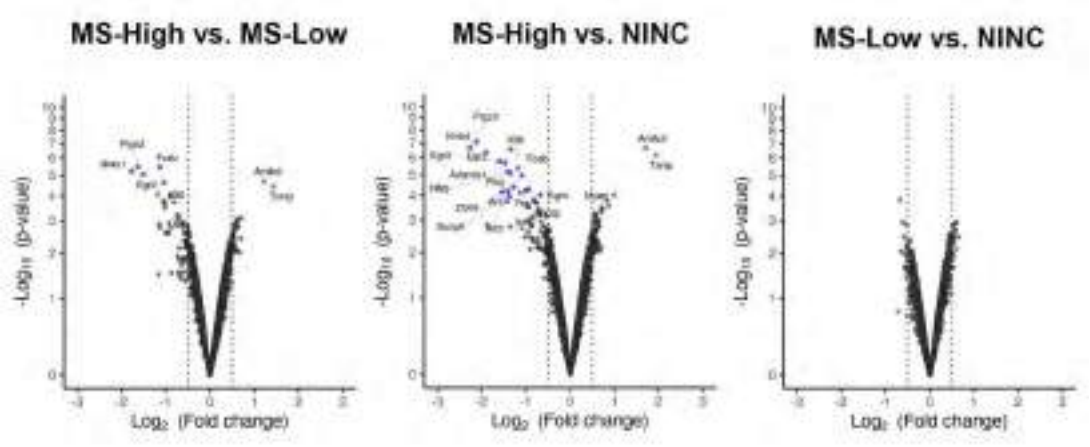

Figure 22. Astrocytes exposed to CSF from MS patients with high inflammatory activity present a specific gene expression signature. Volcano plots showing normalized Log_2 gene expression satisfying p-value <0.01 and absolute fold change >0.5. FDR analysis; n=3 independent biological samples per group. Significant differentially expressed genes (adjusted p-value <0.05) are highlighted in blue (down-regulated) and red (up-regulated). Abbreviations: MS-High: high inflammatory multiple sclerosis; MS-Low: low inflammatory multiple sclerosis; NINC: non-inflammatory neurological controls.

Regarding protein expression profile, we found a specific expression pattern characterized by an up-regulation of intracellular protein expression in MS-High-stimulated astrocytes compared to those exposed to low or non-inflammatory conditions (**Figure 21B**). Astrocytes exposed to MS-High CSF exhibited significantly enhanced expression of 8 intracellular proteins when compared to the MS-Low condition (**Table 8**), and 9 differentially expressed proteins (3 up-regulated and 6 down-regulated) when compared with the non-inflammatory control condition (adjusted p-values <0.05, **Table 9**).

Table 6. Top genes differentially expressed in astrocytes exposed to CSF from MS-High patients compared to MS-Low.

Gene	Log_2 (Fold change)	p-value	Adjusted p-value
Ptgs2	-1.6	3.3×10^{-6}	0.01
Fosb	-1.1	3.5×10^{-6}	0.01
Nr4a1	-1.8	5.8×10^{-6}	0.01
Egr2	-1.5	$8.7\ 10^{-6}$	0.01
Arrdc3	1.2	1.9×10^{-5}	0.02
Klf6	-1.0	2.3×10^{-5}	0.02
Txnip	1.4	3.6×10^{-5}	0.03
Egr3	-1.2	8.3×10^{-5}	0.07
Zfp36	-0.9	1.0×10^{-4}	0.08
Fos	-1.0	1.7×10^{-4}	0.11
Adamts1	-1.0	1.7×10^{-4}	0.11
Gdf15	-0.8	1.8×10^{-4}	0.11
Plk2	-1.0	2.3×10^{-4}	0.12
Nfil3	-1.0	3.3×10^{-4}	0.17
Klf2	-0.7	6.2×10^{-4}	0.12
Dusp1	-0.7	7.8×10^{-4}	0.34
Zfp712	0.7	8.2×10^{-4}	0.34
Zfp101	0.6	8.8×10^{-4}	0.35
BC147527	0.6	9.5×10^{-4}	0.35
Ier3	-0.7	0.001	0.35
Dclk3	0.6	0.001	0.35
Egr1	-0.6	0.001	0.35
Dusp5	-0.9	0.001	0.35
Ccdc116	-0.6	0.001	0.35
Lpar6	-0.6	0.001	0.35
Arc	-1.1	0.001	0.35
Akr1c19	0.6	0.001	0.35
Mfsd9	0.5	0.001	0.35
Prxl2b	-0.7	0.001	0.35
Zfp72	0.6	0.001	0.35
Prl3d3	0.6	0.001	0.35
Vmn2r39	-0.5	0.001	0.35
Slc25a25	-0.6	0.002	0.35
Zkscan4	0.6	0.002	0.35

Rgs16	-1.1	0.002	0.35
Nfkbiz	-0.9	0.002	0.35
Sash3	-0.5	0.002	0.35
Zfp202	0.5	0.002	0.36
Ddit4	0.5	0.002	0.41
Cyb5r2	-0.5	0.002	0.41
Zfp790	0.5	0.002	0.41
Atf3	-1.0	0.002	0.41
Csrnp1	-1.0	0.002	0.41
Spry1	-0.6	0.002	0.41
Spry4	-0.9	0.002	0.41
Dnajc5g	-0.5	0.003	0.41
Ephb2	0.5	0.003	0.42
Prg4	-0.5	0.003	0.42
1700018L02Rik	0.5	0.003	0.43
Cplane2	0.5	0.003	0.45

Top 50 differentially expressed genes obtained from microarrays data set of MS-High- compared to MS-Low condition. Genes are classified according to their adjusted p-value. Significant differentially expressed genes (adjusted p-value <0.05) are highlighted in bold. Mouse gene ID symbols are shown.

Table 7. Top genes differentially expressed in astrocytes exposed to CSF from MS-High patients compared to NINC controls.

Gene	Log_2 (Fold change)	p-value	Adjusted p-value
Ptgs2	-2.1	7.8×10^{-8}	4.9×10^{-4}
Nr4a1	-2.2	2.0×10^{-7}	4.9×10^{-4}
Arrdc3	1.7	$2.2\ 4.9 \times 10^{-7}$	4.9×10^{-4}
Fosb	-1.3	2.7×10^{-7}	4.9×10^{-4}
Egr2	-1.9	4.1×10^{-7}	5.9×10^{-4}
Txnip	1.9	4.13×10^{-7}	8.7×10^{-4}
Egr3	-1.6	1.7×10^{-6}	0.002
Adamts1	-1.5	2.2×10^{-6}	0.002
Klf6	-1.2	4.3×10^{-6}	0.003
Nfil3	-1.4	6.8×10^{-6}	0.005
Plk2	-1.3	8.3×10^{-6}	0.005
Zfp36	-1.1	1.1×10^{-5}	0.006
Dusp5	-1.3	4.1×10^{-5}	0.02
Klf2	-0.9	5.2×10^{-5}	0.02
Ier3	-1.0	6.1×10^{-5}	0.02
Atf3	-1.4	6.5×10^{-5}	0.02
Arc	-1.5	6.9×10^{-5}	0.02
Fos	-1.1	7.6×10^{-5}	0.03
Egr4	-0.7	9.4×10^{-5}	0.03
Mycn	1.0	9.8×10^{-5}	0.03
Mfsd9	0.7	1.1×10^{-4}	0.03
Csrnp1	-1.4	1.1×10^{-4}	0.03
Ogt	-0.8	1.5×10^{-4}	0.04
Zfp217	0.8	1.7×10^{-4}	0.05
Rgs16	-1.4	1.8×10^{-4}	0.05
Dusp1	-0.8	1.9×10^{-4}	0.05
Egr1	-0.7	2.1×10^{-4}	0.05
Clec2d	0.8	2.9×10^{-4}	0.07
Idi1	-0.9	3.1×10^{-4}	0.08
Pik3ip1	0.7	3.3×10^{-4}	0.08
Noct	-0.9	3.3×10^{-4}	0.08
Sgk1	-0.7	3.7×10^{-4}	0.08
Zkscan4	0.7	4.0×10^{-4}	0.08
Pcdh18	-0.6	5.0×10^{-4}	0.10
Gem	-0.7	5.0×10^{-4}	0.10

Cdk20	0.7	5.1×10^{-4}	0.10
Tnfaip8l1	0.5	6.0×10^{-4}	0.11
Crb1	0.6	6.1×10^{-4}	0.11
Gdf15	-0.7	6.3×10^{-4}	0.11
4632415L05Rik	0.6	6.8×10^{-4}	0.12
Dusp6	-0.6	6.8×10^{-4}	0.12
F3	-0.8	7.4×10^{-4}	0.12
Nudt16l2	-0.5	7.5×10^{-4}	0.12
Zfp870	0.6	8.9×10^{-4}	0.14
Nr4a3	-0.8	9.3×10^{-4}	0.15
Zfp72	0.6	0.001	0.16
Cyb561d1	0.6	0.001	0.16
Ccdc185	0.5	0.001	0.16
Nfkbiz	-0.9	0.001	0.16
Slc25a25	-0.6	0.001	0.16

Top 50 differentially expressed genes obtained from microarrays data set of MS-High- compared to NINC condition. Genes are classified according to their adjusted p-value. Significant differentially expressed genes (adjusted p-value <0.05) are highlighted in bold. Mouse gene ID symbols are shown.

Table 8. Top intracellular proteins differentially expressed in astrocytes exposed to CSF from MS-High patients compared to MS-Low.

Gene	Log_2 (Fold change)	p-value	Adjusted p-value
Eprs1	0.3	9.2×10^{-5}	0.006
Hmgb1	0.3	1.5×10^{-4}	0.009
Ndufa3	0.6	2.2×10^{-4}	0.01
Lima1	0.1	5.2×10^{-4}	0.03
Nup88	2.4	6.6×10^{-4}	0.04
Nudt18	0.9	6.6×10^{-4}	0.04
Mtarc2	0.8	6.8×10^{-4}	0.04
Apex1	0.3	7.1×10^{-4}	0.04
Psmd4	0.6	0.001	0.05
Psmg2	-4.2	0.001	0.06
Hspa4	0.2	0.001	0.07
Ndufaf3	0.3	0.001	0.07
Dnajc10	1.2	0.001	0.09
Lactb	0.5	0.002	0.09
Lars1	0.4	0.002	0.10
Nup133	1.0	0.002	0.10
Camk2d	0.1	0.002	0.11
Rab7a	0.4	0.002	0.11
Kctd5	1.3	0.003	0.15
Pdcl	0.9	0.003	0.15
Rpl37	1.9	0.003	0.15
Farsb	0.2	0.003	0.16
Lars2	1.4	0.004	0.16
Sorl1	0.8	0.004	0.18
Ogt	0.6	0.004	0.19
Eef1a1	0.2	0.005	0.19
Hnrnpul1	0.2	0.005	0.19
Adsl	0.4	0.005	0.19
Ddr1	2.1	0.005	0.19
Snx33	0.5	0.005	0.19
Nemf	1.8	0.006	0.21
Lsm12	0.8	0.006	0.21
Abcf3	0.6	0.006	0.22
Cars1	0.9	0.006	0.23

Gca	0.3	0.006	0.23
Msto1	1.4	0.007	0.24
Btf3	0.3	0.007	0.24
Tsr2	-0.7	0.007	0.24
Tpd52	0.1	0.007	0.24
Npepps	0.4	0.007	0.24
Rnf40	-0.5	0.007	0.24
Eif3a	0.3	0.008	0.25
Drg2	0.3	0.008	0.25
Sec61g	0.8	0.008	0.25
Rdh14	0.5	0.008	0.25
Zhx3	-0.6	0.008	0.26
Serhl	-1.1	0.009	0.27
Mrpl3	0.6	0.009	0.27
Epb41l3	0.6	0.009	0.27
Tmx3	0.5	0.010	0.30

Top 50 differentially expressed intracellular proteins obtained from LC/MS data set of MS-High compared to MS-Low condition. Proteins are classified according to their adjusted p-value. Significant differentially expressed proteins (adjusted p-value <0.05) are highlighted in bold. Mouse gene ID symbols are shown.

Table 9. Top intracellular proteins differentially expressed in astrocytes exposed to CSF from MS-High patients compared to NINC controls.

Gene	Log_2 (Fold change)	p-value	Adjusted p-value
Rabggtb	-1.5	1.2×10^{-4}	0.007
Atp6v1g1	-0.5	1.7×10^{-4}	0.01
Med22	-0.7	2.3×10^{-4}	0.01
Rdh14	0.5	2.7×10^{-4}	0.01
Pon2	-1.7	2.7×10^{-4}	0.01
Grb2	-1.2	3.3×10^{-4}	0.02
Samd1	2.5	5.6×10^{-4}	0.03
Prpf6	-1.0	7.0×10^{-4}	0.03
Aldh3a2	0.7	7.0×10^{-4}	0.03
Zfp27	-2.0	0.001	0.06
Hnrnpul1	0.5	0.001	0.06
Ppp1r7	0.3	0.001	0.06
Snx2	-0.3	0.001	0.08
Hspb11	-0.4	0.002	0.08
Zfyve21	0.9	0.002	0.08
Ywhaq	-0.3	0.002	0.09
Tkfc	-0.4	0.002	0.09
Mtch2	0.7	0.002	0.09
Mtss2	-0.4	0.002	0.09
Cuta	0.5	0.002	0.09
Acp2	0.5	0.002	0.09
Mrrf	1.7	0.002	0.10
Apex1	0.3	0.002	0.10
Aars2	4.3	0.002	0.10
Lrrc40	0.7	0.003	0.10
Thoc3	0.8	0.003	0.10
Pmpca	0.3	0.003	0.11
Isy1	-1.4	0.003	0.11
Kifbp	-0.7	0.003	0.11
Ptpn23	-0.6	0.003	0.11
Cox17	-0.7	0.003	0.11
Egln1	-1.6	0.003	0.11
Ubtd2	-0.7	0.003	0.12
Taldo1	-0.3	0.004	0.13

Smarcc2	0.8	0.004	0.13
Ssbp1	-1.3	0.004	0.13
Hspa13	0.8	0.004	0.13
Srgap2	-0.4	0.004	0.14
Isoc1	-0.5	0.004	0.14
Gripap1	-1.2	0.004	0.14
Ptgr2	-0.8	0.004	0.14
Csnk2a1	0.5	0.004	0.14
Pcnp	-0.8	0.004	0.14
Eif3g	-0.4	0.005	0.14
Txndc5	0.3	0.005	0.14
Rps19	-0.3	0.005	0.14
Slc16a1	-1.3	0.005	0.14
Clip2	-1.0	0.005	0.15
Actr1a	0.5	0.005	0.15
Tmx3	0.9	0.005	0.15

Top 50 differentially expressed intracellular proteins obtained from LC/MS data set of MS-High compared to NINC condition. Proteins are classified according to their adjusted p-value. Significant differentially expressed proteins (adjusted p-value <0.05) are highlighted in bold. Mouse gene ID symbols are shown.

This gene expression signature obtained with microarrays was successfully validated by qPCR (**Figure 23**) and was mostly comprised of down-regulated immediate early response genes (*Nr4a1, Fosb, Egr2* and *Klf6*), which are transcription factors that regulate gene expression. In fact, *Nr4a1* and *Klf6* have been associated to anti-inflammatory responses by specifically repressing NF-kB activity and thus inhibiting its downstream targeted genes (254-256). Also, down-regulated *Ptgs2* gene has been associated to an astrocyte A2 reactive state marker and was found to be decreased in neuroinflammatory-exposed astrocytes *in vitro* (216). *Ptgs2* has also been involved in synaptic plasticity regulation through the synthesis of prostaglandin E2 (257, 258).

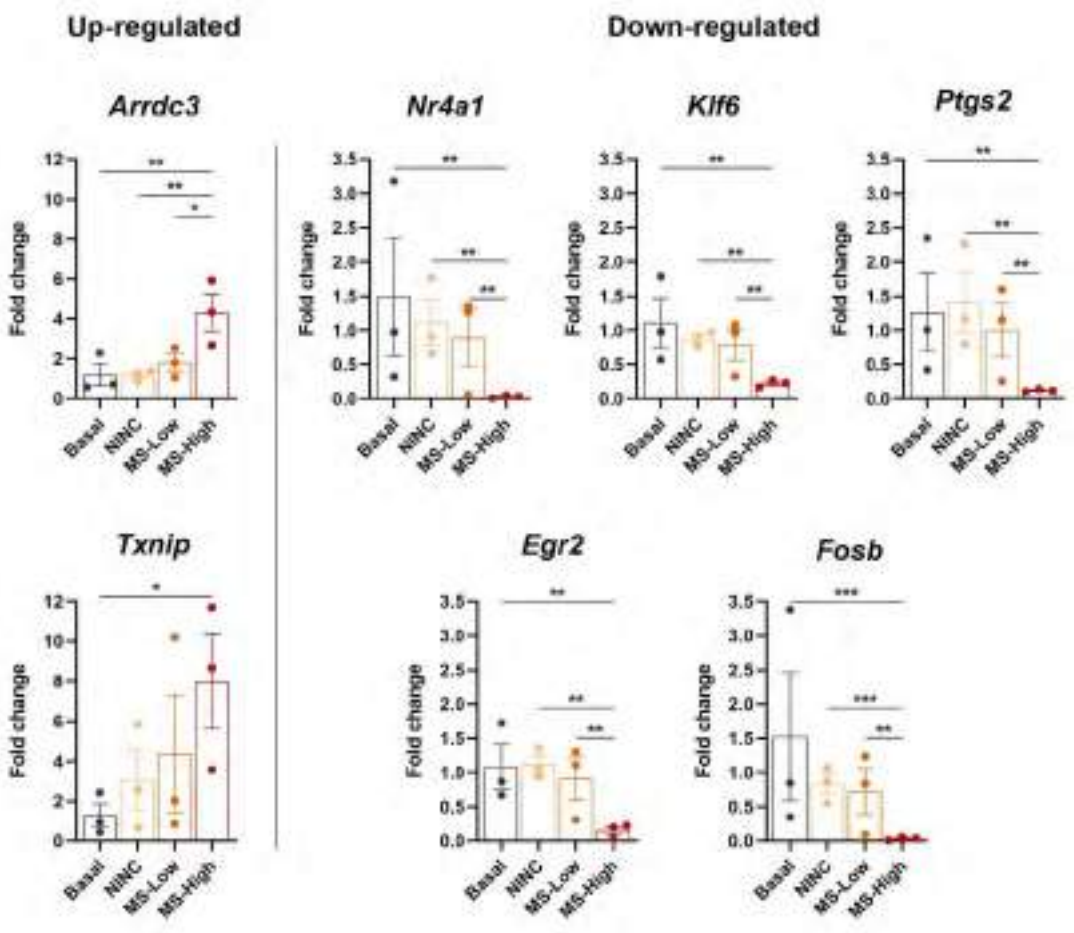

Figure 23. Validation of the astrocyte-specific gene expression signature associated to the exposure to CSF from MS patients with high inflammatory activity. mRNA expression levels measured by qPCR of the specific gene expression signature associated with astrocyte exposure to CSF from MS-High patients. Individual values represent fold change = $2^{-(\text{average } \Delta\Delta Ct)}$ in mRNAs of CSF-exposed astrocytes relative to non-stimulated astrocytes (Basal). Least Squares Means Estimates test and Dunnett-Hsu test for multiple comparisons; n=3 independent biological samples per group. Data are shown as mean (SEM). *p<0.05, **p<0.01, ***p<0.001. Abbreviations: NINC: non-inflammatory neurological controls; MS-Low: low inflammatory multiple sclerosis; MS-High: high inflammatory multiple sclerosis Arrdc3: arrestin domain containing 3; Nr4a1: nuclear receptor subfamily 4 group A member 1; Klf6: Kruppel like factor 6; Ptgs2: prostaglandin-endoperoxide synthase 2; Txnip: thioredoxin interacting protein; Egr2: early growth response 2; Fosb: FosB proto-oncogene.

To further decipher the specific MS-High-induced reactive astrocyte state, we performed a functional enrichment analysis integrating all data sets obtained from CSF exposed astrocytes. Overall, this revealed a prominent pro-inflammatory signature when compared with both the MS-Low (**Figure 24A**) and non-inflammatory control (**Figure 24B**) conditions. In concordance with these data, we found that *Nfkb1* was the main regulatory transcription factor of the MS-High-exposed astrocyte-specific fingerprint, compared to both the MS-Low (FDR=2.0 x 10^{-8}, **Figure 24A**) and non-inflammatory control exposures (FDR=1 x 10^{-13}, **Figure 24B**), together with transcription factor p65 (*Rela*), that forms an heterodimeric complex with *Nfkb1,* in the MS-High versus the non-inflammatory control condition (FDR=1.2 x 10^{-6}, **Figure 24B**). *Trp53*, which is known to induce NF-kB activation (248), was also overrepresented in astrocytes exposed to CSF from MS-High patients compared to both the MS-Low (FDR=6.3 x 10^{-10}, **Figure 24A**) and non-inflammatory control exposures (FDR=6.3 x 10^{-7}, **Figure 24B**).

Taken together, these findings indicate that astrocytes exposed to CSF from MS patients with high inflammatory activity acquire a specific reactive state characterized by an enhanced pro-inflammatory signature mainly associated with NF-kB signalling.

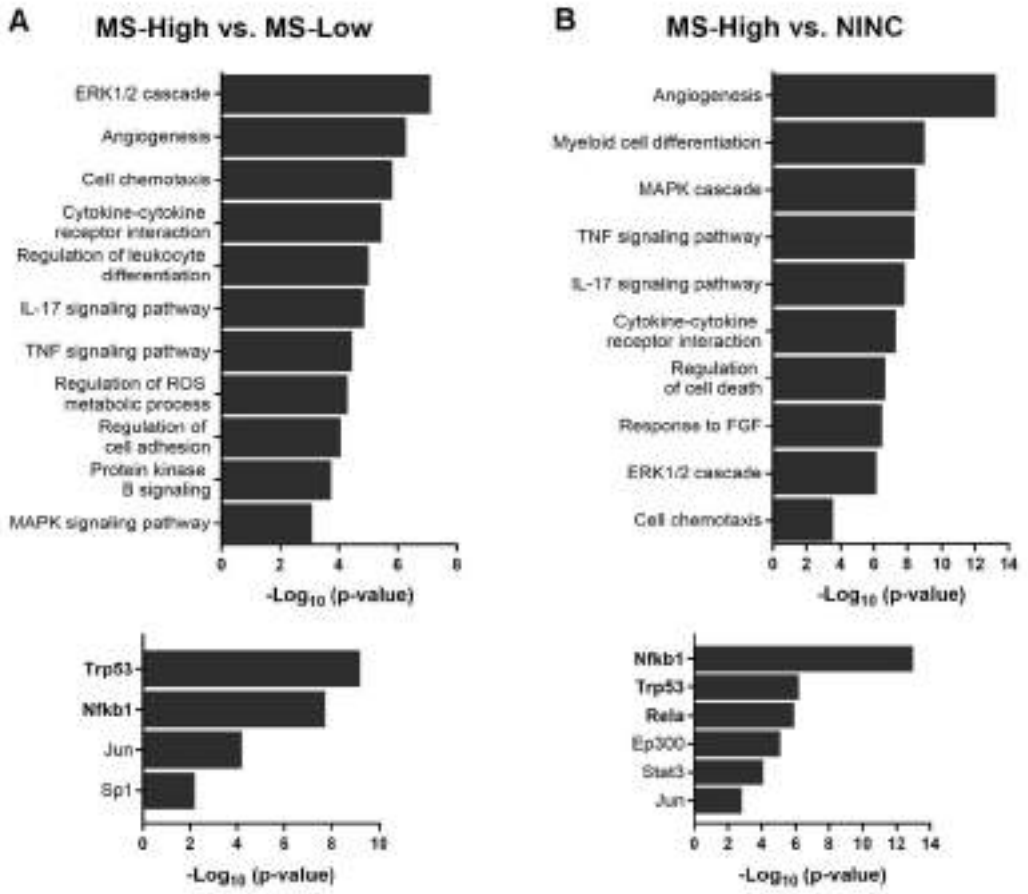

Figure 24. Astrocytes exposed to MS-High-derived CSF exhibit a pro-inflammatory signature characterized by an enhanced NF-kB signalling. Plots showing functional annotation enrichment analysis integrating transcriptomic, proteomic and secretomic data of MS-High compared to MS-Low (A) and non-inflammatory (NINC, B) exposed reactive astrocytes. Abbreviations: MS-High: high inflammatory multiple sclerosis; MS-Low: low inflammatory multiple sclerosis; NINC: non-inflammatory neurological controls; IL: interleukin; TNF: tumour necrosis factor; MAPK: mitogen-activated protein kinase; FGF: fibroblast growth factor; ERK1: mitogen-activated protein kinase 3; ERK2: mitogen-activated protein kinase 2; Trp53: cellular tumour antigen p53; Nfkb1: nuclear factor-kappa-B p105 subunit; Jun: transcription factor AP-1; Sp1: transcription factor Sp1; Rela: transcription factor p65; Ep300: histone acetyltransferase p300; Stat3: signal transducer and activator of transcription 3.

Chitinase 3-like 1 is a potential mediator of the reactive astrocyte state by enhancing the pro-inflammatory NF-kB signalling pathway

Finally, we investigated whether the pro-inflammatory reactive astrocyte state is associated with a specific CSF protein profile in MS patients with high inflammatory activity, with the ultimate goal of identifying potential mediators of the astrocytic alteration. To this aim, we fully characterized CSF pools samples using LC/MS analysis. The CSF proteome of MS-High patients clearly differed from the proteomes of MS-Low patients and non-inflammatory controls (**Figure 25A**). Of note, further characterization of the CSF proteome revealed prognostic biomarkers previously identified by our group in patients at the time of the first demyelinating event such as Semaphorin-7A (SEMA7A, FC=-0.9, p=8.7 x 10^{-5}, adjusted p=0.003, versus NINC) (139, 259), Beta-Ala-His dipeptidase (CNDP1, FC=-1.0, p=0.014, adjusted p=0.1, versus NINC) (139), and CHI3L1 (FC=1.0, p=0.005, adjusted p=0.08, versus MS-Low) (139, 140) (**Figure 25B**, **Table 10** and **Table 11**).

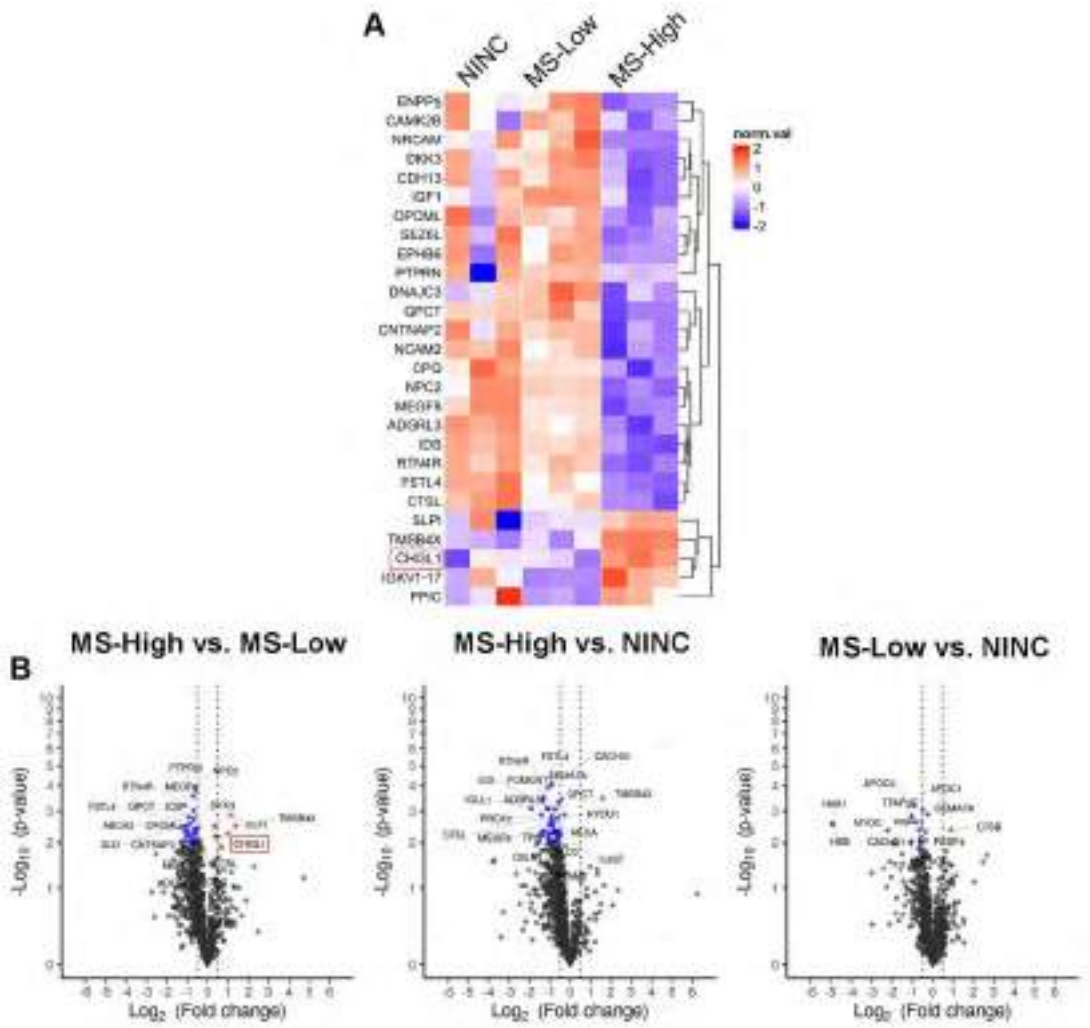

Figure 25. CSF proteome of MS-High patients exhibit a specific profile. Liquid chromatography/mass spectrometry analysis of CSF from MS patients with inflammatory activity (MS-High), low inflammatory activity (MS-Low), and non-inflammatory neurological controls (NINC). (A) Heatmap and (B) volcano plots showing normalized Log_2 protein expression satisfying p-value <0.01 and absolute fold change >0.5 identifying up-regulation of CHI3L1 in MS-High CSF (inset). (B) Significant differentially expressed proteins (adjusted p-value <0.05) are highlighted in blue (down-regulated) and red (up-regulated). Abbreviations: NINC: non-inflammatory neurological controls; MS-Low: low inflammatory multiple sclerosis; MS-High: high inflammatory multiple sclerosis; CHI3L1: chitinase 3-like 1.

Table 10. Top proteins differentially expressed in CSF pools from MS-High patients compared to MS-Low.

Gene	Log_2 (Fold Change)	p-value	Adjusted p-value
NPC2	-0.6	1.4×10^{-4}	0.004
PTPRN	-0.7	2.7×10^{-4}	0.008
RTN4R	-1.1	6.3×10^{-4}	0.02
MEGF8	-0.7	9.7×10^{-4}	0.02
SLPI	1.1	0.001	0.03
IDS	-0.9	0.001	0.04
QPCT	-0.7	0.002	0.04
IGKV1D-39	4.1	0.001	0.04
FSTL4	-0.8	0.002	0.06
ABCA2	-1.1	0.003	0.06
OPCML	-1.0	0.003	0.06
IGKV1-17	1.4	0.003	0.06
CD109	0.3	0.003	0.06
TMSB4X	1.4	0.003	0.06
DLD	-1.3	0.003	0.06
IGHV1-46	2.3	0.003	0.06
DKK3	-0.6	0.004	0.07
SUSD5	-0.4	0.004	0.07
ADGRL3	-0.7	0.004	0.07
CNTNAP2	-1.1	0.005	0.07
IGF1	-0.9	0.005	0.07
CTSL	-0.6	0.005	0.08
CHI3L1	1.0	0.005	0.08
ENPP5	-0.9	0.006	0.09
CPQ	-0.7	0.006	0.09
EPHB6	-1.0	0.006	0.09
SERPING1	0.4	0.006	0.09
PPIC	0.5	0.007	0.09
DNAJC3	-1.1	0.008	0.10
SEZ6L	-0.6	0.008	0.10
SEMA7A	-0.4	0.008	0.10
CDH13	-0.8	0.008	0.10
KLK6	-0.5	0.009	0.10
NRCAM	-0.6	0.009	0.10

NCAM2	-0.7	0.009	0.10
CAMK2B	-1.3	0.009	0.10
PTPRZ1	-0.8	0.01	0.11
IGLV1-47	1.1	0.01	0.11
IGLV2-14	2.7	0.01	0.11
CNTN1	-0.3	0.01	0.11
LY6H	-0.4	0.01	0.11
MT1G	-1.2	0.01	0.11
THY1	-0.5	0.01	0.12
NPTX1	-0.7	0.01	0.12
SEMA6D	-1.1	0.01	0.12
GLDN	0.7	0.01	0.12
IGHV6-1	2.4	0.01	0.12
PCDH1	-1.0	0.01	0.12
NCAN	-0.8	0.01	0.12
APLP2	-1.3	0.01	0.12

Top 50 differentially expressed CSF proteins obtained from LC/MS data set of MS-High compared to MS-Low condition. Proteins are classified according to their adjusted p-value. Significant differentially expressed proteins (adjusted p-value <0.05) and CHI3L1 are highlighted in bold. Human gene ID symbols are shown.

Table 11. Top 50 proteins differentially expressed in CSF pools from MS-High patients compared to NINC controls.

Gene	Log_2 (Fold Change)	p-value	Adjusted p-value
SEMA7A	-0.9	8.7×10^{-5}	0.003
CACHD1	-1.1	1.2×10^{-4}	0.003
FSTL4	-1.3	3.1×10^{-4}	0.009
TMSB4X	1.6	3.3×10^{-4}	0.009
LCAT	-0.4	3.6×10^{-4}	0.009
RTN4R	-1.3	4.3×10^{-4}	0.01
QPCT	-0.6	4.8×10^{-4}	0.01
IDS	-1.1	8.0×10^{-4}	0.02
POMGNT1	-0.7	8.7×10^{-4}	0.02
IGLL1	-1.9	8.1×10^{-4}	0.02
ADGRL3	-1.0	8.4×10^{-4}	0.02
AGT	-0.3	0.001	0.02
PRDX2	-1.4	0.001	0.02
CTSL	-0.9	0.001	0.03
HYOU1	-0.6	0.001	0.03
MEGF8	-0.9	0.001	0.03
HEXA	-0.8	0.002	0.04
TPI1	-0.9	0.002	0.04
CBLN1	-1.0	0.003	0.04
NCAM2	-0.9	0.003	0.05
IL6ST	-0.7	0.004	0.06
CNTN2	-0.6	0.004	0.06
PLD3	-1.3	0.004	0.06
SEMA3B	-0.8	0.004	0.06
MGAT1	-0.8	0.005	0.06
GOT1	-0.7	0.005	0.06
NPEPPS	-1.4	0.005	0.06
SORL1	-0.9	0.005	0.07
LRP1	-0.5	0.005	0.07
HYAL1	-1.1	0.005	0.07
FAT2	-0.7	0.006	0.07
CLSTN1	-0.5	0.006	0.07
FSCN1	-1.4	0.006	0.07
LINGO1	-1.5	0.006	0.07
SCG5	-0.6	0.007	0.07

SEMA6D	-1.1	0.007	0.07
IGLV2-14	3.5	0.008	0.08
WFDC2	-0.6	0.008	0.08
PTPRZ1	-1.0	0.008	0.08
NDRG4	-0.9	0.008	0.08
EFNA3	-0.8	0.009	0.09
NPC2	-0.7	0.009	0.09
IGKV2-40	2.6	0.009	0.09
NTNG1	-1.5	0.009	0.09
NFASC	-0.8	0.01	0.09
CEMIP	-1.0	0.01	0.09
PCDH9	-0.8	0.01	0.09
CDH15	-1.1	0.01	0.09
ATP6AP1	-0.8	0.01	0.09
MT1G	-1.6	0.01	0.09

Top 50 differentially expressed CSF proteins obtained from LC/MS data set of MS-High compared to NINC condition. Proteins are classified according to their adjusted p-value. Significant differentially expressed proteins (adjusted p-value <0.05) are highlighted in bold. Human gene ID symbols are shown.

To elucidate the primary mechanisms underlying astrocyte reactivity, we further depeened our study by performing an integrative omics data analysis with data sets at 3 different levels: (i) CSF from MS-High and MS-Low phenotypes (LC/MS); (ii) CSF-stimulated reactive astrocytes (microarrays and LC/MS); and (iii) CSF-stimulated reactive astrocytic secretomes (proteome array). Bioinformatic functional annotation analysis revealed the mitogen-activated protein kinase (ERK)-1/2 cascade ($p=4.7 \times 10^{-11}$), NF-κB-inducing kinase (NIK)/NF-kB signalling (p=0.004), *Nfkb1* (FDR=5.3×10^{-8}) and *Trp53* (FDR=5.3×10^{-8}) as the most significantly enriched pathways and transcription factors, respectively, by the exposure to a highly inflammatory MS microenvironment (**Figure 26**). These data reinforce the role of an enhanced NF-kB signalling in the MS-High-exposed reactive astrocytes.

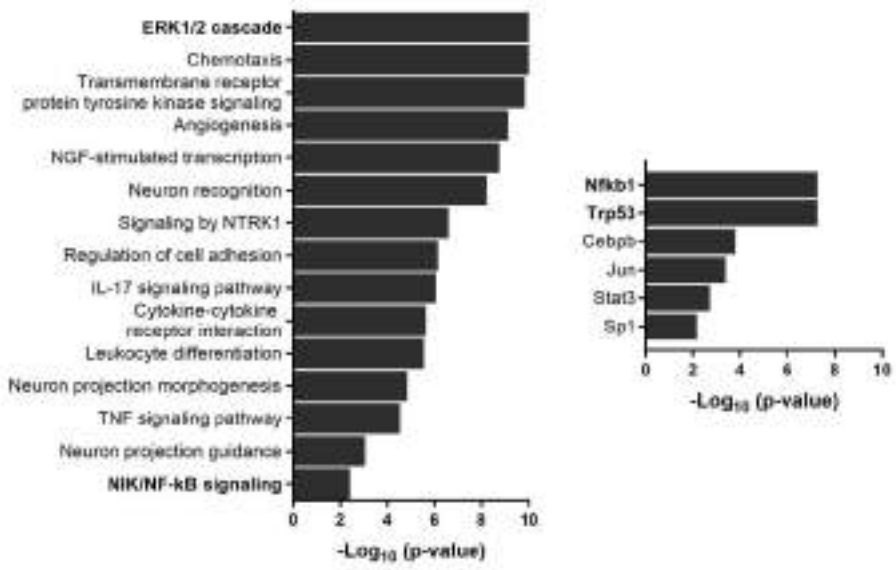

Figure 26. Bioinformatic analysis integrating the astrocyte reactive signature point to enhanced NF-kB signalling. Plots showing bioinformatic annotation analysis integrating CSF, reactive astrocytes and astrocytic secretome data sets of MS-high compared to MS-Low condition. Abbreviations: ERK1: mitogen-activated protein kinase 3; ERK2: mitogen-activated protein kinase 1; NGF: nerve growth factor; NTRK1: high affinity nerve growth factor receptor; IL: interleukin; TNF: tumour necrosis factor; NIK: NF-κB-inducing kinase; NF-kB: nuclear factor-kappa B; Nfkb1: nuclear factor-kappa-B p105 subunit; Trp53: cellular tumour antigen p53; Cebpb: CCAAT/enhancer-binding protein beta; Jun: transcription factor AP-1; Stat3: signal transducer and activator of transcription 3; Sp1: transcription factor Sp1.

Remarkably, we identified CHI3L1 up-regulated in the CSF proteome of MS-High patients, which was also represented in the aforementioned pathways (**Table 12**).

Table 12. CHI3L1 representation in astrocyte-specific fingerprint.

Pathways	Adjusted p-value	Genes
ERK1/2 cascade	4.7×10^{-11}	*ATF3, CASR,* ***CHI3L1****, DUSP1, DUSP6, EPHB2, HMGB1, IGF1, KDR, LIF, PDGFB, CCL12, CCL19, SPRY1, SPRY2, SPRY4, DUSP5, IL11, LEP, SORL1, GDF15, DDR1, CSF1, EGR1, EPHB6, ARRDC3, IRGM, IGFBP5, AKR1C3*
Angiogenesis	7.8×10^{-10}	*CDH13,* ***CHI3L1****, EGR3, EPHB2, HMGB1, NR4A1, KDR, LEP, MMP2, NRCAM, SERPINE1, PRL, PTGS2, CCL12, SP1, ADAMTS1, SPRY2, KLF2, PLK2*
Regulation of cell adhesion	7.5×10^{-7}	*DDR1, CDH13, CSF1, DUSP1, EGR3, HMGB1, IGF1, KDR, LEP, LIF, SERPINE1, PDGFB, CCL12, CCL19, SASH3, NFKBIZ, SPRY4, FOS, KLF6, CTSL, EGR1, IL11, ZFP36,* ***CHI3L1****, TMSB4X, TBK1, PSMD4, PTGS2, SORL1, KLF2*
NIK/NF-kB signaling	0.004	***CHI3L1****, HMGB1, PSMD4, CCL19, TMSB4X*

Bioinformatic functional annotation analysis integrating CSF, reactive astrocytes and astrocytic secretome data sets of MS-high compared to MS-Low condition. CHI3L1 is highlighted in bold. Human gene ID symbols are shown. Abbreviations: CHI3L1: chitinase 3-like 1; CCL: C-C motif chemokine; CSF1: M-CSF; IL: interleukin; LEP: leptin; LIF: leukemia inhibitor factor; PDGFB: platelet-derived growth factor subunit B; IGFBP5: insulin-like growth factor-binding protein 5; MMP2: matrix metalloproteinase-2.

Taking into account that CHI3L1 is considered an astrocytic reactive marker (189), and has been proposed as a prognostic biomaker in MS patients (139, 140), we wondered whether CHI3L1 could be a potential mediator of the reactive astrocyte state observed following stimulation with CSF from MS-High patients. To achieve this, we stimulated primary purified astrocyte cultures with two different CHI3L1 concentrations above 170 ng/ml (300 ng/ml and 600 ng/ml), a cut-off value that was demonstrated to have prognostic implications in patients at the time of the first demyelinating event (140), using the same exposure conditions as previously in the CSF stimulation experiments (**Figure 27A**). We next tested whether CHI3L1 was able to reproduce the gene expression signature found in MS-High reactive astrocytes. Two out of the 7 genes comprising the MS-High specific gene expression signature were significantly reduced by CHI3L1 stimulation at 600 ng/ml, *Nr4a1* ($p=0.03$) and *Klf6* ($p=0.02$) (**Figure 27B** and **Figure 28**). Of note, as previously mentioned, both genes coincide in their inhibitory role of NF-kB transcription factor and its downstream signalling, which leads to an anti-inflammatory response (254-256).

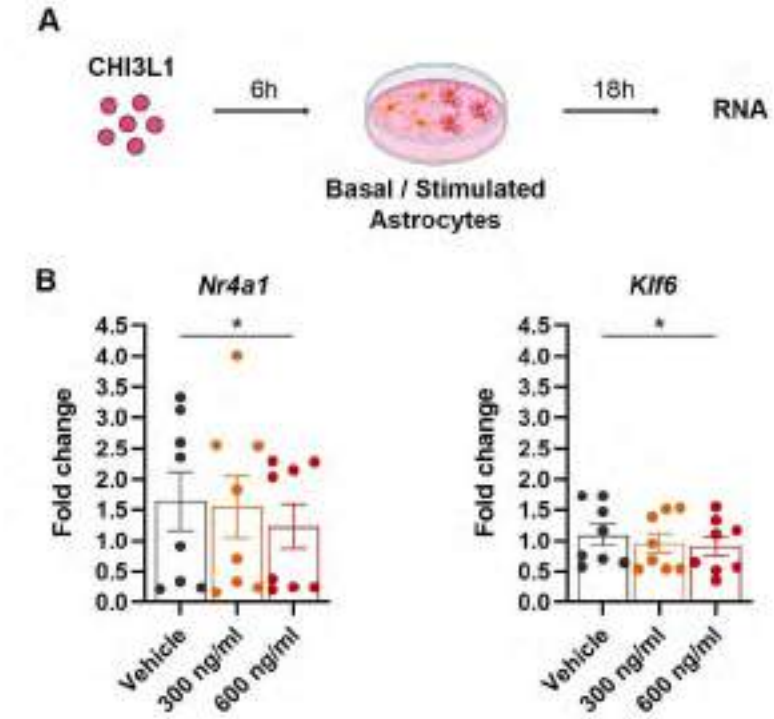

Figure 27. CHI3L1 stimulation of astrocytes reproduce down-regulation of *Nr4a1* and *Klf6*. (A) Flowchart illustrating primary purified astrocyte cultures stimulated with either PBS (Vehicle) or CHI3L1 at 300 and 600 ng/ml, using the same exposure conditions as previously in the CSF stimulation experiments. (B) qPCR assessment of CHI3L1 stimulation. Individual values represent fold change = $2^{-(\text{average } \Delta\Delta Ct)}$ in mRNAs in CHI3L1-stimulated astrocytes relative to vehicle. Least Squares Means Estimates test and Tukey-Kramer multiple comparisons test; n=8 independent biological samples per group. Data are shown as mean (SEM). *p<0.05. Abbreviations: CHI3L1: chitinase 3-like 1; RNA: ribonucleic acid; Nr4a1: nuclear receptor subfamily 4 group A member 1; Klf6: Kruppel like factor 6.

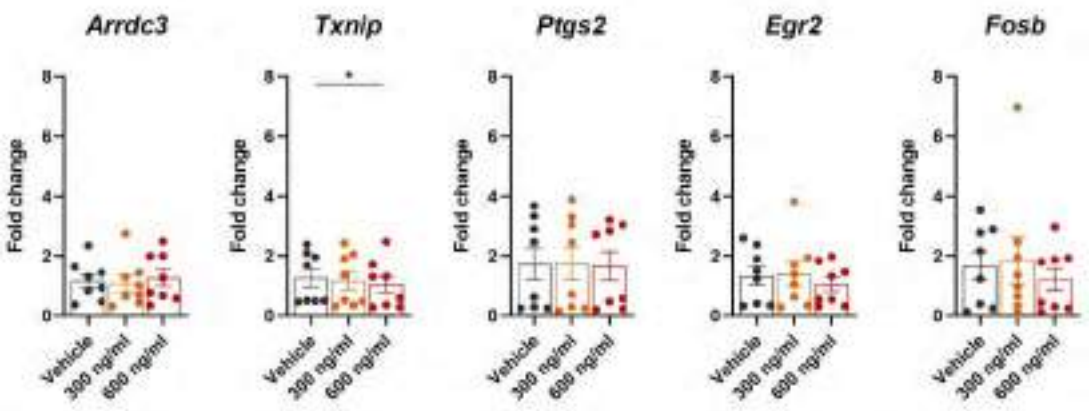

Figure 28. Expression levels of genes associated with the specific astrocyte-derived gene expression signature following CHI3L1 stimulation. qPCR assessment of CHI3L1 stimulation. Individual values represent fold change = $2^{-(\text{average } \Delta\Delta Ct)}$ in mRNAs in CHI3L1-stimulated astrocytes relative to vehicle. Least Squares Means Estimates test and Tukey-Kramer multiple comparisons test; n=8 independent biological samples per group. Data are shown as mean (SEM). *p<0.05. Abbreviations: Arrdc3: arrestin domain containing 3; Nr4a1: nuclear receptor subfamily 4 group A member 1; Klf6: Kruppel like factor 6; Ptgs2: prostaglandin-endoperoxide synthase 2; Txnip: thioredoxin interacting protein; Egr2: early growth response 2; Fosb: FosB proto-oncogene.

Protein interactome computation aiming to explore a potential cause and effect between CHI3L1 and the dysregulated transcriptional response observed in astrocytes exposed to CSF from High-MS patients, revealed an interaction between the NF-kB transcription module and both *Nr4a1* and *Klf6* molecules, which was potentially controlled by CHI3L1 ($p=3.5 \times 10^{-5}$, **Figure 29A**). Noteworthy, we found a node of interaction between mitogen-activated protein kinase (Mapk)-3 (ERK1), *Mapk1* (ERK2) and *Nr4a1* in the NF-kB transcription module, which might potentially be regulated by CHI3L1 and would also affect *Serpine1* expression (p=0.0003, **Figure 29B**), thus connecting the main molecular mediators identified at the 3 experimental levels analysed in the study, i.e., CSF - astrocyte - secretomes.

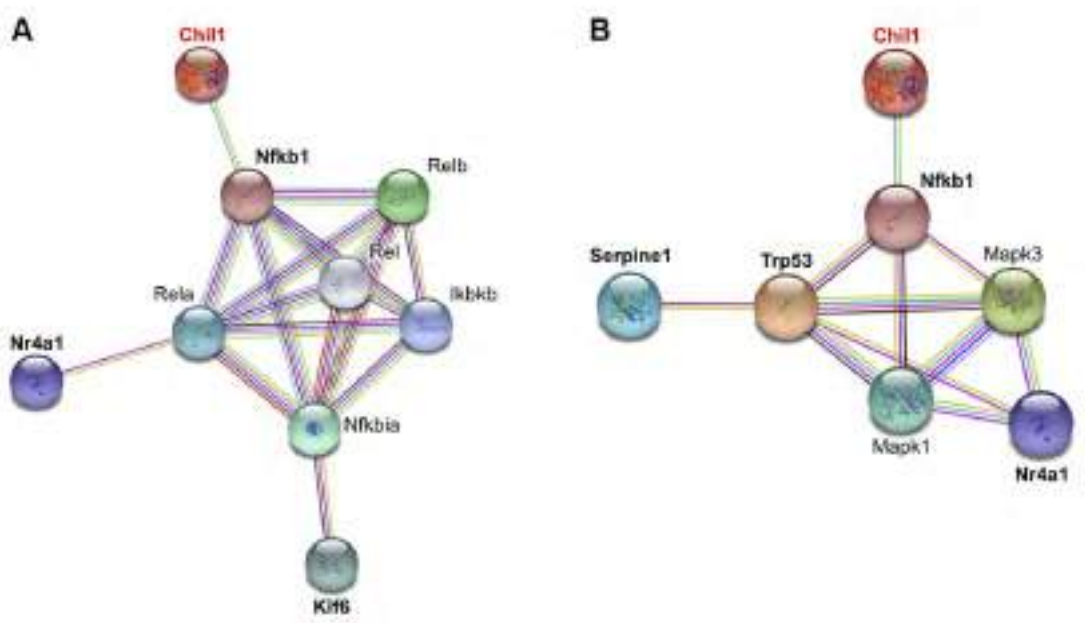

Figure 29. Protein interactome computation connecting the main potential mediators of astrocyte-specific reactive state. (A, B) Network diagrams of differentially regulated contributors of enhanced NF-kB signalling in MS-High-exposed reactive astrocytes. Abbreviations: Chil1: chitinase 3-like 1; Nfkb1: nuclear factor-kappa-B p105 subunit; Mapk1: mitogen-activated protein kinase 1, Mapk3: mitogen-activated protein kinase 3; Rela: transcription factor p65; Rel: proto-oncogene c-Rel; Ikbkb: inhibitor of nuclear factor kappa-B kinase subunit beta; Nfkbia: NF-kappa-B inhibitor alpha; Trp53: cellular tumour antigen p53.

These results indicate that the CSF of MS patients with high inflammatory activity is characterized by a unique proteome profile that induces a specific reactive astrocyte state, which is dependent on enhanced NF-kB signalling, and contains CHI3L1 as a potential mediator of astrocyte alteration.

Discussion

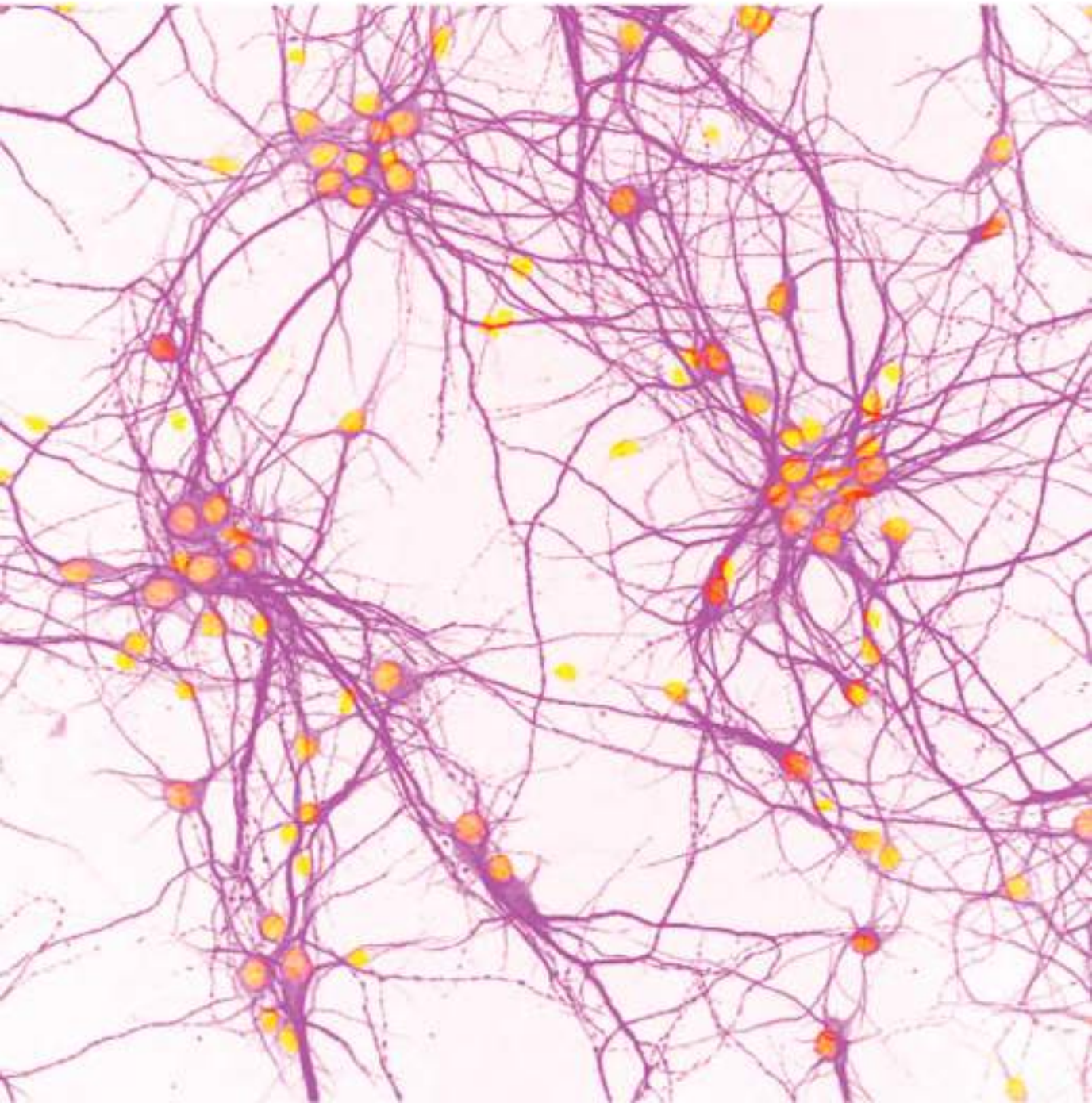

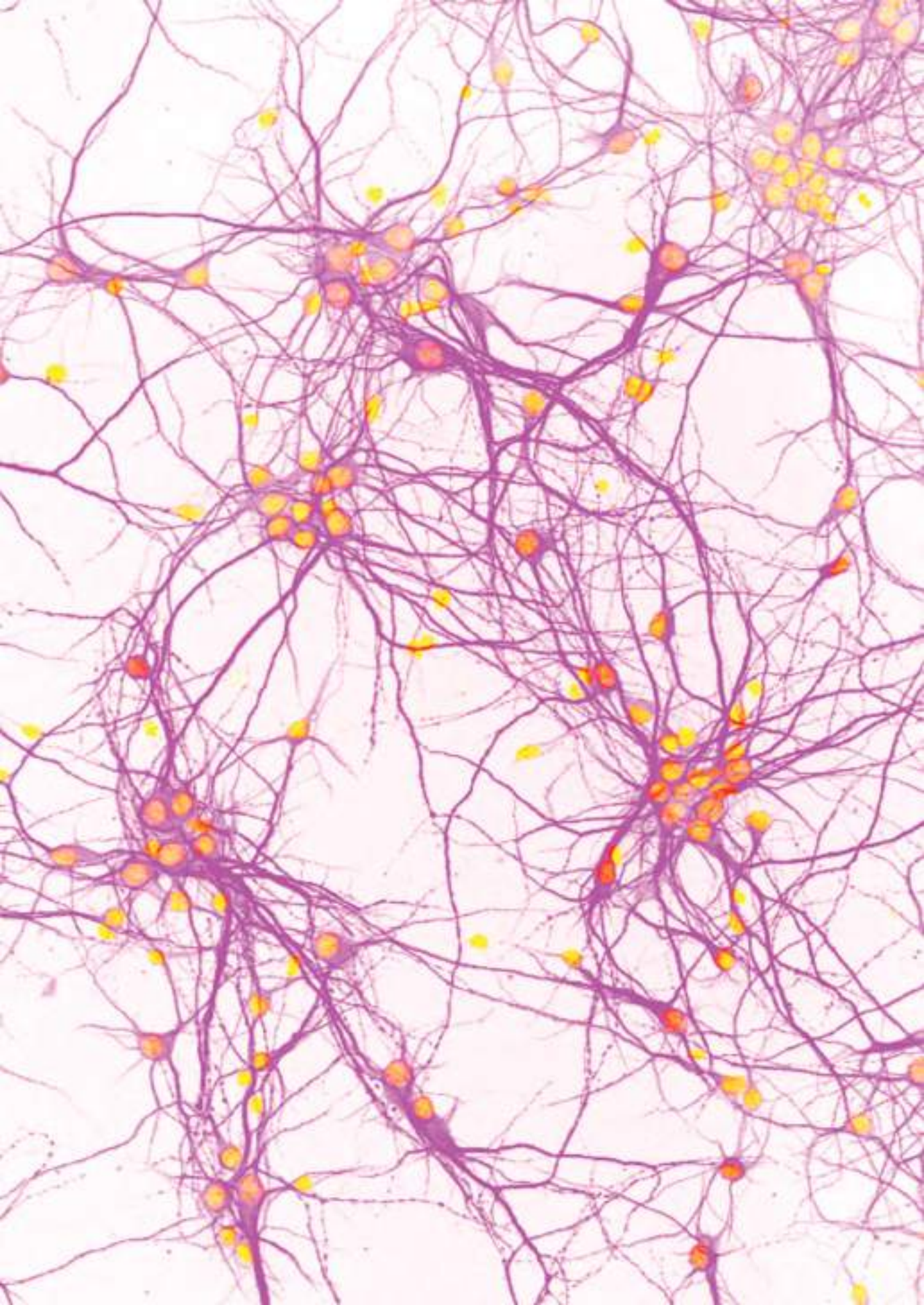

5. Discussion

An in-depth understanding of the neurodegenerative component taking place in the CNS of MS patients at the earliest phases of disease pathogenesis is crucial for the design of therapeutic approaches that may stop disease progression. Despite the centrist view of MS as an immune-mediated condition, the essential contribution of astrocytes to the neurodegenerative component of the disease is increasingly supported by several lines of evidence: (i) severe myelin alterations and neurodegeneration are observed in disorders characterized by primary astrocyte defects, such as in Alexander's disease caused by mutations in the GFAP gene (260); (ii) neuromyelitis optica is associated with antibodies targeting the astrocyte-specific water channel AQP4 (261); (iii) the potassium channel Kir4.1 expressed in astrocytes is a target of the autoantibody responses in a subgroup of MS patients (25); (iv) astrocytes regulates tightness and permeability of the BBB (19); (v) in EAE, astrocyte responses occurred before CNS inflammatory infiltrates (262) and coincided with the earliest manifestations of axonal damage (196); (vi) selective transgenic inhibition of NF-κB signalling in astrocytes exhibited reduced disease severity and better functional recovery in EAE (263); (vii) in toxic-induced demyelination model, laquinimod, an oral immunomodulatory treatment in MS with proposed neuroprotective effects, reduced NF-kB activation in astrocytes (264); (viii) a potential non-immunological CNS effect of fingolimod may occur via specific modulation of the S1P receptor 1 (S1PR1) in astrocytes (265); (ix) CCL2 production by astrocytes drove the recruitment of monocytes that promote neurodegeneration in EAE (266, 267); (x) astrocytes control disease progression in an experimental model of SPMS (204, 268); (xi) microglia-astrocyte interactions promote CNS pathology (216, 269); (xii) astrocyte-specific biomarkers, such as GFAP (270) and CHI3L1 (139, 140), determined in CSF from MS patients correlated with disability progression.

However, the mechanisms underlying astrocytic responses associated to neurodegeneration in MS are still largely unknown. In the present work, we found that exposure of astrocytes to CSF from MS patients with high inflammatory activity

induced a maladaptive response altering their secretome pattern, which ultimately impaired synaptic plasticity and induced neuronal dysfunction in a non-cell-autonomous manner.

We report for the first time an exhaustive molecular and functional characterization of astrocyte reactivity in a MS-specific inflammatory context, through the exposure of mouse primary astrocytes to the CSF from MS patients classified according to the degree of inflammatory activity. We focused on CSF from MS patients at the time of the first demyelinating event as it is the first available sample from early disease onset, because the CSF is collected for diagnostic purposes, and because at this stage disease follow-up can be long enough to confirm a higher degree of neurological disability in MS patients with high inflammatory activity. Since the CSF is the closest body fluid to the CNS that can be examined, and considering it circulates in proximity to the brain sites of inflammation, we hypothesised that the CSF would certainly reflects the pathological microenvironment occurring in the CNS of MS patients. Thus, it would reliably simulate astrocyte reactivity during the early inflammatory phase of the disease. In addition, given that the CNS inflammation is considered one of the major drivers of axonal loss in MS patients (79), we explored whether a highly inflammatory microenvironment conveyed through the CSF could contribute to neurodegeneration by modulating disease-specific astrocyte function.

Since our main goal was to specifically investigate the astrocyte response in a context of high inflammation in MS, we needed to generate an *in vitro* system that allowed us to induce astrocyte reactivity through CSF stimulation and to discriminatively elucidate the effects on astrocyte function. For this purpose, we first generated primary mixed glial cultures, in which we found a considerable microglia contamination. Most *in vitro* models used to investigate astrocytes reported in the literature are astroglial-enriched cultures with an important contamination of microglial cells present both above and below the astrocyte monolayer (271). The main problems about the presence of contaminating microglia in cell cultures are: (i) microglia is highly sensitive to a wide variety of stimuli (272); (ii) reactive microglia is very plastic and can exert both neuroinflammatory and neuroprotective responses

(273); (iii) activated microglia releases cytokines, chemokines and reactive oxygen and nitrogen species (274); (iv) an inflammatory microenvironment has the potential to induce microglia proliferation (275, 276); (v) microglial cells can modify the extracellular milieu of the cell cultures by both secreting and taking up factors of the culture medium; and (vi) small amounts of microglial cells (<5%) can be responsible for the observed effects in cultures even though astrocytes are the predominant cell type (271). Moreover, it has been reported that microglia can cause direct neuronal death by secreting neurotoxic factors (ROS, glutamate, proteases) (60, 277) as well as promote inflammation-mediated neurodegeneration through the release of pro-inflammatory cytokines (TNF, IL-1 and IL-6) (278). Considering its involvement in MS pathogenesis and that our approach was focused on the astrocyte contribution to neuronal damage through secreted factors, we addressed the removal of microglial cells from our cultures. We thus tested two different methods in order to purify mixed glial cultures: shaking and magnetic cell sorting based on MACS® technology. As expected, we found a significant reduction of contaminating microglia when purifying cultures with both methods. Indeed, MACS-purification resulted in a complete elimination of microglial cell from astrocyte cultures. Consistently, shaking was effective to reduce the proportion of contaminating microglia. However, as not all microglial cells are on the top of the astroglial monolayer, it does not allow a complete elimination of these cells (234). Taking into account we achieved a successful removal of microglia applying MACS purification at the time of culture generation without the need of subculturing or any other direct astrocyte cell manipulation, we chose this method for our astrocyte *in vitro* model.

Astrocytes exposed to CSF from MS patients with high inflammatory activity manifested an aberrant pattern of activation that modified their secretome. Remarkably, this was sufficient to alter synaptic plasticity and induce neuronal dysfunction in a non-cell autonomous manner, in agreement with other reports (216, 279). Furthermore, we observed a strong direct correlation between the degree of the inflammatory microenvironment, the exacerbation of astrocyte reactivity and the extent of neuronal damage. These findings were only observed in patients with high

inflammatory activity but not in patients with low inflammatory activity, who showed a pattern more similar to non-inflammatory neurological controls. We thus postulate that the degree of inflammation during MS leads to an astrocyte-mediated impairment of the cellular homeostasis of neurons, making them more prone to degenerate from environmental stressors along the course of the disease. Other studies already suggested a direct link between the inflammatory activity of MS patients, conveyed through the CSF, with synaptopathy processes (95, 280). However, these studies were focused on CSF neuromodulators and did not address whether these effects were mediated by a particular cell type.

A particular strength of our study was the unbiased quantification of hundreds of neurons, ensuring a robust sample size and statistical power. More importantly, the use of a well-defined unique cohort of patients allowed us to develop an *in vitro* model that discriminated the effect of different levels of physiological CNS inflammation on astrocyte reactivity. To the best of our knowledge, *in vitro* models mimicking neuroinflammation are mainly based on simplified pro-inflammatory cytokine stimulation, mostly using TNFα, IL-1β, IFN-γ and IL-6, among others (217, 281-283), or activated microglia-secreted factors IL-1α, TNFα and C1q (216). Indeed, animal models of neuroinflammation provide useful experimental systems that reproduce CNS inflammation in a fancy physiological manner to study the pathogenic role of astrocytes. However, the degree of inflammation cannot be modulated, thus, the influence of inflammation on astrocyte reactivity in terms of prognosis cannot be addressed.

To unravel the mechanisms underlying a maladaptive response to a high inflammatory microenvironment, which results in malfunctional astrocytes, we performed a unique characterization of their reactive state at the transcriptomic, proteomic and secretomic levels. Data obtained from both secretome and gene expression profiling, together with thorough bioinformatic analysis pointed to a prominent pro-inflammatory signature in astrocytes exposed to CSF derived from MS patients with high inflammatory activity, in agreement with other studies conducted in neuroinflammation models (246, 284). First, a large panel of **astrocyte-secreted**

factors, mainly cytokines, chemokines, and growth factors, were up-regulated in the highly inflammatory condition, predominantly involved in inflammatory response, immune cell chemotaxis and extracellular matrix organization. This supports existing evidence suggesting that astrocytes perpetuate immune-mediated demyelination by secreting chemokines that promote lymphocyte trafficking into the CNS and cytokines that provide suitable environment for T cell activation (66). It is worth stressing a number of particularly interesting astrocyte soluble factors that were identified. For instance, C-C motif chemokine (CCL)-19, a chemokine that in homeostasis guides B cells, naive T cells and mature dendritic cells into the secondary lymphatic organs. Its receptor, CC receptor-like 2 (CCRL2), was found overexpressed in microglia and astrocytes as well as in infiltrating macrophages during EAE (285). CCL19 has been involved in APC and lymphocyte homing into the CNS in both EAE (286) and MS patients (287), which promotes a continuous antigen stimulation and thus the chronification of inflammation. Moreover, CCL19 was found increased both in active and inactive lesions from MS patients, and elevated CSF levels correlated with intrathecal IgG production in RRMS and SPMS patients (287). On the other hand, a study demonstrated that CCL19 secretion by lymphocytes from MS patients was associated with their low remyelination ability, and exogenous addition of CCL19 abolished OPC differentiation and increased the pro-inflammatory M1 phenotype in macrophages *in vitro* (288).

Previous studies already reported the expression of CXCL1 by reactive astrocytes both in MS lesions (289) and EAE models (262, 290), in which its increased expression resulted in more severe EAE by promoting neutrophil trafficking into the CNS (291). In contrast, other studies suggested neuroprotective and remyelinating effects of the CXCL1 released by reactive astrocytes (228). Interestingly, CXCL1 up-regulation in astrocytes has also been linked to NF-κB-dependent signalling, which has shown to play a role in astrocyte-neuron interactions as neurons express its receptor (CXC receptor-like 2, CXCRL2) (292, 293). Also, CXCL1 released by astrocytes after inflammation mediated spinal cord neurons increased excitatory

synaptic transmission which ultimately contributed to the pathogenesis of inflammatory pain (294, 295).

Studies using knock-out mice for matrix metalloproteinase (MMP)-2 and MMP-9 reported resistance to EAE development (296, 297). Later, a study demonstrated that MMP-2 and MMP-9 modulated chemokine expression at the BBB, resulting in an acceleration of leukocyte infiltration into the CNS parenchyma. Moreover, this induction of chemokine expression by astrocytes was associated to the protein kinase B (AKT)/NF-kB-signalling pathway (298). Similarly, Fetuin-A deficient EAE mice showed delayed onset and reduced disease severity (299), as well as reduced immune cell trafficking into the CNS (300). Moreover, elevated Fetuin-A levels were found in the CSF from MS patients and thus was proposed as a potential biomarker (299).

In addition, proprotein convertase 9 (PCSK9) pro-inflammatory nature was confirmed when the inhibition of PCSK9 expression resulted in prevention of dendritic spine loss mediated by the attenuation of microglia activation (301). In this line, macrophage colony-stimulating factor (M-CSF) was also associated with regulation of microglia activation and was found to increase its proliferation and phagocytic capacity (302).

Consistent with the dual role of reactive astrocytes, which can exert both detrimental and beneficial effects in a disease context, a number of soluble factors identified are known to play beneficial roles in a context of CNS inflammation. For instance, the leukemia inhibitor factor (LIF) released by astrocytes has been linked to neuroprotective and remyelination effects; to mention a few: (i) LIF promoted survival of mature oligodendrocytes and myelination (303, 304); (ii) LIF induced sustained neuronal survival against excitotoxicity (305); (iii) LIF inhibition in EAE led to enhanced disease severity, demyelination, axonal injury and oligodendrocyte death (306). Also, Leptin, has been involved in regulating and enhancing synaptic transmission in the hippocampus (307) as well as in neuroprotective effects against different CNS insults (308, 309). Granulocyte colony-stimulating factor (G-CSF), a

hematopoietic growth factor, has been found to be protective in animal models of both acute and chronic neurodegenerative diseases (reviewed in (310)), in which G-CSF seems to protect oligodendrocytes by supressing inflammatory cytokines and up-regulating anti-apoptotic factors (311). Similarly, fibroblast growth factor 21 (FGF-21) has demonstrated to induce proliferation of OPCs, which could have an important role on promoting CNS regeneration (312). Recently, a study reported that growth/differentiation factor 15 (GDF-15) expression in astrocytes triggered BBB remodelling through enhanced tight junction strengthening (313). Finally, platelet-derived growth factor subtype BB (PDGF-BB), an important mitogenic factor, demonstrated protective properties in neurons exposed to oxidative stress (314) as well as in astrocytes itself by reducing ROS production and activating antioxidant mechanisms, altogether suggesting a potential compensatory mechanism of the cellular stress caused by its reactive state (315).

An important finding of the present study was the identification of **SerpinE1** among the astrocyte-secreted factors more robustly increased in the highly inflammatory condition. SerpinE1, also known as plasminogen activator inhibitor 1 (PAI-1), is the major serine protease inhibitor of tissue-type plasminogen activator (tPA/PLAT) and urokinase-type plasminogen activator (PLAU), involved in the proteolysis of plasminogen to plasmin. The plasmin system and its inhibitors are involved in many physiological and pathological processes in the CNS, particularly by promoting neurite outgrowth and supporting synaptic plasticity through the interaction with extracellular matrix proteoglycans (316-318). Consistently, our functional enrichment analysis involved SerpinE1 released from MS-High-reactive astrocytes in inflammatory response, myeloid leukocyte migration and extracellular matrix organization pathways, angiogenesis, regulation of cell adhesion and chemotaxis. In this line, previous studies have shown that SerpinE1 induces neuronal apoptosis and synaptic impairment (251, 319, 320), and exacerbates axonal damage and demyelination in EAE (252, 253). Moreover, significant increased PAI-1 expression was detected in acute MS lesions (321) as well as in the CSF of progressive MS patients with high disability, compared to those with low disability (322). Some reports

also showed a significant association between PAI-1 polymorphism and susceptibility to MS (323, 324). Taking all these data into account, we propose secreted SerpinE1 as a potential toxic mediator of the detrimental effect of astrocytes on neuronal function and plasticity.

The gene expression pattern of astrocytes exposed to CSF from MS patients with high inflammatory activity showed down-regulation of transcription factors, particularly *Nr4a1* and *Klf6*, which have been involved in responses of anti-inflammatory nature (254-256). Also, we identified *Nfkb1*, together with *Rela* and *Trp53*, as the main transcription factors regulating the MS-High-derived reactive astrocyte signature. **NF-κB** is considered a key canonical signalling cascade regulating astrocyte reactivity and an essential mediator of neuroinflammation. The inhibition of NF-κB activation in astrocytes ameliorates immune infiltrate, axonal damage, and demyelination, by preventing the establishment of the astrocyte-mediated pro-inflammatory microenvironment that leads to disease progression in EAE (263, 325). Moreover, a common MS risk variant (rs7665090) has been found associated to increased NF-κB signalling in astrocytes, driving increased lymphocyte infiltrate and lesion size (282). Altogether, our findings provide evidence that a high inflammatory microenvironment in MS patients may mediate disease progression by enhancing NF-κB signalling in astrocytes, which modifies their secretome content resulting in both immune-mediated neurodegeneration and potential direct neurotoxic effects.

Fitting all pieces together, we found a high abundance of **CHI3L1** in the CSF of MS patients with high inflammatory activity, which is in accordance with previous studies conducted by our group (139, 140) and others (326, 327). In addition, treatment of astrocytes with CHI3L1 was associated with reduced expression of negative regulators of NF-kB, which are essential for maintaining immune homeostasis and suggest that CHI3L1 is acting by enhancing NF-kB signalling in astrocytes, as it has been proposed in other pathological conditions (328-331). CHI3L1, also known as YKL-40 in humans and breast regression protein 39 (BRP-39) in mice, is a secreted glycoprotein member of the glycoside hydrolase 18

chitinase family that targets chitin but lacks enzymatic activity (332). Within the CNS, CHI3L1 is mainly secreted by reactive astrocytes (140, 333), particularly in lesions with high inflammatory activity, but also by macrophages/microglia in lesions with low inflammatory activity (140). The mechanisms of action of CHI3L1 are complex and depends on the cellular context (reviewed in (334)). What we know for now is that CHI3L1 is an acute-phase protein overall involved in triggering an inflammatory response. For instance, it has been reported that in response to pro-inflammatory stimuli, CHI3L1 secretion is induced by immune cells (335) (IFN-γ, IL-1β, or TNF-α) and astrocytes (IL-1β and TNF-α) (336, 337). Also, CHI3L1 has been linked to a regulating role in the Th1/Th2 ratio (338). But, surprisingly, both M1- and M2-polarized macrophages have shown increased expression of CHI3L1 (339), pointing to pleiotropic functions during inflammation. Recently, we described a direct neurotoxic effect of CHI3L1 that, when added to cortical neurons induced an early shortening of dendrite length that ultimately provoked a significant reduction on neuronal survival (142). It is worth stressing that CHI3L1-derived toxic effect was neuron-specific as the addition of CHI3L1 to splenocyte, microglia, and astrocyte cultures showed no changes on cell survival. Taken all together, our results support the notion that CHI3L1 may contribute to MS disease progression both by inducing a direct neurotoxic effect (142) and also by inducing a specific reactive astrocyte state with neurotoxic potential.

In conclusion, our findings provide evidence that the degree of inflammatory activity in MS patients at disease onset has the potential to induce a specific pro-inflammatory reactive state in astrocytes, which is characterized by activation of NF-kB signalling. Such maladaptive response in astrocytes triggers neuronal dysfunction and may ultimately contribute to disease progression in MS patients. These results have several implications in MS. First, the assessment of this specific astrocyte reactive state following exposure of mouse astrocytes to CSF from MS patients can be exploited as a prognostic biomarker that reflects a potential toxic effect of MS astrocytes on neuronal function. Second, the gene expression signature induced in astrocytes following exposure to CSF from MS patients with high inflammatory

activity can be utilized for the identification of therapeutic compounds that may revert the pro-inflammatory signature and reduce neuronal loss in MS patients. And last, CHI3L1 is a potential therapeutic target whose binding to astrocytes can be blocked in order to prevent the induction of the pro-inflammatory reactive astrocyte state with potential toxic effects on neurons. Altogether, these approaches may ultimately be used to identify MS patients at high risk for disease progression who are candidates for therapies that target either specific astrocyte signatures or CHI3L1 directly (**Figure 30**).

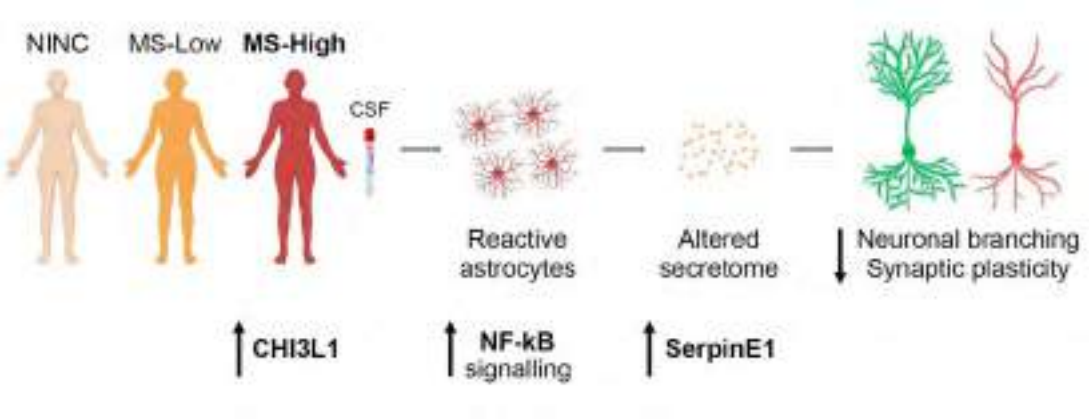

Figure 30. Role of astrocytes exposed to CSF from MS patients with high inflammatory activity. High inflammatory activity in patients with MS (MS-High) induces a specific reactive astrocyte state *in vitro* characterized by an enhanced NF-κB activation, which confers a maladaptive response accompanied by an altered secretome that leads to neuronal dysfunction and synaptic plasticity impairment. SerpinE1 up-regulated in astrocytic secretomes is a potential downstream mediator of non-cell-autonomous neuronal damage. In addition, chitinase 3-like 1 (CHI3L1), increased in CSF from MS-High patients, is a potential upstream modulator of astrocyte reactivity. Abbreviations: NINC: non-inflammatory neurological controls; MS: multiple sclerosis; MS-Low: low inflammatory multiple sclerosis; MS-High: high inflammatory multiple sclerosis; CHI3L1: chitinase 3-like 1; CSF: cerebrospinal fluid; NF-κB: nuclear factor kappa B.

Conclusions

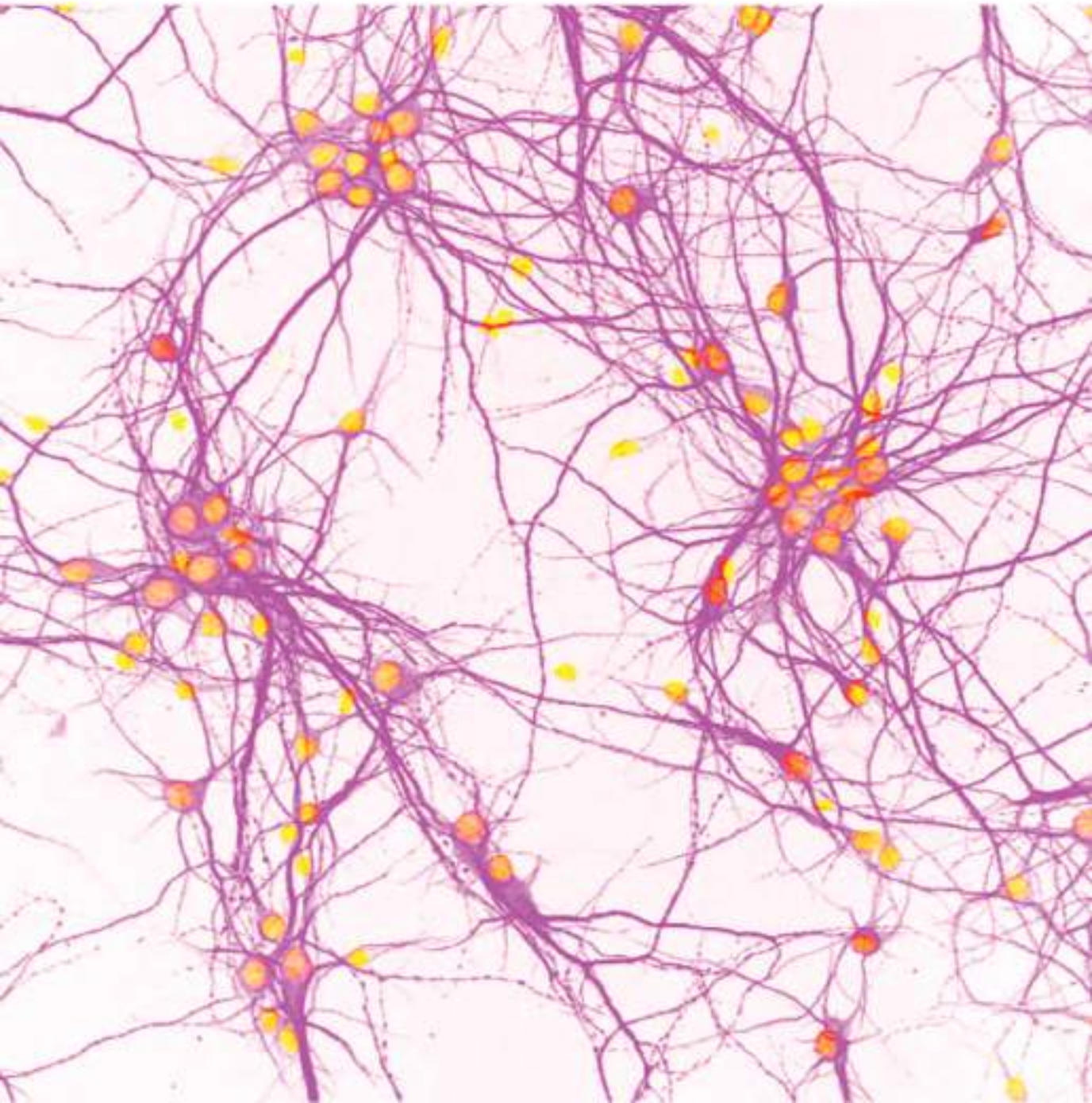

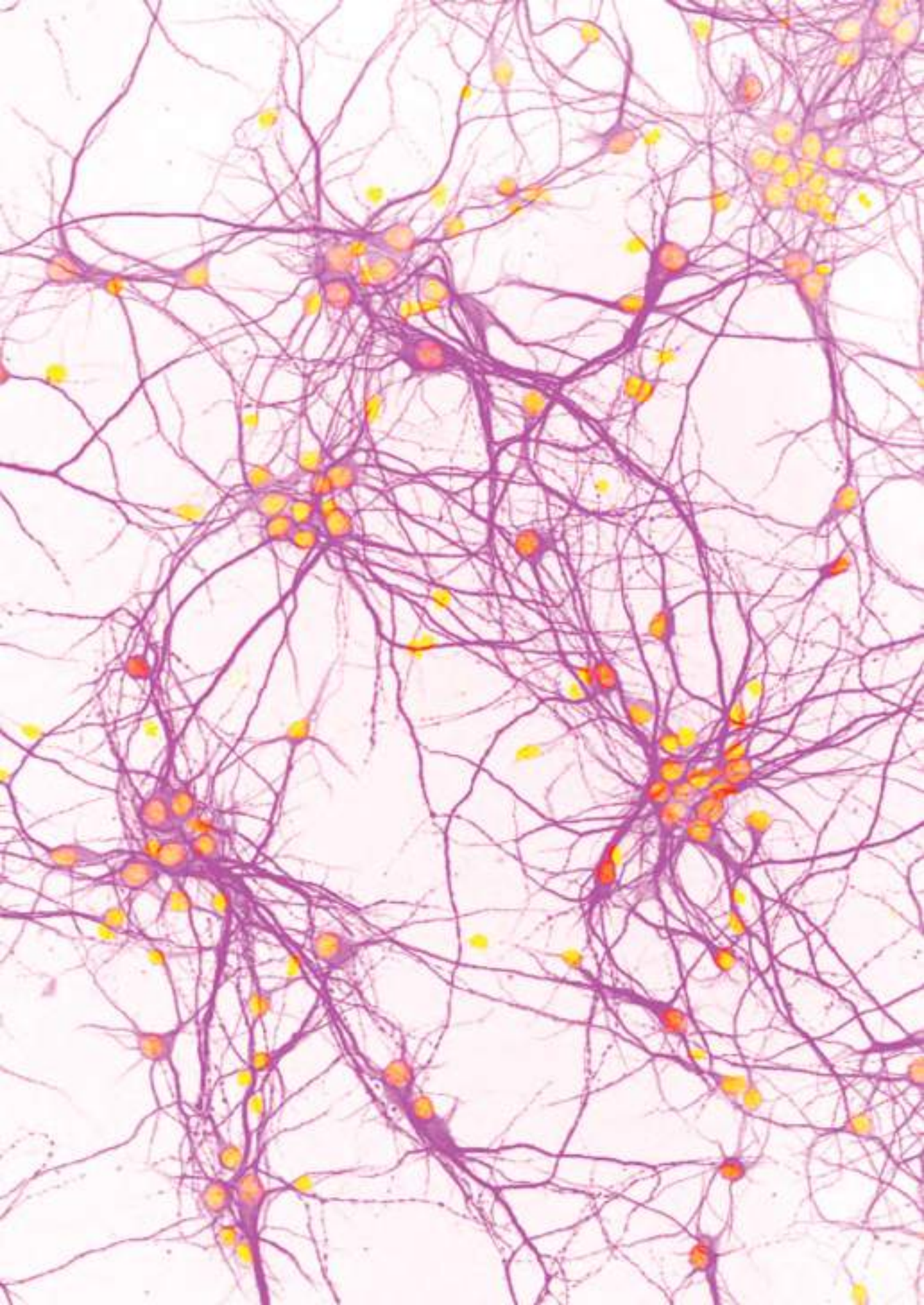

6. Conclusions

1. Astrocytes exposed to a high inflammatory MS microenvironment induce non-cell-autonomous **neuronal dysfunction**.

2. **Secretomes** from astrocytes exposed to CSF from MS patients with high inflammatory activity have a prominent pro-inflammatory content that is potentially regulated by NF-kB signalling.

3. **SerpinE1** is increased in secretomes derived from astrocytes exposed to CSF from MS patients with high inflammatory activity and may be one of the toxic mediators of the paracrine effect of astrocytes on neuronal function and plasticity.

4. Astrocytes exposed to CSF from MS patients with high inflammatory activity acquire a **specific pro-inflammatory reactive state** characterized by an enhanced pro-inflammatory signature mainly associated with NF-kB signalling.

5. The CSF of MS patients with high inflammatory activity is characterized by a unique proteome profile that induces a specific reactive astrocyte state and is potentially mediated by **CHI3L1**.

6. The maladaptive response of astrocytes to a high inflammatory MS microenvironment triggering neuronal dysfunction may ultimately contribute to disease progression in MS patients.

Future perspectives

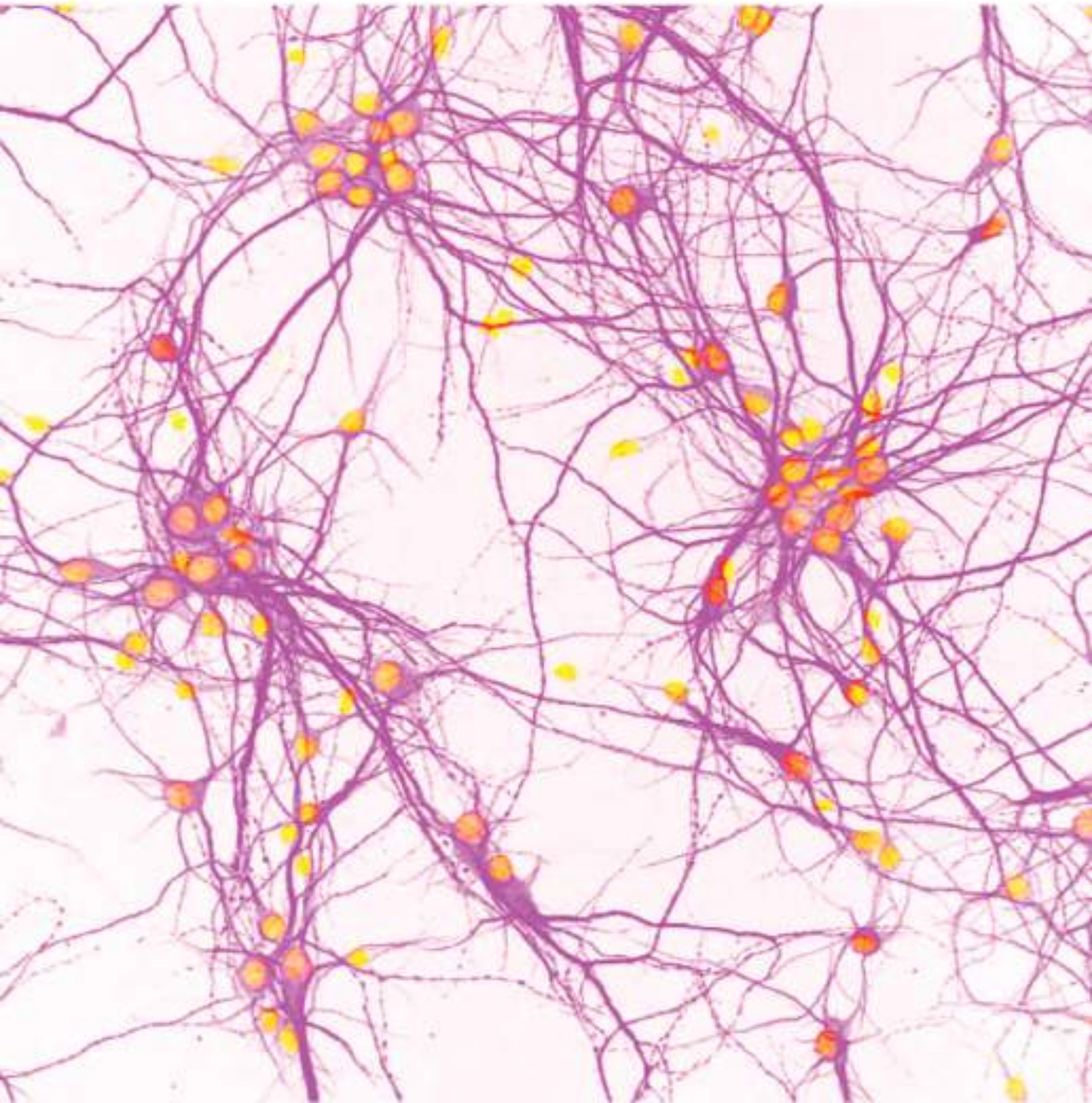

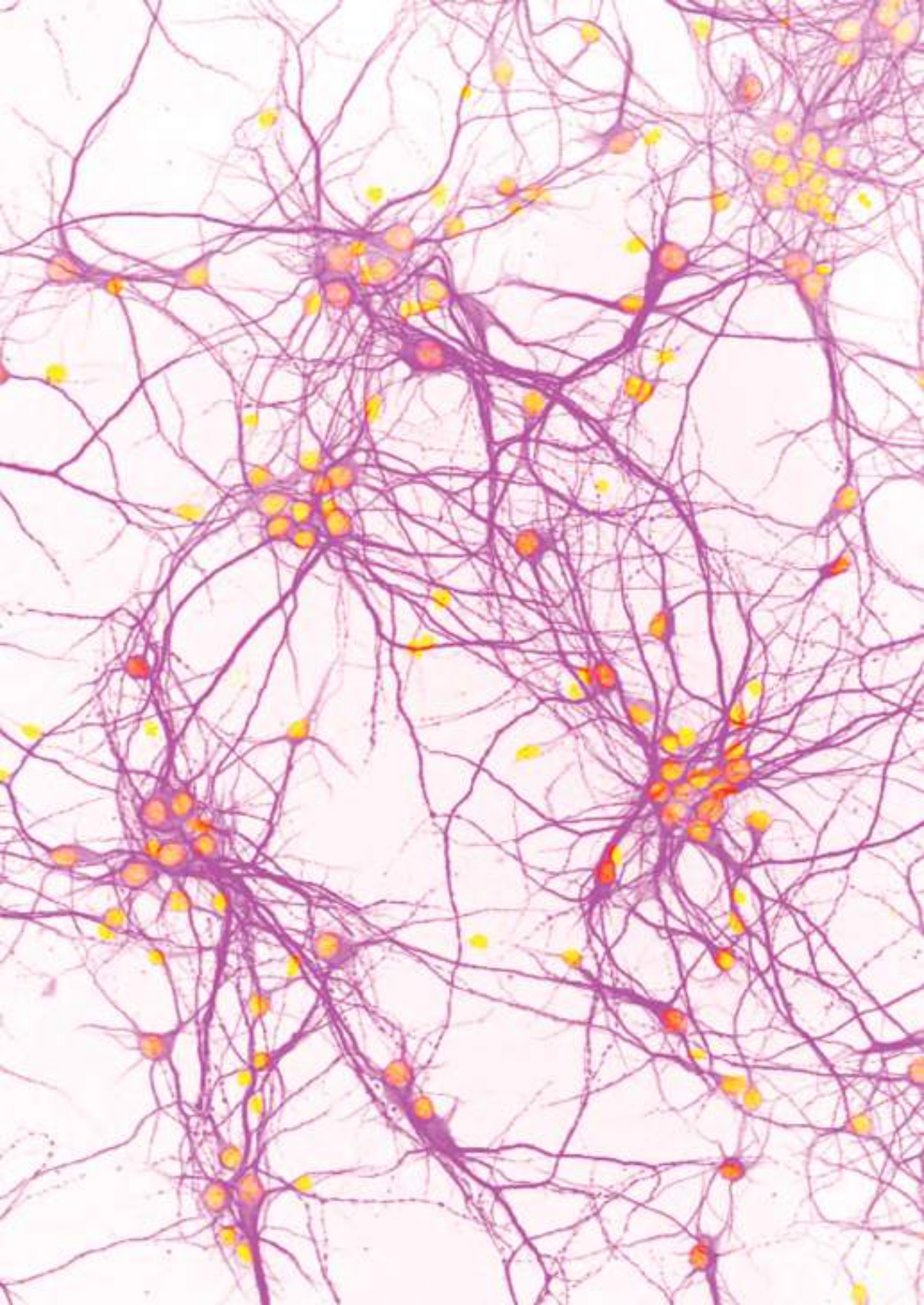

7. Future perspectives

The present study was focused on the functional assessment of the role of astrocyte secretomes on neuronal function and plasticity in a context of MS-specific CNS inflammation. The well-defined functions of astrocytes in synaptic signalling in healthy CNS led to the rationale of studying its role in disease.

The field of interest in the contribution of astrocytes in MS is huge. The crosstalk between astrocytes and other CNS-resident cells is essential for the maintenance of CNS homeostasis and function, as so is in neuroinflammation. Growing evidence points to the relevance of the interaction between astrocytes and oligodendrocytes in MS. Likewise, several studies have described both beneficial and detrimental roles played by astrocytes in remyelination. Based on these observations, we aim in the future to also investigate whether our astrocytes exposed to a MS-specific inflammatory microenvironment contribute to oligodendroglial damage. To this end, we have established collaboration with Prof. Denise Fitzgerald, who leads the Regenerative NeuroImmunology research group at Queen's University of Belfast (UK). Her group will provide the expertise necessary to successfully perform the evaluation of the effect of reactive astrocyte secretomes on OPC and oligodendrocytes. This collaboration will be performed as a three month stay for Clara Matute, and will be supported by two international grants that the doctoral student successfully applied, the IBRO-PERC InEurope Short Stay Grant and the EMBO Short-Term Fellowship.

Despite the important contribution of mouse models on the knowledge of astrocyte biology, some astrocytic responses show species-specific differences. In this regard, we have been actively working on the differentiation of astrocytes derived from human induced pluripotent stem cells (iPSC). At the moment, we have successfully achieved the obtention of fully differentiated human mature astrocytes. In this context, we also aim in the future to validate the findings generated from the present work in a model of iPSC-derived astrocytes from both controls and MS patients.

Bibliography

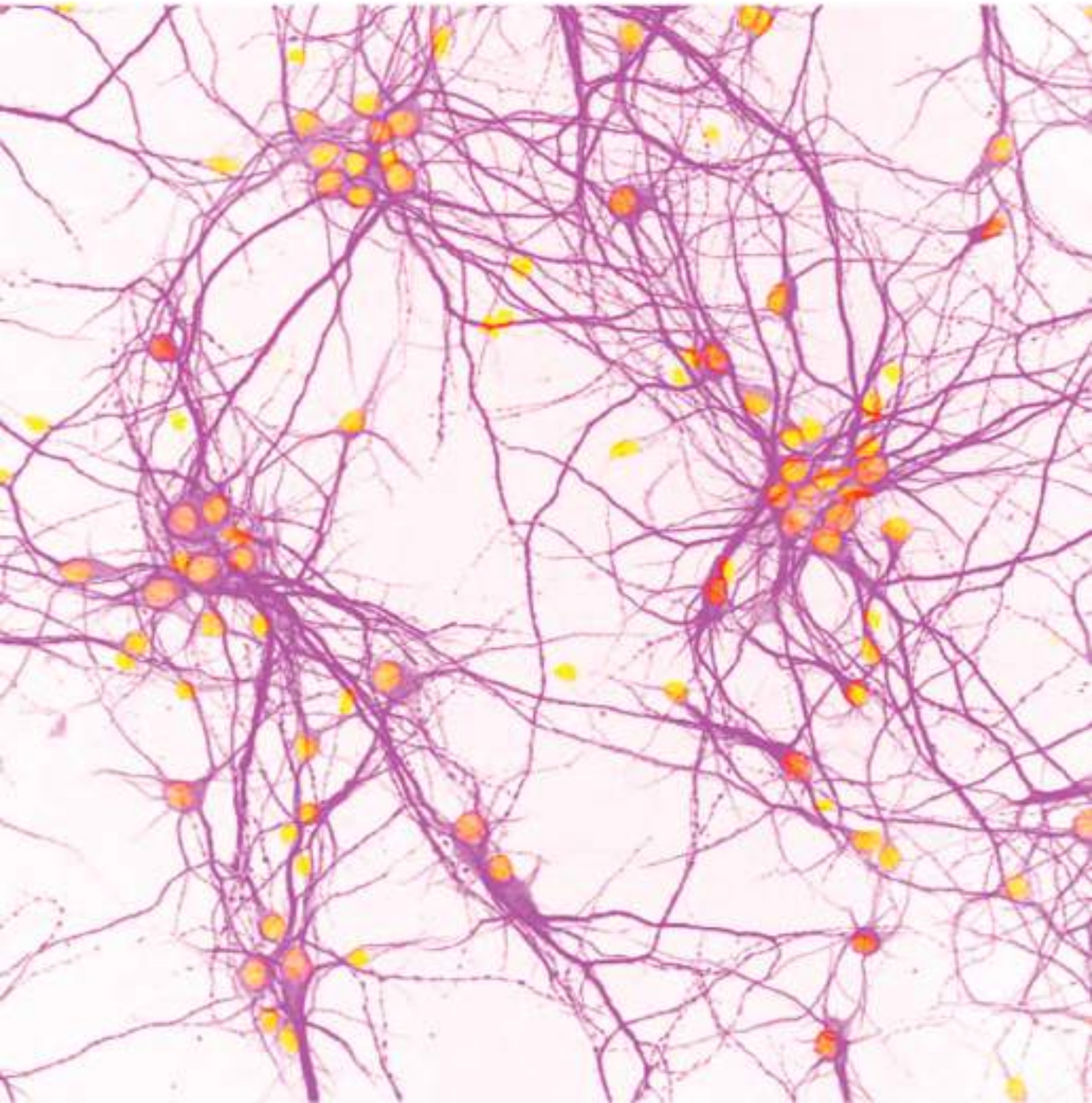

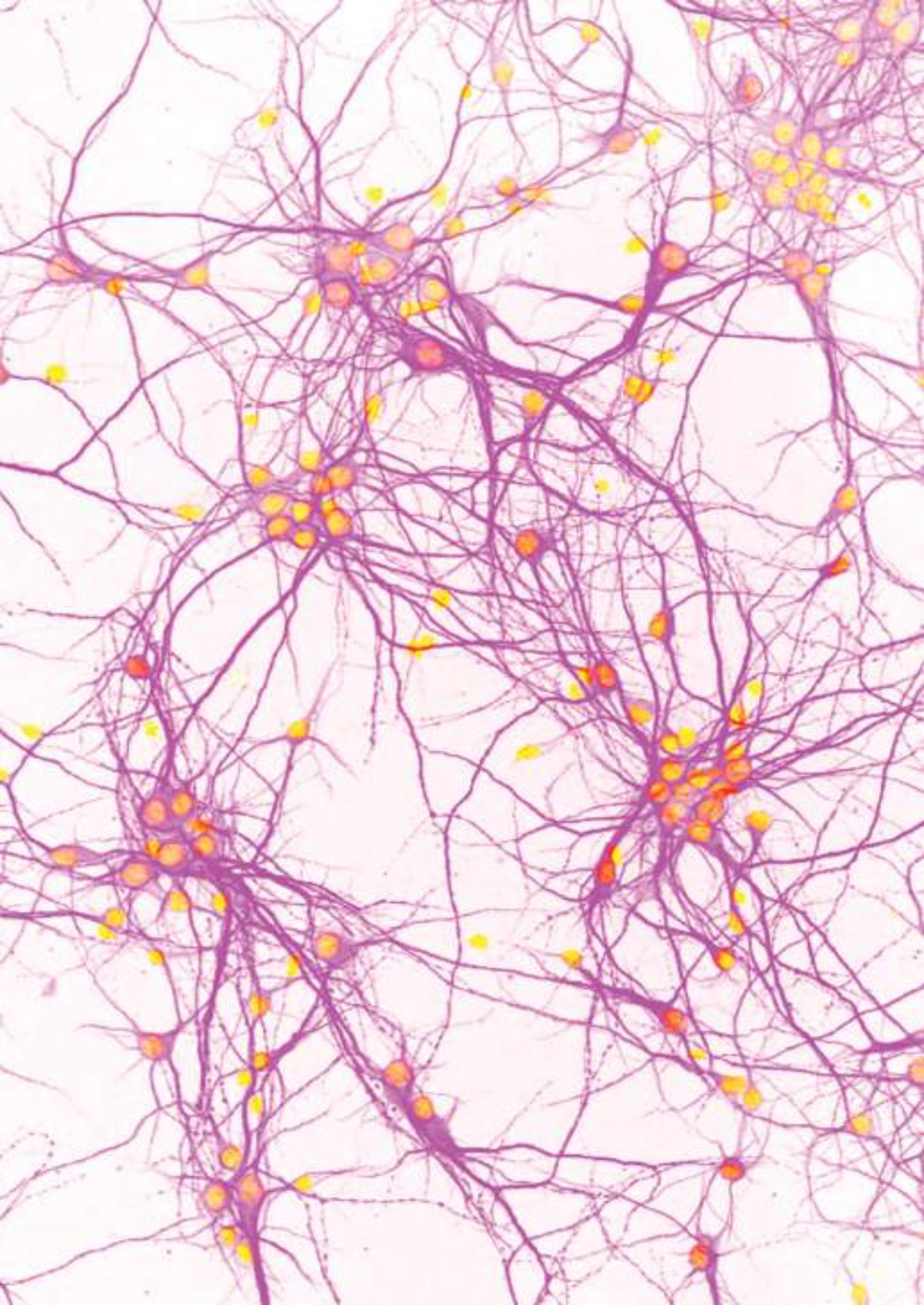

1. Baecher-Allan C, Kaskow BJ, Weiner HL. Multiple Sclerosis: Mechanisms and Immunotherapy. Neuron. 2018;97(4):742-68.

2. Thompson AJ, Baranzini SE, Geurts J, Hemmer B, Ciccarelli O. Multiple sclerosis. Lancet. 2018;391(10130):1622-36.

3. Tintore M, Vidal-Jordana A, Sastre-Garriga J. Treatment of multiple sclerosis - success from bench to bedside. Nat Rev Neurol. 2019;15(1):53-8.

4. Sofroniew MV, Vinters HV. Astrocytes: biology and pathology. Acta Neuropathol. 2010;119(1):7-35.

5. Collaborators GBDMS. Global, regional, and national burden of multiple sclerosis 1990-2016: a systematic analysis for the Global Burden of Disease Study 2016. Lancet Neurol. 2019;18(3):269-85.

6. Boiko A, Vorobeychik G, Paty D, Devonshire V, Sadovnick D, University of British Columbia MSCN. Early onset multiple sclerosis: a longitudinal study. Neurology. 2002;59(7):1006-10.

7. Tremlett H, Devonshire V. Is late-onset multiple sclerosis associated with a worse outcome? Neurology. 2006;67(6):954-9.

8. Harbo HF, Gold R, Tintore M. Sex and gender issues in multiple sclerosis. Ther Adv Neurol Disord. 2013;6(4):237-48.

9. Ascherio A, Munger KL, Lunemann JD. The initiation and prevention of multiple sclerosis. Nat Rev Neurol. 2012;8(11):602-12.

10. International Multiple Sclerosis Genetics C. Multiple sclerosis genomic map implicates peripheral immune cells and microglia in susceptibility. Science. 2019;365(6460).

11. Ascherio A. Environmental factors in multiple sclerosis. Expert Rev Neurother. 2013;13(12 Suppl):3-9.

12. Frohman EM, Racke MK, Raine CS. Multiple sclerosis--the plaque and its pathogenesis. N Engl J Med. 2006;354(9):942-55.

13. Trapp BD, Nave KA. Multiple sclerosis: an immune or neurodegenerative disorder? Annu Rev Neurosci. 2008;31:247-69.

14. Filippi M, Rocca MA, Barkhof F, Bruck W, Chen JT, Comi G, et al. Association between pathological and MRI findings in multiple sclerosis. Lancet Neurol. 2012;11(4):349-60.

15. Compston A, Coles A. Multiple sclerosis. Lancet. 2008;372(9648):1502-17.

16. Stys PK, Zamponi GW, van Minnen J, Geurts JJ. Will the real multiple sclerosis please stand up? Nat Rev Neurosci. 2012;13(7):507-14.

17. Louveau A, Smirnov I, Keyes TJ, Eccles JD, Rouhani SJ, Peske JD, et al. Structural and functional features of central nervous system lymphatic vessels. Nature. 2015;523(7560):337-41.

18. Hemmer B, Kerschensteiner M, Korn T. Role of the innate and adaptive immune responses in the course of multiple sclerosis. Lancet Neurol. 2015;14(4):406-19.

19. Abbott NJ, Ronnback L, Hansson E. Astrocyte-endothelial interactions at the blood-brain barrier. Nat Rev Neurosci. 2006;7(1):41-53.

20. Maggi P, Macri SM, Gaitan MI, Leibovitch E, Wholer JE, Knight HL, et al. The formation of inflammatory demyelinated lesions in cerebral white matter. Ann Neurol. 2014;76(4):594-608.

21. Dendrou CA, Fugger L, Friese MA. Immunopathology of multiple sclerosis. Nat Rev Immunol. 2015;15(9):545-58.

22. Levin MC, Lee S, Gardner LA, Shin Y, Douglas JN, Cooper C. Autoantibodies to Non-myelin Antigens as Contributors to the Pathogenesis of Multiple Sclerosis. J Clin Cell Immunol. 2013;4.

23. Derfuss T, Parikh K, Velhin S, Braun M, Mathey E, Krumbholz M, et al. Contactin-2/TAG-1-directed autoimmunity is identified in multiple sclerosis patients and mediates gray matter pathology in animals. Proc Natl Acad Sci U S A. 2009;106(20):8302-7.

24. Mathey EK, Derfuss T, Storch MK, Williams KR, Hales K, Woolley DR, et al. Neurofascin as a novel target for autoantibody-mediated axonal injury. J Exp Med. 2007;204(10):2363-72.

25. Srivastava R, Aslam M, Kalluri SR, Schirmer L, Buck D, Tackenberg B, et al. Potassium channel KIR4.1 as an immune target in multiple sclerosis. N Engl J Med. 2012;367(2):115-23.

26. Olsson T, Zhi WW, Hojeberg B, Kostulas V, Jiang YP, Anderson G, et al. Autoreactive T lymphocytes in multiple sclerosis determined by antigen-induced secretion of interferon-gamma. J Clin Invest. 1990;86(3):981-5.

27. Olsson T, Wallstrom E. IFN-secreting cells. Neurology. 1996;47(3):854-5.

28. Lassmann H, Ransohoff RM. The CD4-Th1 model for multiple sclerosis: a critical [correction of crucial] re-appraisal. Trends Immunol. 2004;25(3):132-7.

29. Codarri L, Gyulveszi G, Tosevski V, Hesske L, Fontana A, Magnenat L, et al. RORgammat drives production of the cytokine GM-CSF in helper T cells, which is essential for the effector phase of autoimmune neuroinflammation. Nat Immunol. 2011;12(6):560-7.

30. Kebir H, Kreymborg K, Ifergan I, Dodelet-Devillers A, Cayrol R, Bernard M, et al. Human TH17 lymphocytes promote blood-brain barrier disruption and central nervous system inflammation. Nat Med. 2007;13(10):1173-5.

31. Langrish CL, Chen Y, Blumenschein WM, Mattson J, Basham B, Sedgwick JD, et al. IL-23 drives a pathogenic T cell population that induces autoimmune inflammation. J Exp Med. 2005;201(2):233-40.

32. Neumann H, Medana IM, Bauer J, Lassmann H. Cytotoxic T lymphocytes in autoimmune and degenerative CNS diseases. Trends Neurosci. 2002;25(6):313-9.

33. Hauser SL, Bhan AK, Gilles F, Kemp M, Kerr C, Weiner HL. Immunohistochemical analysis of the cellular infiltrate in multiple sclerosis lesions. Ann Neurol. 1986;19(6):578-87.

34. Bitsch A, Schuchardt J, Bunkowski S, Kuhlmann T, Bruck W. Acute axonal injury in multiple sclerosis. Correlation with demyelination and inflammation. Brain. 2000;123 (Pt 6):1174-83.

35. Kuhlmann T, Lingfeld G, Bitsch A, Schuchardt J, Bruck W. Acute axonal damage in multiple sclerosis is most extensive in early disease stages and decreases over time. Brain. 2002;125(Pt 10):2202-12.

36. Esiri MM. Multiple sclerosis: a quantitative and qualitative study of immunoglobulin-containing cells in the central nervous system. Neuropathol Appl Neurobiol. 1980;6(1):9-21.

37. Sospedra M. B cells in multiple sclerosis. Curr Opin Neurol. 2018;31(3):256-62.

38. Chen Y, Kuchroo VK, Inobe J, Hafler DA, Weiner HL. Regulatory T cell clones induced by oral tolerance: suppression of autoimmune encephalomyelitis. Science. 1994;265(5176):1237-40.

39. Falcone M, Lee J, Patstone G, Yeung B, Sarvetnick N. B lymphocytes are crucial antigen-presenting cells in the pathogenic autoimmune response to GAD65 antigen in nonobese diabetic mice. J Immunol. 1998;161(3):1163-8.

40. Suri-Payer E, Amar AZ, Thornton AM, Shevach EM. CD4+CD25+ T cells inhibit both the induction and effector function of autoreactive T cells and represent a unique lineage of immunoregulatory cells. J Immunol. 1998;160(3):1212-8.

41. Kohm AP, Carpentier PA, Anger HA, Miller SD. Cutting edge: CD4+CD25+ regulatory T cells suppress antigen-specific autoreactive immune responses and central nervous system inflammation during active experimental autoimmune encephalomyelitis. J Immunol. 2002;169(9):4712-6.

42. Friese MA, Schattling B, Fugger L. Mechanisms of neurodegeneration and axonal dysfunction in multiple sclerosis. Nat Rev Neurol. 2014;10(4):225-38.

43. Heneka MT, Kummer MP, Latz E. Innate immune activation in neurodegenerative disease. Nat Rev Immunol. 2014;14(7):463-77.

44. Trapp BD, Peterson J, Ransohoff RM, Rudick R, Mork S, Bo L. Axonal transection in the lesions of multiple sclerosis. N Engl J Med. 1998;338(5):278-85.

45. Ghione E, Bergsland N, Dwyer MG, Hagemeier J, Jakimovski D, Paunkoski I, et al. Brain Atrophy Is Associated with Disability Progression in Patients with MS followed in a Clinical Routine. AJNR Am J Neuroradiol. 2018;39(12):2237-42.

46. Medana IM, Gallimore A, Oxenius A, Martinic MM, Wekerle H, Neumann H. MHC class I-restricted killing of neurons by virus-specific CD8+ T lymphocytes is effected through the Fas/FasL, but not the perforin pathway. Eur J Immunol. 2000;30(12):3623-33.

47. Na SY, Cao Y, Toben C, Nitschke L, Stadelmann C, Gold R, et al. Naive CD8 T-cells initiate spontaneous autoimmunity to a sequestered model antigen of the central nervous system. Brain. 2008;131(Pt 9):2353-65.

48. Saxena A, Bauer J, Scheikl T, Zappulla J, Audebert M, Desbois S, et al. Cutting edge: Multiple sclerosis-like lesions induced by effector CD8 T cells recognizing a sequestered antigen on oligodendrocytes. J Immunol. 2008;181(3):1617-21.

49. Meuth SG, Herrmann AM, Simon OJ, Siffrin V, Melzer N, Bittner S, et al. Cytotoxic CD8+ T cell-neuron interactions: perforin-dependent electrical silencing precedes but is not causally linked to neuronal cell death. J Neurosci. 2009;29(49):15397-409.

50. Vanguri P, Shin ML. Activation of complement by myelin: identification of C1-binding proteins of human myelin from central nervous tissue. J Neurochem. 1986;46(5):1535-41.

51. Linington C, Bradl M, Lassmann H, Brunner C, Vass K. Augmentation of demyelination in rat acute allergic encephalomyelitis by circulating mouse monoclonal antibodies directed against a myelin/oligodendrocyte glycoprotein. Am J Pathol. 1988;130(3):443-54.

52. Huizinga R, Heijmans N, Schubert P, Gschmeissner S, t Hart BA, Herrmann H, et al. Immunization with neurofilament light protein induces spastic paresis and axonal degeneration in Biozzi ABH mice. J Neuropathol Exp Neurol. 2007;66(4):295-304.

53. Nitsch R, Pohl EE, Smorodchenko A, Infante-Duarte C, Aktas O, Zipp F. Direct impact of T cells on neurons revealed by two-photon microscopy in living brain tissue. J Neurosci. 2004;24(10):2458-64.

54. Mizuno T, Zhang G, Takeuchi H, Kawanokuchi J, Wang J, Sonobe Y, et al. Interferon-gamma directly induces neurotoxicity through a neuron specific, calcium-permeable complex of IFN-gamma receptor and AMPA GluR1 receptor. FASEB J. 2008;22(6):1797-806.

55. Venters HD, Dantzer R, Kelley KW. A new concept in neurodegeneration: TNFalpha is a silencer of survival signals. Trends Neurosci. 2000;23(4):175-80.

56. Wang T, Allie R, Conant K, Haughey N, Turchan-Chelowo J, Hahn K, et al. Granzyme B mediates neurotoxicity through a G-protein-coupled receptor. FASEB J. 2006;20(8):1209-11.

57. Dong Y, Benveniste EN. Immune function of astrocytes. Glia. 2001;36(2):180-90.

58. DeWitt DA, Perry G, Cohen M, Doller C, Silver J. Astrocytes regulate microglial phagocytosis of senile plaque cores of Alzheimer's disease. Exp Neurol. 1998;149(2):329-40.

59. Krumbholz M, Theil D, Derfuss T, Rosenwald A, Schrader F, Monoranu CM, et al. BAFF is produced by astrocytes and up-regulated in multiple sclerosis lesions and primary central nervous system lymphoma. J Exp Med. 2005;201(2):195-200.

60. Nikic I, Merkler D, Sorbara C, Brinkoetter M, Kreutzfeldt M, Bareyre FM, et al. A reversible form of axon damage in experimental autoimmune encephalomyelitis and multiple sclerosis. Nat Med. 2011;17(4):495-9.

61. Gan L, Ye S, Chu A, Anton K, Yi S, Vincent VA, et al. Identification of cathepsin B as a mediator of neuronal death induced by Abeta-activated microglial cells using a functional genomics approach. J Biol Chem. 2004;279(7):5565-72.

62. Mahad DJ, Ziabreva I, Campbell G, Lax N, White K, Hanson PS, et al. Mitochondrial changes within axons in multiple sclerosis. Brain. 2009;132(Pt 5):1161-74.

63. Campbell GR, Ziabreva I, Reeve AK, Krishnan KJ, Reynolds R, Howell O, et al. Mitochondrial DNA deletions and neurodegeneration in multiple sclerosis. Ann Neurol. 2011;69(3):481-92.

64. Hametner S, Wimmer I, Haider L, Pfeifenbring S, Bruck W, Lassmann H. Iron and neurodegeneration in the multiple sclerosis brain. Ann Neurol. 2013;74(6):848-61.

65. Brown GC, Neher JJ. Microglial phagocytosis of live neurons. Nat Rev Neurosci. 2014;15(4):209-16.

66. Nair A, Frederick TJ, Miller SD. Astrocytes in multiple sclerosis: a product of their environment. Cell Mol Life Sci. 2008;65(17):2702-20.

67. Domingues HS, Portugal CC, Socodato R, Relvas JB. Oligodendrocyte, Astrocyte, and Microglia Crosstalk in Myelin Development, Damage, and Repair. Front Cell Dev Biol. 2016;4:71.

68. Dutta R, McDonough J, Yin X, Peterson J, Chang A, Torres T, et al. Mitochondrial dysfunction as a cause of axonal degeneration in multiple sclerosis patients. Ann Neurol. 2006;59(3):478-89.

69. Mahad D, Ziabreva I, Lassmann H, Turnbull D. Mitochondrial defects in acute multiple sclerosis lesions. Brain. 2008;131(Pt 7):1722-35.

70. Matute C, Sanchez-Gomez MV, Martinez-Millan L, Miledi R. Glutamate receptor-mediated toxicity in optic nerve oligodendrocytes. Proc Natl Acad Sci U S A. 1997;94(16):8830-5.

71. Matute C, Alberdi E, Domercq M, Sanchez-Gomez MV, Perez-Samartin A, Rodriguez-Antiguedad A, et al. Excitotoxic damage to white matter. J Anat. 2007;210(6):693-702.

72. Schirmer L, Velmeshev D, Holmqvist S, Kaufmann M, Werneburg S, Jung D, et al. Neuronal vulnerability and multilineage diversity in multiple sclerosis. Nature. 2019;573(7772):75-82.

73. Jakel S, Agirre E, Mendanha Falcao A, van Bruggen D, Lee KW, Knuesel I, et al. Altered human oligodendrocyte heterogeneity in multiple sclerosis. Nature. 2019;566(7745):543-7.

74. Nicaise AM, Wagstaff LJ, Willis CM, Paisie C, Chandok H, Robson P, et al. Cellular senescence in progenitor cells contributes to diminished remyelination potential in progressive multiple sclerosis. Proc Natl Acad Sci U S A. 2019;116(18):9030-9.

75. Kornek B, Storch MK, Bauer J, Djamshidian A, Weissert R, Wallstroem E, et al. Distribution of a calcium channel subunit in dystrophic axons in multiple sclerosis and experimental autoimmune encephalomyelitis. Brain. 2001;124(Pt 6):1114-24.

76. Black JA, Waxman SG, Smith KJ. Remyelination of dorsal column axons by endogenous Schwann cells restores the normal pattern of Nav1.6 and Kv1.2 at nodes of Ranvier. Brain. 2006;129(Pt 5):1319-29.

77. Friese MA, Craner MJ, Etzensperger R, Vergo S, Wemmie JA, Welsh MJ, et al. Acid-sensing ion channel-1 contributes to axonal degeneration in autoimmune inflammation of the central nervous system. Nat Med. 2007;13(12):1483-9.

78. Mandolesi G, Gentile A, Musella A, Fresegna D, De Vito F, Bullitta S, et al. Synaptopathy connects inflammation and neurodegeneration in multiple sclerosis. Nat Rev Neurol. 2015;11(12):711-24.

79. Absinta M, Lassmann H, Trapp BD. Mechanisms underlying progression in multiple sclerosis. Curr Opin Neurol. 2020;33(3):277-85.

80. Zhu B, Luo L, Moore GR, Paty DW, Cynader MS. Dendritic and synaptic pathology in experimental autoimmune encephalomyelitis. Am J Pathol. 2003;162(5):1639-50.

81. Marques KB, Santos LM, Oliveira AL. Spinal motoneuron synaptic plasticity during the course of an animal model of multiple sclerosis. Eur J Neurosci. 2006;24(11):3053-62.

82. Freria CM, Zanon RG, Santos LM, Oliveira AL. Major histocompatibility complex class I expression and glial reaction influence spinal motoneuron synaptic plasticity during the course of experimental autoimmune encephalomyelitis. J Comp Neurol. 2010;518(7):990-1007.

83. Centonze D, Muzio L, Rossi S, Cavasinni F, De Chiara V, Bergami A, et al. Inflammation triggers synaptic alteration and degeneration in experimental autoimmune encephalomyelitis. J Neurosci. 2009;29(11):3442-52.

84. Vitkovic L, Bockaert J, Jacque C. "Inflammatory" cytokines: neuromodulators in normal brain? J Neurochem. 2000;74(2):457-71.

85. Bauer S, Kerr BJ, Patterson PH. The neuropoietic cytokine family in development, plasticity, disease and injury. Nat Rev Neurosci. 2007;8(3):221-32.

86. Schafers M, Sorkin L. Effect of cytokines on neuronal excitability. Neurosci Lett. 2008;437(3):188-93.

87. Rossi S, De Chiara V, Furlan R, Musella A, Cavasinni F, Muzio L, et al. Abnormal activity of the Na/Ca exchanger enhances glutamate transmission in experimental autoimmune encephalomyelitis. Brain Behav Immun. 2010;24(8):1379-85.

88. Dutta R, Chang A, Doud MK, Kidd GJ, Ribaudo MV, Young EA, et al. Demyelination causes synaptic alterations in hippocampi from multiple sclerosis patients. Ann Neurol. 2011;69(3):445-54.

89. Michailidou I, Willems JG, Kooi EJ, van Eden C, Gold SM, Geurts JJ, et al. Complement C1q-C3-associated synaptic changes in multiple sclerosis hippocampus. Ann Neurol. 2015;77(6):1007-26.

90. Mandolesi G, Musella A, Gentile A, Grasselli G, Haji N, Sepman H, et al. Interleukin-1beta alters glutamate transmission at purkinje cell synapses in a mouse model of multiple sclerosis. J Neurosci. 2013;33(29):12105-21.

91. Haji N, Mandolesi G, Gentile A, Sacchetti L, Fresegna D, Rossi S, et al. TNF-alpha-mediated anxiety in a mouse model of multiple sclerosis. Exp Neurol. 2012;237(2):296-303.

92. Mori F, Nistico R, Mandolesi G, Piccinin S, Mango D, Kusayanagi H, et al. Interleukin-1beta promotes long-term potentiation in patients with multiple sclerosis. Neuromolecular Med. 2014;16(1):38-51.

93. Nistico R, Mango D, Mandolesi G, Piccinin S, Berretta N, Pignatelli M, et al. Inflammation subverts hippocampal synaptic plasticity in experimental multiple sclerosis. PLoS One. 2013;8(1):e54666.

94. Musumeci G, Grasselli G, Rossi S, De Chiara V, Musella A, Motta C, et al. Transient receptor potential vanilloid 1 channels modulate the synaptic effects of TNF-alpha and of IL-1beta in experimental autoimmune encephalomyelitis. Neurobiol Dis. 2011;43(3):669-77.

95. Rossi S, Furlan R, De Chiara V, Motta C, Studer V, Mori F, et al. Interleukin-1beta causes synaptic hyperexcitability in multiple sclerosis. Ann Neurol. 2012;71(1):76-83.

96. Mandolesi G, Grasselli G, Musella A, Gentile A, Musumeci G, Sepman H, et al. GABAergic signaling and connectivity on Purkinje cells are impaired in experimental autoimmune encephalomyelitis. Neurobiol Dis. 2012;46(2):414-24.

97. Kurtzke JF. Rating neurologic impairment in multiple sclerosis: an expanded disability status scale (EDSS). Neurology. 1983;33(11):1444-52.

98. Lublin FD, Reingold SC. Defining the clinical course of multiple sclerosis: results of an international survey. National Multiple Sclerosis Society (USA) Advisory Committee on Clinical Trials of New Agents in Multiple Sclerosis. Neurology. 1996;46(4):907-11.

99. Lublin FD, Reingold SC, Cohen JA, Cutter GR, Sorensen PS, Thompson AJ, et al. Defining the clinical course of multiple sclerosis: the 2013 revisions. Neurology. 2014;83(3):278-86.

100. Miller D, Barkhof F, Montalban X, Thompson A, Filippi M. Clinically isolated syndromes suggestive of multiple sclerosis, part I: natural history, pathogenesis, diagnosis, and prognosis. Lancet Neurol. 2005;4(5):281-8.

101. Okuda DT, Siva A, Kantarci O, Inglese M, Katz I, Tutuncu M, et al. Radiologically isolated syndrome: 5-year risk for an initial clinical event. PLoS One. 2014;9(3):e90509.

102. Ransohoff RM, Hafler DA, Lucchinetti CF. Multiple sclerosis-a quiet revolution. Nat Rev Neurol. 2015;11(3):134-42.

103. Klineova S, Lublin FD. Clinical Course of Multiple Sclerosis. Cold Spring Harb Perspect Med. 2018;8(9).

104. Jacobs LD, Beck RW, Simon JH, Kinkel RP, Brownscheidle CM, Murray TJ, et al. Intramuscular interferon beta-1a therapy initiated during a first demyelinating event in multiple sclerosis. CHAMPS Study Group. N Engl J Med. 2000;343(13):898-904.

105. Comi G, Filippi M, Barkhof F, Durelli L, Edan G, Fernandez O, et al. Effect of early interferon treatment on conversion to definite multiple sclerosis: a randomised study. Lancet. 2001;357(9268):1576-82.

106. Kappos L, Polman CH, Freedman MS, Edan G, Hartung HP, Miller DH, et al. Treatment with interferon beta-1b delays conversion to clinically definite and McDonald MS in patients with clinically isolated syndromes. Neurology. 2006;67(7):1242-9.

107. Thompson AJ, Banwell BL, Barkhof F, Carroll WM, Coetzee T, Comi G, et al. Diagnosis of multiple sclerosis: 2017 revisions of the McDonald criteria. Lancet Neurol. 2018;17(2):162-73.

108. Tintore M, Rovira A, Rio J, Nos C, Grive E, Tellez N, et al. Baseline MRI predicts future attacks and disability in clinically isolated syndromes. Neurology. 2006;67(6):968-72.

109. Fisniku LK, Brex PA, Altmann DR, Miszkiel KA, Benton CE, Lanyon R, et al. Disability and T2 MRI lesions: a 20-year follow-up of patients with relapse onset of multiple sclerosis. Brain. 2008;131(Pt 3):808-17.

110. Optic Neuritis Study G. Multiple sclerosis risk after optic neuritis: final optic neuritis treatment trial follow-up. Arch Neurol. 2008;65(6):727-32.

111. Young J, Quinn S, Hurrell M, Taylor B. Clinically isolated acute transverse myelitis: prognostic features and incidence. Mult Scler. 2009;15(11):1295-302.

112. Tintore M, Rovira A, Rio J, Otero-Romero S, Arrambide G, Tur C, et al. Defining high, medium and low impact prognostic factors for developing multiple sclerosis. Brain. 2015;138(Pt 7):1863-74.

113. Wattjes MP, Rovira A, Miller D, Yousry TA, Sormani MP, de Stefano MP, et al. Evidence-based guidelines: MAGNIMS consensus guidelines on the use of MRI in multiple sclerosis--establishing disease prognosis and monitoring patients. Nat Rev Neurol. 2015;11(10):597-606.

114. Filippi M, Preziosa P, Copetti M, Riccitelli G, Horsfield MA, Martinelli V, et al. Gray matter damage predicts the accumulation of disability 13 years later in MS. Neurology. 2013;81(20):1759-67.

115. Dobson R, Ramagopalan S, Davis A, Giovannoni G. Cerebrospinal fluid oligoclonal bands in multiple sclerosis and clinically isolated syndromes: a meta-analysis of prevalence, prognosis and effect of latitude. J Neurol Neurosurg Psychiatry. 2013;84(8):909-14.

116. Arrambide G, Tintore M, Espejo C, Auger C, Castillo M, Rio J, et al. The value of oligoclonal bands in the multiple sclerosis diagnostic criteria. Brain. 2018;141(4):1075-84.

117. Weber F, Janovskaja J, Polak T, Poser S, Rieckmann P. Effect of interferon beta on human myelin basic protein-specific T-cell lines: comparison of IFNbeta-1a and IFNbeta-1b. Neurology. 1999;52(5):1069-71.

118. Johnson KP, Brooks BR, Cohen JA, Ford CC, Goldstein J, Lisak RP, et al. Copolymer 1 reduces relapse rate and improves disability in relapsing-remitting multiple sclerosis: results of a phase III multicenter, double-blind placebo-controlled trial. The Copolymer 1 Multiple Sclerosis Study Group. Neurology. 1995;45(7):1268-76.

119. Comi G, Filippi M, Wolinsky JS. European/Canadian multicenter, double-blind, randomized, placebo-controlled study of the effects of glatiramer acetate on magnetic resonance imaging--measured disease activity and burden in patients with relapsing multiple sclerosis. European/Canadian Glatiramer Acetate Study Group. Ann Neurol. 2001;49(3):290-7.

120. Cohen JA, Barkhof F, Comi G, Hartung HP, Khatri BO, Montalban X, et al. Oral fingolimod or intramuscular interferon for relapsing multiple sclerosis. N Engl J Med. 2010;362(5):402-15.

121. Kappos L, Radue EW, O'Connor P, Polman C, Hohlfeld R, Calabresi P, et al. A placebo-controlled trial of oral fingolimod in relapsing multiple sclerosis. N Engl J Med. 2010;362(5):387-401.

122. Confavreux C, O'Connor P, Comi G, Freedman MS, Miller AE, Olsson TP, et al. Oral teriflunomide for patients with relapsing multiple sclerosis (TOWER): a randomised, double-blind, placebo-controlled, phase 3 trial. Lancet Neurol. 2014;13(3):247-56.

123. O'Connor P, Wolinsky JS, Confavreux C, Comi G, Kappos L, Olsson TP, et al. Randomized trial of oral teriflunomide for relapsing multiple sclerosis. N Engl J Med. 2011;365(14):1293-303.

124. Dubey D, Kieseier BC, Hartung HP, Hemmer B, Warnke C, Menge T, et al. Dimethyl fumarate in relapsing-remitting multiple sclerosis: rationale, mechanisms of action, pharmacokinetics, efficacy and safety. Expert Rev Neurother. 2015;15(4):339-46.

125. Giovannoni G, Comi G, Cook S, Rammohan K, Rieckmann P, Soelberg-Sorensen P, et al. Safety and Efficacy of Oral Cladribine in Patients with Relapsing-Remitting Multiple Sclerosis: Results from the 96 Week Phase IIIb Extension Trial to the CLARITY Study (P07.119). Neurology. 2013;80(7 Supplement):P07.119-P07.

126. Yednock TA, Cannon C, Fritz LC, Sanchez-Madrid F, Steinman L, Karin N. Prevention of experimental autoimmune encephalomyelitis by antibodies against alpha 4 beta 1 integrin. Nature. 1992;356(6364):63-6.

127. Polman CH, O'Connor PW, Havrdova E, Hutchinson M, Kappos L, Miller DH, et al. A randomized, placebo-controlled trial of natalizumab for relapsing multiple sclerosis. N Engl J Med. 2006;354(9):899-910.

128. Ruck T, Bittner S, Wiendl H, Meuth SG. Alemtuzumab in Multiple Sclerosis: Mechanism of Action and Beyond. Int J Mol Sci. 2015;16(7):16414-39.

129. Coles AJ, Twyman CL, Arnold DL, Cohen JA, Confavreux C, Fox EJ, et al. Alemtuzumab for patients with relapsing multiple sclerosis after disease-modifying therapy: a randomised controlled phase 3 trial. Lancet. 2012;380(9856):1829-39.

130. Hauser SL, Bar-Or A, Comi G, Giovannoni G, Hartung HP, Hemmer B, et al. Ocrelizumab versus Interferon Beta-1a in Relapsing Multiple Sclerosis. N Engl J Med. 2017;376(3):221-34.

131. Akaishi T, Nakashima I. Efficiency of antibody therapy in demyelinating diseases. Int Immunol. 2017;29(7):327-35.

132. Montalban X, Hauser SL, Kappos L, Arnold DL, Bar-Or A, Comi G, et al. Ocrelizumab versus Placebo in Primary Progressive Multiple Sclerosis. N Engl J Med. 2017;376(3):209-20.

133. Matute-Blanch C, Montalban X, Comabella M. Multiple sclerosis, and other demyelinating and autoimmune inflammatory diseases of the central nervous system. Handb Clin Neurol. 2017;146:67-84.

134. Paul A, Comabella M, Gandhi R. Biomarkers in Multiple Sclerosis. Cold Spring Harb Perspect Med. 2019;9(3).

135. Delcoigne B, Manouchehrinia A, Barro C, Benkert P, Michalak Z, Kappos L, et al. Blood neurofilament light levels segregate treatment effects in multiple sclerosis. Neurology. 2020;94(11):e1201-e12.

136. Villar LM, Masjuan J, Gonzalez-Porque P, Plaza J, Sadaba MC, Roldan E, et al. Intrathecal IgM synthesis predicts the onset of new relapses and a worse disease course in MS. Neurology. 2002;59(4):555-9.

137. Ferraro D, Simone AM, Bedin R, Galli V, Vitetta F, Federzoni L, et al. Cerebrospinal fluid oligoclonal IgM bands predict early conversion to clinically definite multiple sclerosis in patients with clinically isolated syndrome. J Neuroimmunol. 2013;257(1-2):76-81.

138. Khademi M, Kockum I, Andersson ML, Iacobaeus E, Brundin L, Sellebjerg F, et al. Cerebrospinal fluid CXCL13 in multiple sclerosis: a suggestive prognostic marker for the disease course. Mult Scler. 2011;17(3):335-43.

139. Comabella M, Fernandez M, Martin R, Rivera-Vallve S, Borras E, Chiva C, et al. Cerebrospinal fluid chitinase 3-like 1 levels are associated with conversion to multiple sclerosis. Brain. 2010;133(Pt 4):1082-93.

140. Canto E, Tintore M, Villar LM, Costa C, Nurtdinov R, Alvarez-Cermeno JC, et al. Chitinase 3-like 1: prognostic biomarker in clinically isolated syndromes. Brain. 2015;138(Pt 4):918-31.

141. Teunissen CE, Iacobaeus E, Khademi M, Brundin L, Norgren N, Koel-Simmelink MJ, et al. Combination of CSF N-acetylaspartate and neurofilaments in multiple sclerosis. Neurology. 2009;72(15):1322-9.

142. Matute-Blanch C, Calvo-Barreiro L, Carballo-Carbajal I, Gonzalo R, Sanchez A, Vila M, et al. Chitinase 3-like 1 is neurotoxic in primary cultured neurons. Sci Rep. 2020;10(1):7118.

143. Nedergaard M, Ransom B, Goldman SA. New roles for astrocytes: redefining the functional architecture of the brain. Trends Neurosci. 2003;26(10):523-30.

144. Garcia-Marin V, Garcia-Lopez P, Freire M. Cajal's contributions to glia research. Trends Neurosci. 2007;30(9):479-87.

145. Verkhratsky A, Steinhauser C. Ion channels in glial cells. Brain Res Brain Res Rev. 2000;32(2-3):380-412.

146. Cornell-Bell AH, Finkbeiner SM, Cooper MS, Smith SJ. Glutamate induces calcium waves in cultured astrocytes: long-range glial signaling. Science. 1990;247(4941):470-3.

147. Charles AC, Merrill JE, Dirksen ER, Sanderson MJ. Intercellular signaling in glial cells: calcium waves and oscillations in response to mechanical stimulation and glutamate. Neuron. 1991;6(6):983-92.

148. Halassa MM, Fellin T, Haydon PG. The tripartite synapse: roles for gliotransmission in health and disease. Trends Mol Med. 2007;13(2):54-63.

149. Shigetomi E, Bowser DN, Sofroniew MV, Khakh BS. Two forms of astrocyte calcium excitability have distinct effects on NMDA receptor-mediated slow inward currents in pyramidal neurons. J Neurosci. 2008;28(26):6659-63.

150. Perea G, Navarrete M, Araque A. Tripartite synapses: astrocytes process and control synaptic information. Trends Neurosci. 2009;32(8):421-31.

151. Volterra A, Meldolesi J. Astrocytes, from brain glue to communication elements: the revolution continues. Nat Rev Neurosci. 2005;6(8):626-40.

152. Higashi K, Fujita A, Inanobe A, Tanemoto M, Doi K, Kubo T, et al. An inwardly rectifying K(+) channel, Kir4.1, expressed in astrocytes surrounds synapses and blood vessels in brain. Am J Physiol Cell Physiol. 2001;281(3):C922-31.

153. Verkman AS. More than just water channels: unexpected cellular roles of aquaporins. J Cell Sci. 2005;118(Pt 15):3225-32.

154. Amiry-Moghaddam M, Frydenlund DS, Ottersen OP. Anchoring of aquaporin-4 in brain: molecular mechanisms and implications for the physiology and pathophysiology of water transport. Neuroscience. 2004;129(4):999-1010.

155. Danbolt NC. Glutamate uptake. Prog Neurobiol. 2001;65(1):1-105.

156. Bergles DE, Diamond JS, Jahr CE. Clearance of glutamate inside the synapse and beyond. Curr Opin Neurobiol. 1999;9(3):293-8.

157. Spampinato SF, Copani A, Nicoletti F, Sortino MA, Caraci F. Metabotropic Glutamate Receptors in Glial Cells: A New Potential Target for Neuroprotection? Front Mol Neurosci. 2018;11:414.

158. Theis M, Sohl G, Eiberger J, Willecke K. Emerging complexities in identity and function of glial connexins. Trends Neurosci. 2005;28(4):188-95.

159. Koehler RC, Roman RJ, Harder DR. Astrocytes and the regulation of cerebral blood flow. Trends Neurosci. 2009;32(3):160-9.

160. Gordon GR, Mulligan SJ, MacVicar BA. Astrocyte control of the cerebrovasculature. Glia. 2007;55(12):1214-21.

161. Iadecola C, Nedergaard M. Glial regulation of the cerebral microvasculature. Nat Neurosci. 2007;10(11):1369-76.

162. Lecuyer MA, Kebir H, Prat A. Glial influences on BBB functions and molecular players in immune cell trafficking. Biochim Biophys Acta. 2016;1862(3):472-82.

163. Robinson CJ, Stringer SE. The splice variants of vascular endothelial growth factor (VEGF) and their receptors. J Cell Sci. 2001;114(Pt 5):853-65.

164. Shibuya M. Vascular endothelial growth factor-dependent and -independent regulation of angiogenesis. BMB Rep. 2008;41(4):278-86.

165. Pfaff D, Fiedler U, Augustin HG. Emerging roles of the Angiopoietin-Tie and the ephrin-Eph systems as regulators of cell trafficking. J Leukoc Biol. 2006;80(4):719-26.

166. Phelps CH. Barbiturate-induced glycogen accumulation in brain. An electron microscopic study. Brain Res. 1972;39(1):225-34.

167. Voutsinos-Porche B, Bonvento G, Tanaka K, Steiner P, Welker E, Chatton JY, et al. Glial glutamate transporters mediate a functional metabolic crosstalk between neurons and astrocytes in the mouse developing cortex. Neuron. 2003;37(2):275-86.

168. Brown AM, Baltan Tekkok S, Ransom BR. Energy transfer from astrocytes to axons: the role of CNS glycogen. Neurochem Int. 2004;45(4):529-36.

169. Pellerin L, Bouzier-Sore AK, Aubert A, Serres S, Merle M, Costalat R, et al. Activity-dependent regulation of energy metabolism by astrocytes: an update. Glia. 2007;55(12):1251-62.

170. Freeman MR. Specification and morphogenesis of astrocytes. Science. 2010;330(6005):774-8.

171. Allen NJ, Eroglu C. Cell Biology of Astrocyte-Synapse Interactions. Neuron. 2017;96(3):697-708.

172. Christopherson KS, Ullian EM, Stokes CC, Mullowney CE, Hell JW, Agah A, et al. Thrombospondins are astrocyte-secreted proteins that promote CNS synaptogenesis. Cell. 2005;120(3):421-33.

173. Kucukdereli H, Allen NJ, Lee AT, Feng A, Ozlu MI, Conatser LM, et al. Control of excitatory CNS synaptogenesis by astrocyte-secreted proteins Hevin and SPARC. Proc Natl Acad Sci U S A. 2011;108(32):E440-9.

174. Allen NJ, Bennett ML, Foo LC, Wang GX, Chakraborty C, Smith SJ, et al. Astrocyte glypicans 4 and 6 promote formation of excitatory synapses via GluA1 AMPA receptors. Nature. 2012;486(7403):410-4.

175. Stellwagen D, Beattie EC, Seo JY, Malenka RC. Differential regulation of AMPA receptor and GABA receptor trafficking by tumor necrosis factor-alpha. J Neurosci. 2005;25(12):3219-28.

176. Diniz LP, Almeida JC, Tortelli V, Vargas Lopes C, Setti-Perdigao P, Stipursky J, et al. Astrocyte-induced synaptogenesis is mediated by transforming growth factor beta signaling through modulation of D-serine levels in cerebral cortex neurons. J Biol Chem. 2012;287(49):41432-45.

177. Diniz LP, Tortelli V, Garcia MN, Araujo AP, Melo HM, Silva GS, et al. Astrocyte transforming growth factor beta 1 promotes inhibitory synapse formation via CaM kinase II signaling. Glia. 2014;62(12):1917-31.

178. Bialas AR, Stevens B. TGF-beta signaling regulates neuronal C1q expression and developmental synaptic refinement. Nat Neurosci. 2013;16(12):1773-82.

179. Schafer DP, Lehrman EK, Kautzman AG, Koyama R, Mardinly AR, Yamasaki R, et al. Microglia sculpt postnatal neural circuits in an activity and complement-dependent manner. Neuron. 2012;74(4):691-705.

180. Chung WS, Clarke LE, Wang GX, Stafford BK, Sher A, Chakraborty C, et al. Astrocytes mediate synapse elimination through MEGF10 and MERTK pathways. Nature. 2013;504(7480):394-400.

181. Vainchtein ID, Chin G, Cho FS, Kelley KW, Miller JG, Chien EC, et al. Astrocyte-derived interleukin-33 promotes microglial synapse engulfment and neural circuit development. Science. 2018;359(6381):1269-73.

182. Araque A, Parpura V, Sanzgiri RP, Haydon PG. Tripartite synapses: glia, the unacknowledged partner. Trends Neurosci. 1999;22(5):208-15.

183. Ponath G, Park C, Pitt D. The Role of Astrocytes in Multiple Sclerosis. Front Immunol. 2018;9:217.

184. Bechmann I, Mor G, Nilsen J, Eliza M, Nitsch R, Naftolin F. FasL (CD95L, Apo1L) is expressed in the normal rat and human brain: evidence for the existence of an immunological brain barrier. Glia. 1999;27(1):62-74.

185. Choi C, Benveniste EN. Fas ligand/Fas system in the brain: regulator of immune and apoptotic responses. Brain Res Brain Res Rev. 2004;44(1):65-81.

186. Gimsa U, A OR, Pandiyan P, Teichmann D, Bechmann I, Nitsch R, et al. Astrocytes protect the CNS: antigen-specific T helper cell responses are inhibited by astrocyte-induced upregulation of CTLA-4 (CD152). J Mol Med (Berl). 2004;82(6):364-72.

187. Sofroniew MV. Astrocyte barriers to neurotoxic inflammation. Nat Rev Neurosci. 2015;16(5):249-63.

188. Chai H, Diaz-Castro B, Shigetomi E, Monte E, Octeau JC, Yu X, et al. Neural Circuit-Specialized Astrocytes: Transcriptomic, Proteomic, Morphological, and Functional Evidence. Neuron. 2017;95(3):531-49 e9.

189. Escartin C, Galea E, Lakatos A, O'Callaghan JP, Petzold GC, Serrano-Pozo A, et al. Reactive astrocyte nomenclature, definitions, and future directions. Nat Neurosci. 2021;24(3):312-25.

190. Sofroniew MV. Molecular dissection of reactive astrogliosis and glial scar formation. Trends Neurosci. 2009;32(12):638-47.

191. Sofroniew MV. Astrogliosis. Cold Spring Harb Perspect Biol. 2014;7(2):a020420.

192. Escartin C, Guillemaud O, Carrillo-de Sauvage MA. Questions and (some) answers on reactive astrocytes. Glia. 2019;67(12):2221-47.

193. Brosnan CF, Raine CS. The astrocyte in multiple sclerosis revisited. Glia. 2013;61(4):453-65.

194. Ponath G, Ramanan S, Mubarak M, Housley W, Lee S, Sahinkaya FR, et al. Myelin phagocytosis by astrocytes after myelin damage promotes lesion pathology. Brain. 2017;140(2):399-413.

195. D'Amelio FE, Smith ME, Eng LF. Sequence of tissue responses in the early stages of experimental allergic encephalomyelitis (EAE): immunohistochemical, light microscopic, and ultrastructural observations in the spinal cord. Glia. 1990;3(4):229-40.

196. Wang D, Ayers MM, Catmull DV, Hazelwood LJ, Bernard CC, Orian JM. Astrocyte-associated axonal damage in pre-onset stages of experimental autoimmune encephalomyelitis. Glia. 2005;51(3):235-40.

197. Pham H, Ramp AA, Klonis N, Ng SW, Klopstein A, Ayers MM, et al. The astrocytic response in early experimental autoimmune encephalomyelitis occurs across both the grey and white matter compartments. J Neuroimmunol. 2009;208(1-2):30-9.

198. Bush TG, Puvanachandra N, Horner CH, Polito A, Ostenfeld T, Svendsen CN, et al. Leukocyte infiltration, neuronal degeneration, and neurite outgrowth after ablation of scar-forming, reactive astrocytes in adult transgenic mice. Neuron. 1999;23(2):297-308.

199. Faulkner JR, Herrmann JE, Woo MJ, Tansey KE, Doan NB, Sofroniew MV. Reactive astrocytes protect tissue and preserve function after spinal cord injury. J Neurosci. 2004;24(9):2143-55.

200. Voskuhl RR, Peterson RS, Song B, Ao Y, Morales LB, Tiwari-Woodruff S, et al. Reactive astrocytes form scar-like perivascular barriers to leukocytes during adaptive immune inflammation of the CNS. J Neurosci. 2009;29(37):11511-22.

201. Toft-Hansen H, Fuchtbauer L, Owens T. Inhibition of reactive astrocytosis in established experimental autoimmune encephalomyelitis favors infiltration by myeloid cells over T cells and enhances severity of disease. Glia. 2011;59(1):166-76.

202. Liedtke W, Edelmann W, Chiu FC, Kucherlapati R, Raine CS. Experimental autoimmune encephalomyelitis in mice lacking glial fibrillary acidic protein is

characterized by a more severe clinical course and an infiltrative central nervous system lesion. Am J Pathol. 1998;152(1):251-9.

203. Herrmann JE, Imura T, Song B, Qi J, Ao Y, Nguyen TK, et al. STAT3 is a critical regulator of astrogliosis and scar formation after spinal cord injury. J Neurosci. 2008;28(28):7231-43.

204. Mayo L, Trauger SA, Blain M, Nadeau M, Patel B, Alvarez JI, et al. Regulation of astrocyte activation by glycolipids drives chronic CNS inflammation. Nat Med. 2014;20(10):1147-56.

205. Alvarez JI, Dodelet-Devillers A, Kebir H, Ifergan I, Fabre PJ, Terouz S, et al. The Hedgehog pathway promotes blood-brain barrier integrity and CNS immune quiescence. Science. 2011;334(6063):1727-31.

206. Alvarez JI, Katayama T, Prat A. Glial influence on the blood brain barrier. Glia. 2013;61(12):1939-58.

207. Bell RD, Winkler EA, Singh I, Sagare AP, Deane R, Wu Z, et al. Apolipoprotein E controls cerebrovascular integrity via cyclophilin A. Nature. 2012;485(7399):512-6.

208. Haroon F, Drogemuller K, Handel U, Brunn A, Reinhold D, Nishanth G, et al. Gp130-dependent astrocytic survival is critical for the control of autoimmune central nervous system inflammation. J Immunol. 2011;186(11):6521-31.

209. Norden DM, Fenn AM, Dugan A, Godbout JP. TGFbeta produced by IL-10 redirected astrocytes attenuates microglial activation. Glia. 2014;62(6):881-95.

210. Cekanaviciute E, Dietrich HK, Axtell RC, Williams AM, Egusquiza R, Wai KM, et al. Astrocytic TGF-beta signaling limits inflammation and reduces neuronal damage during central nervous system Toxoplasma infection. J Immunol. 2014;193(1):139-49.

211. Cekanaviciute E, Fathali N, Doyle KP, Williams AM, Han J, Buckwalter MS. Astrocytic transforming growth factor-beta signaling reduces subacute neuroinflammation after stroke in mice. Glia. 2014;62(8):1227-40.

212. Anderson MA, Burda JE, Ren Y, Ao Y, O'Shea TM, Kawaguchi R, et al. Astrocyte scar formation aids central nervous system axon regeneration. Nature. 2016;532(7598):195-200.

213. Goldmann T, Prinz M. Role of microglia in CNS autoimmunity. Clin Dev Immunol. 2013;2013:208093.

214. Colombo E, Farina C. Astrocytes: Key Regulators of Neuroinflammation. Trends Immunol. 2016;37(9):608-20.

215. Linnerbauer M, Wheeler MA, Quintana FJ. Astrocyte Crosstalk in CNS Inflammation. Neuron. 2020;108(4):608-22.

216. Liddelow SA, Guttenplan KA, Clarke LE, Bennett FC, Bohlen CJ, Schirmer L, et al. Neurotoxic reactive astrocytes are induced by activated microglia. Nature. 2017;541(7638):481-7.

217. Rothhammer V, Borucki DM, Tjon EC, Takenaka MC, Chao CC, Ardura-Fabregat A, et al. Microglial control of astrocytes in response to microbial metabolites. Nature. 2018;557(7707):724-8.

218. Bezzi P, Domercq M, Brambilla L, Galli R, Schols D, De Clercq E, et al. CXCR4-activated astrocyte glutamate release via TNFalpha: amplification by microglia triggers neurotoxicity. Nat Neurosci. 2001;4(7):702-10.

219. Hamilton JA. Colony-stimulating factors in inflammation and autoimmunity. Nat Rev Immunol. 2008;8(7):533-44.

220. Wheeler MA, Clark IC, Tjon EC, Li Z, Zandee SEJ, Couturier CP, et al. MAFG-driven astrocytes promote CNS inflammation. Nature. 2020;578(7796):593-9.

221. Sanchis P, Fernandez-Gayol O, Comes G, Escrig A, Giralt M, Palmiter RD, et al. Interleukin-6 Derived from the Central Nervous System May Influence the Pathogenesis of Experimental Autoimmune Encephalomyelitis in a Cell-Dependent Manner. Cells. 2020;9(2).

222. Nguyen PT, Dorman LC, Pan S, Vainchtein ID, Han RT, Nakao-Inoue H, et al. Microglial Remodeling of the Extracellular Matrix Promotes Synapse Plasticity. Cell. 2020;182(2):388-403 e15.

223. Liddelow SA, Barres BA. Reactive Astrocytes: Production, Function, and Therapeutic Potential. Immunity. 2017;46(6):957-67.

224. Calabrese V, Mancuso C, Calvani M, Rizzarelli E, Butterfield DA, Stella AM. Nitric oxide in the central nervous system: neuroprotection versus neurotoxicity. Nat Rev Neurosci. 2007;8(10):766-75.

225. Colombo E, Cordiglieri C, Melli G, Newcombe J, Krumbholz M, Parada LF, et al. Stimulation of the neurotrophin receptor TrkB on astrocytes drives nitric oxide production and neurodegeneration. J Exp Med. 2012;209(3):521-35.

226. Pitt D, Werner P, Raine CS. Glutamate excitotoxicity in a model of multiple sclerosis. Nat Med. 2000;6(1):67-70.

227. Chao CC, Gutierrez-Vazquez C, Rothhammer V, Mayo L, Wheeler MA, Tjon EC, et al. Metabolic Control of Astrocyte Pathogenic Activity via cPLA2-MAVS. Cell. 2019;179(7):1483-98 e22.

228. Omari KM, John GR, Sealfon SC, Raine CS. CXC chemokine receptors on human oligodendrocytes: implications for multiple sclerosis. Brain. 2005;128(Pt 5):1003-15.

229. Moyon S, Dubessy AL, Aigrot MS, Trotter M, Huang JK, Dauphinot L, et al. Demyelination causes adult CNS progenitors to revert to an immature state and express immune cues that support their migration. J Neurosci. 2015;35(1):4-20.

230. Kim S, Steelman AJ, Koito H, Li J. Astrocytes promote TNF-mediated toxicity to oligodendrocyte precursors. J Neurochem. 2011;116(1):53-66.

231. Valentin-Torres A, Savarin C, Barnett J, Bergmann CC. Blockade of sustained tumor necrosis factor in a transgenic model of progressive autoimmune encephalomyelitis limits oligodendrocyte apoptosis and promotes oligodendrocyte maturation. J Neuroinflammation. 2018;15(1):121.

232. Li W, Maeda Y, Ming X, Cook S, Chapin J, Husar W, et al. Apoptotic death following Fas activation in human oligodendrocyte hybrid cultures. J Neurosci Res. 2002;69(2):189-96.

233. Tzartos JS, Friese MA, Craner MJ, Palace J, Newcombe J, Esiri MM, et al. Interleukin-17 production in central nervous system-infiltrating T cells and glial cells is associated with active disease in multiple sclerosis. Am J Pathol. 2008;172(1):146-55.

234. Giulian D, Baker TJ. Characterization of ameboid microglia isolated from developing mammalian brain. J Neurosci. 1986;6(8):2163-78.

235. Garcia-Diaz Barriga G, Giralt A, Anglada-Huguet M, Gaja-Capdevila N, Orlandi JG, Soriano J, et al. 7,8-dihydroxyflavone ameliorates cognitive and motor

deficits in a Huntington's disease mouse model through specific activation of the PLCgamma1 pathway. Hum Mol Genet. 2017;26(16):3144-60.

236. Smyth GK. Linear models and empirical bayes methods for assessing differential expression in microarray experiments. Stat Appl Genet Mol Biol. 2004;3:Article3.

237. Chiva C, Olivella R, Borras E, Espadas G, Pastor O, Sole A, et al. QCloud: A cloud-based quality control system for mass spectrometry-based proteomics laboratories. PLoS One. 2018;13(1):e0189209.

238. Perkins DN, Pappin DJ, Creasy DM, Cottrell JS. Probability-based protein identification by searching sequence databases using mass spectrometry data. Electrophoresis. 1999;20(18):3551-67.

239. Beer LA, Liu P, Ky B, Barnhart KT, Speicher DW. Efficient Quantitative Comparisons of Plasma Proteomes Using Label-Free Analysis with MaxQuant. Methods Mol Biol. 2017;1619:339-52.

240. Vizcaino JA, Csordas A, Del-Toro N, Dianes JA, Griss J, Lavidas I, et al. 2016 update of the PRIDE database and its related tools. Nucleic Acids Res. 2016;44(22):11033.

241. Livak KJ, Schmittgen TD. Analysis of relative gene expression data using real-time quantitative PCR and the 2(-Delta Delta C(T)) Method. Methods. 2001;25(4):402-8.

242. Borovecki F, Lovrecic L, Zhou J, Jeong H, Then F, Rosas HD, et al. Genome-wide expression profiling of human blood reveals biomarkers for Huntington's disease. Proc Natl Acad Sci U S A. 2005;102(31):11023-8.

243. Bustin SA, Benes V, Garson JA, Hellemans J, Huggett J, Kubista M, et al. The MIQE guidelines: minimum information for publication of quantitative real-time PCR experiments. Clin Chem. 2009;55(4):611-22.

244. Zhou Y, Zhou B, Pache L, Chang M, Khodabakhshi AH, Tanaseichuk O, et al. Metascape provides a biologist-oriented resource for the analysis of systems-level datasets. Nat Commun. 2019;10(1):1523.

245. Han H, Cho JW, Lee S, Yun A, Kim H, Bae D, et al. TRRUST v2: an expanded reference database of human and mouse transcriptional regulatory interactions. Nucleic Acids Res. 2018;46(D1):D380-D6.

246. Zamanian JL, Xu L, Foo LC, Nouri N, Zhou L, Giffard RG, et al. Genomic analysis of reactive astrogliosis. J Neurosci. 2012;32(18):6391-410.

247. Ben Haim L, Carrillo-de Sauvage MA, Ceyzeriat K, Escartin C. Elusive roles for reactive astrocytes in neurodegenerative diseases. Front Cell Neurosci. 2015;9:278.

248. Ryan KM, Ernst MK, Rice NR, Vousden KH. Role of NF-kappaB in p53-mediated programmed cell death. Nature. 2000;404(6780):892-7.

249. Kasza A, Kiss DL, Gopalan S, Xu W, Rydel RE, Koj A, et al. Mechanism of plasminogen activator inhibitor-1 regulation by oncostatin M and interleukin-1 in human astrocytes. J Neurochem. 2002;83(3):696-703.

250. Hou B, Eren M, Painter CA, Covington JW, Dixon JD, Schoenhard JA, et al. Tumor necrosis factor alpha activates the human plasminogen activator inhibitor-1 gene through a distal nuclear factor kappaB site. J Biol Chem. 2004;279(18):18127-36.

251. Xin H, Li Y, Shen LH, Liu X, Wang X, Zhang J, et al. Increasing tPA activity in astrocytes induced by multipotent mesenchymal stromal cells facilitate neurite outgrowth after stroke in the mouse. PLoS One. 2010;5(2):e9027.

252. East E, Gveric D, Baker D, Pryce G, Lijnen HR, Cuzner ML. Chronic relapsing experimental allergic encephalomyelitis (CREAE) in plasminogen activator inhibitor-1 knockout mice: the effect of fibrinolysis during neuroinflammation. Neuropathol Appl Neurobiol. 2008;34(2):216-30.

253. Pelisch N, Dan T, Ichimura A, Sekiguchi H, Vaughan DE, van Ypersele de Strihou C, et al. Plasminogen Activator Inhibitor-1 Antagonist TM5484 Attenuates Demyelination and Axonal Degeneration in a Mice Model of Multiple Sclerosis. PLoS One. 2015;10(4):e0124510.

254. Popichak KA, Hammond SL, Moreno JA, Afzali MF, Backos DS, Slayden RD, et al. Compensatory Expression of Nur77 and Nurr1 Regulates NF-kappaB-

Dependent Inflammatory Signaling in Astrocytes. Mol Pharmacol. 2018;94(4):1174-86.

255. McEvoy C, de Gaetano M, Giffney HE, Bahar B, Cummins EP, Brennan EP, et al. NR4A Receptors Differentially Regulate NF-kappaB Signaling in Myeloid Cells. Front Immunol. 2017;8:7.

256. Masilamani AP, Ferrarese R, Kling E, Thudi NK, Kim H, Scholtens DM, et al. KLF6 depletion promotes NF-kappaB signaling in glioblastoma. Oncogene. 2017;36(25):3562-75.

257. Chen C, Magee JC, Bazan NG. Cyclooxygenase-2 regulates prostaglandin E2 signaling in hippocampal long-term synaptic plasticity. J Neurophysiol. 2002;87(6):2851-7.

258. Sang N, Zhang J, Marcheselli V, Bazan NG, Chen C. Postsynaptically synthesized prostaglandin E2 (PGE2) modulates hippocampal synaptic transmission via a presynaptic PGE2 EP2 receptor. J Neurosci. 2005;25(43):9858-70.

259. Canto E, Tintore M, Villar LM, Borras E, Alvarez-Cermeno JC, Chiva C, et al. Validation of semaphorin 7A and ala-beta-his-dipeptidase as biomarkers associated with the conversion from clinically isolated syndrome to multiple sclerosis. J Neuroinflammation. 2014;11:181.

260. Kohlschutter A, Eichler F. Childhood leukodystrophies: a clinical perspective. Expert Rev Neurother. 2011;11(10):1485-96.

261. Wingerchuk DM, Weinshenker BG. Neuromyelitis optica (Devic's syndrome). Handb Clin Neurol. 2014;122:581-99.

262. Luo J, Ho P, Steinman L, Wyss-Coray T. Bioluminescence in vivo imaging of autoimmune encephalomyelitis predicts disease. J Neuroinflammation. 2008;5:6.

263. Brambilla R, Persaud T, Hu X, Karmally S, Shestopalov VI, Dvoriantchikova G, et al. Transgenic inhibition of astroglial NF-kappa B improves functional outcome in experimental autoimmune encephalomyelitis by suppressing chronic central nervous system inflammation. J Immunol. 2009;182(5):2628-40.

264. Bruck W, Pfortner R, Pham T, Zhang J, Hayardeny L, Piryatinsky V, et al. Reduced astrocytic NF-kappaB activation by laquinimod protects from cuprizone-induced demyelination. Acta Neuropathol. 2012;124(3):411-24.

265. Choi JW, Gardell SE, Herr DR, Rivera R, Lee CW, Noguchi K, et al. FTY720 (fingolimod) efficacy in an animal model of multiple sclerosis requires astrocyte sphingosine 1-phosphate receptor 1 (S1P1) modulation. Proc Natl Acad Sci U S A. 2011;108(2):751-6.

266. Kim RY, Hoffman AS, Itoh N, Ao Y, Spence R, Sofroniew MV, et al. Astrocyte CCL2 sustains immune cell infiltration in chronic experimental autoimmune encephalomyelitis. J Neuroimmunol. 2014;274(1-2):53-61.

267. Moreno M, Bannerman P, Ma J, Guo F, Miers L, Soulika AM, et al. Conditional ablation of astroglial CCL2 suppresses CNS accumulation of M1 macrophages and preserves axons in mice with MOG peptide EAE. J Neurosci. 2014;34(24):8175-85.

268. Farez MF, Quintana FJ, Gandhi R, Izquierdo G, Lucas M, Weiner HL. Toll-like receptor 2 and poly(ADP-ribose) polymerase 1 promote central nervous system neuroinflammation in progressive EAE. Nat Immunol. 2009;10(9):958-64.

269. Clark IC, Gutierrez-Vazquez C, Wheeler MA, Li Z, Rothhammer V, Linnerbauer M, et al. Barcoded viral tracing of single-cell interactions in central nervous system inflammation. Science. 2021;372(6540).

270. Axelsson M, Malmestrom C, Nilsson S, Haghighi S, Rosengren L, Lycke J. Glial fibrillary acidic protein: a potential biomarker for progression in multiple sclerosis. J Neurol. 2011;258(5):882-8.

271. Saura J. Microglial cells in astroglial cultures: a cautionary note. J Neuroinflammation. 2007;4:26.

272. Prinz M, Priller J, Sisodia SS, Ransohoff RM. Heterogeneity of CNS myeloid cells and their roles in neurodegeneration. Nat Neurosci. 2011;14(10):1227-35.

273. Herz J, Filiano AJ, Smith A, Yogev N, Kipnis J. Myeloid Cells in the Central Nervous System. Immunity. 2017;46(6):943-56.

274. Shemer A, Erny D, Jung S, Prinz M. Microglia Plasticity During Health and Disease: An Immunological Perspective. Trends Immunol. 2015;36(10):614-24.

275. Fukushima S, Furube E, Itoh M, Nakashima T, Miyata S. Robust increase of microglia proliferation in the fornix of hippocampal axonal pathway after a single LPS stimulation. J Neuroimmunol. 2015;285:31-40.

276. Bruttger J, Karram K, Wortge S, Regen T, Marini F, Hoppmann N, et al. Genetic Cell Ablation Reveals Clusters of Local Self-Renewing Microglia in the Mammalian Central Nervous System. Immunity. 2015;43(1):92-106.

277. Brown GC, Vilalta A. How microglia kill neurons. Brain Res. 2015;1628(Pt B):288-97.

278. Chabot S, Williams G, Yong VW. Microglial production of TNF-alpha is induced by activated T lymphocytes. Involvement of VLA-4 and inhibition by interferonbeta-1b. J Clin Invest. 1997;100(3):604-12.

279. Lian H, Yang L, Cole A, Sun L, Chiang AC, Fowler SW, et al. NFkappaB-activated astroglial release of complement C3 compromises neuronal morphology and function associated with Alzheimer's disease. Neuron. 2015;85(1):101-15.

280. Rossi S, Motta C, Studer V, Barbieri F, Buttari F, Bergami A, et al. Tumor necrosis factor is elevated in progressive multiple sclerosis and causes excitotoxic neurodegeneration. Mult Scler. 2014;20(3):304-12.

281. Perriot S, Mathias A, Perriard G, Canales M, Jonkmans N, Merienne N, et al. Human Induced Pluripotent Stem Cell-Derived Astrocytes Are Differentially Activated by Multiple Sclerosis-Associated Cytokines. Stem Cell Reports. 2018;11(5):1199-210.

282. Ponath G, Lincoln MR, Levine-Ritterman M, Park C, Dahlawi S, Mubarak M, et al. Enhanced astrocyte responses are driven by a genetic risk allele associated with multiple sclerosis. Nat Commun. 2018;9(1):5337.

283. Trindade P, Loiola EC, Gasparotto J, Ribeiro CT, Cardozo PL, Devalle S, et al. Short and long TNF-alpha exposure recapitulates canonical astrogliosis events in human-induced pluripotent stem cells-derived astrocytes. Glia. 2020;68(7):1396-409.

284. Itoh N, Itoh Y, Tassoni A, Ren E, Kaito M, Ohno A, et al. Cell-specific and region-specific transcriptomics in the multiple sclerosis model: Focus on astrocytes. Proc Natl Acad Sci U S A. 2018;115(2):E302-E9.

285. Zuurman MW, Heeroma J, Brouwer N, Boddeke HW, Biber K. LPS-induced expression of a novel chemokine receptor (L-CCR) in mouse glial cells in vitro and in vivo. Glia. 2003;41(4):327-36.

286. Columba-Cabezas S, Serafini B, Ambrosini E, Aloisi F. Lymphoid chemokines CCL19 and CCL21 are expressed in the central nervous system during experimental autoimmune encephalomyelitis: implications for the maintenance of chronic neuroinflammation. Brain Pathol. 2003;13(1):38-51.

287. Krumbholz M, Theil D, Steinmeyer F, Cepok S, Hemmer B, Hofbauer M, et al. CCL19 is constitutively expressed in the CNS, up-regulated in neuroinflammation, active and also inactive multiple sclerosis lesions. J Neuroimmunol. 2007;190(1-2):72-9.

288. El Behi M, Sanson C, Bachelin C, Guillot-Noel L, Fransson J, Stankoff B, et al. Adaptive human immunity drives remyelination in a mouse model of demyelination. Brain. 2017;140(4):967-80.

289. Omari KM, John G, Lango R, Raine CS. Role for CXCR2 and CXCL1 on glia in multiple sclerosis. Glia. 2006;53(1):24-31.

290. Glabinski AR, Tani M, Strieter RM, Tuohy VK, Ransohoff RM. Synchronous synthesis of alpha- and beta-chemokines by cells of diverse lineage in the central nervous system of mice with relapses of chronic experimental autoimmune encephalomyelitis. Am J Pathol. 1997;150(2):617-30.

291. Grist JJ, Marro BS, Skinner DD, Syage AR, Worne C, Doty DJ, et al. Induced CNS expression of CXCL1 augments neurologic disease in a murine model of multiple sclerosis via enhanced neutrophil recruitment. Eur J Immunol. 2018;48(7):1199-210.

292. Ni H, Wang Y, An K, Liu Q, Xu L, Zhu C, et al. Crosstalk between NFkappaB-dependent astrocytic CXCL1 and neuron CXCR2 plays a role in descending pain facilitation. J Neuroinflammation. 2019;16(1):1.

293. Xu J, Zhu MD, Zhang X, Tian H, Zhang JH, Wu XB, et al. NFkappaB-mediated CXCL1 production in spinal cord astrocytes contributes to the maintenance of bone cancer pain in mice. J Neuroinflammation. 2014;11:38.

294. Zhang ZJ, Cao DL, Zhang X, Ji RR, Gao YJ. Chemokine contribution to neuropathic pain: respective induction of CXCL1 and CXCR2 in spinal cord astrocytes and neurons. Pain. 2013;154(10):2185-97.

295. Cao DL, Zhang ZJ, Xie RG, Jiang BC, Ji RR, Gao YJ. Chemokine CXCL1 enhances inflammatory pain and increases NMDA receptor activity and COX-2 expression in spinal cord neurons via activation of CXCR2. Exp Neurol. 2014;261:328-36.

296. Esparza J, Kruse M, Lee J, Michaud M, Madri JA. MMP-2 null mice exhibit an early onset and severe experimental autoimmune encephalomyelitis due to an increase in MMP-9 expression and activity. FASEB J. 2004;18(14):1682-91.

297. Agrawal S, Anderson P, Durbeej M, van Rooijen N, Ivars F, Opdenakker G, et al. Dystroglycan is selectively cleaved at the parenchymal basement membrane at sites of leukocyte extravasation in experimental autoimmune encephalomyelitis. J Exp Med. 2006;203(4):1007-19.

298. Song J, Wu C, Korpos E, Zhang X, Agrawal SM, Wang Y, et al. Focal MMP-2 and MMP-9 activity at the blood-brain barrier promotes chemokine-induced leukocyte migration. Cell Rep. 2015;10(7):1040-54.

299. Harris VK, Donelan N, Yan QJ, Clark K, Touray A, Rammal M, et al. Cerebrospinal fluid fetuin-A is a biomarker of active multiple sclerosis. Mult Scler. 2013;19(11):1462-72.

300. Harris VK, Bell L, Langan RA, Tuddenham J, Landy M, Sadiq SA. Fetuin-A deficiency protects mice from Experimental Autoimmune Encephalomyelitis (EAE) and correlates with altered innate immune response. PLoS One. 2017;12(4):e0175575.

301. Apaijai N, Moisescu DM, Palee S, McSweeney CM, Saiyasit N, Maneechote C, et al. Pretreatment With PCSK9 Inhibitor Protects the Brain Against Cardiac Ischemia/Reperfusion Injury Through a Reduction of Neuronal Inflammation and Amyloid Beta Aggregation. J Am Heart Assoc. 2019;8(2):e010838.

302. Smith AM, Gibbons HM, Oldfield RL, Bergin PM, Mee EW, Curtis MA, et al. M-CSF increases proliferation and phagocytosis while modulating receptor and transcription factor expression in adult human microglia. J Neuroinflammation. 2013;10:85.

303. Butzkueven H, Zhang JG, Soilu-Hanninen M, Hochrein H, Chionh F, Shipham KA, et al. LIF receptor signaling limits immune-mediated demyelination by enhancing oligodendrocyte survival. Nat Med. 2002;8(6):613-9.

304. Ishibashi T, Dakin KA, Stevens B, Lee PR, Kozlov SV, Stewart CL, et al. Astrocytes promote myelination in response to electrical impulses. Neuron. 2006;49(6):823-32.

305. Moidunny S, Vinet J, Wesseling E, Bijzet J, Shieh CH, van Ijzendoorn SC, et al. Adenosine A2B receptor-mediated leukemia inhibitory factor release from astrocytes protects cortical neurons against excitotoxicity. J Neuroinflammation. 2012;9:198.

306. Butzkueven H, Emery B, Cipriani T, Marriott MP, Kilpatrick TJ. Endogenous leukemia inhibitory factor production limits autoimmune demyelination and oligodendrocyte loss. Glia. 2006;53(7):696-703.

307. McGregor G, Harvey J. Regulation of Hippocampal Synaptic Function by the Metabolic Hormone, Leptin: Implications for Health and Neurodegenerative Disease. Front Cell Neurosci. 2018;12:340.

308. Guo Z, Jiang H, Xu X, Duan W, Mattson MP. Leptin-mediated cell survival signaling in hippocampal neurons mediated by JAK STAT3 and mitochondrial stabilization. J Biol Chem. 2008;283(3):1754-63.

309. Doherty GH, Beccano-Kelly D, Yan SD, Gunn-Moore FJ, Harvey J. Leptin prevents hippocampal synaptic disruption and neuronal cell death induced by amyloid beta. Neurobiol Aging. 2013;34(1):226-37.

310. Diederich K, Schabitz WR, Minnerup J. Seeing old friends from a different angle: novel properties of hematopoietic growth factors in the healthy and diseased brain. Hippocampus. 2012;22(5):1051-7.

311. Kadota R, Koda M, Kawabe J, Hashimoto M, Nishio Y, Mannoji C, et al. Granulocyte colony-stimulating factor (G-CSF) protects oligodendrocyte and promotes hindlimb functional recovery after spinal cord injury in rats. PLoS One. 2012;7(11):e50391.

312. Kuroda M, Muramatsu R, Maedera N, Koyama Y, Hamaguchi M, Fujimura H, et al. Peripherally derived FGF21 promotes remyelination in the central nervous system. J Clin Invest. 2017;127(9):3496-509.

313. Malik VA, Zajicek F, Mittmann LA, Klaus J, Unterseer S, Rajkumar S, et al. GDF15 promotes simultaneous astrocyte remodeling and tight junction strengthening at the blood-brain barrier. J Neurosci Res. 2020;98(7):1433-56.

314. Zheng L, Ishii Y, Tokunaga A, Hamashima T, Shen J, Zhao QL, et al. Neuroprotective effects of PDGF against oxidative stress and the signaling pathway involved. J Neurosci Res. 2010;88(6):1273-84.

315. Cabezas R, Vega-Vela NE, Gonzalez-Sanmiguel J, Gonzalez J, Esquinas P, Echeverria V, et al. PDGF-BB Preserves Mitochondrial Morphology, Attenuates ROS Production, and Upregulates Neuroglobin in an Astrocytic Model Under Rotenone Insult. Mol Neurobiol. 2018;55(4):3085-95.

316. Tzarfaty-Majar V, Lopez-Alemany R, Feinstein Y, Gombau L, Goldshmidt O, Soriano E, et al. Plasmin-mediated release of the guidance molecule F-spondin from the extracellular matrix. J Biol Chem. 2001;276(30):28233-41.

317. Samson AL, Medcalf RL. Tissue-type plasminogen activator: a multifaceted modulator of neurotransmission and synaptic plasticity. Neuron. 2006;50(5):673-8.

318. Nolin WB, Emmetsberger J, Bukhari N, Zhang Y, Levine JM, Tsirka SE. tPA-mediated generation of plasmin is catalyzed by the proteoglycan NG2. Glia. 2008;56(2):177-89.

319. Gerenu G, Martisova E, Ferrero H, Carracedo M, Rantamaki T, Ramirez MJ, et al. Modulation of BDNF cleavage by plasminogen-activator inhibitor-1 contributes to Alzheimer's neuropathology and cognitive deficits. Biochim Biophys Acta Mol Basis Dis. 2017;1863(4):991-1001.

320. Wilhelm CJ, Hashimoto JG, Roberts ML, Zhang X, Goeke CM, Bloom SH, et al. Plasminogen activator system homeostasis and its dysregulation by ethanol in astrocyte cultures and the developing brain. Neuropharmacology. 2018;138:193-209.

321. Gveric D, Hanemaaijer R, Newcombe J, van Lent NA, Sier CF, Cuzner ML. Plasminogen activators in multiple sclerosis lesions: implications for the inflammatory response and axonal damage. Brain. 2001;124(Pt 10):1978-88.

322. Rodriguez-Lorenzo S, Ferreira Francisco DM, Vos R, van Het Hof B, Rijnsburger M, Schroten H, et al. Altered secretory and neuroprotective function of the choroid plexus in progressive multiple sclerosis. Acta Neuropathol Commun. 2020;8(1):35.

323. Zivkovic M, Starcevic Cizmarevic N, Lovrecic L, Klupka-Saric I, Stankovic A, Gasparovic I, et al. The role of TPA I/D and PAI-1 4G/5G polymorphisms in multiple sclerosis. Dis Markers. 2014;2014:362708.

324. Valdes-Alvarado E, Huerta M, Trujillo X, Valle Y, Padilla Gutierrez JR, Mireles-Ramirez MA, et al. Association between the -844 G>A, HindIII C>G, and 4G/5G PAI-1 Polymorphisms and Susceptibility to Multiple Sclerosis in Western Mexican Population. Dis Markers. 2019;2019:9626289.

325. Brambilla R, Morton PD, Ashbaugh JJ, Karmally S, Lambertsen KL, Bethea JR. Astrocytes play a key role in EAE pathophysiology by orchestrating in the CNS the inflammatory response of resident and peripheral immune cells and by suppressing remyelination. Glia. 2014;62(3):452-67.

326. Hinsinger G, Galeotti N, Nabholz N, Urbach S, Rigau V, Demattei C, et al. Chitinase 3-like proteins as diagnostic and prognostic biomarkers of multiple sclerosis. Mult Scler. 2015;21(10):1251-61.

327. Modvig S, Degn M, Roed H, Sorensen TL, Larsson HB, Langkilde AR, et al. Cerebrospinal fluid levels of chitinase 3-like 1 and neurofilament light chain predict multiple sclerosis development and disability after optic neuritis. Mult Scler. 2015;21(14):1761-70.

328. Chen CC, Pekow J, Llado V, Kanneganti M, Lau CW, Mizoguchi A, et al. Chitinase 3-like-1 expression in colonic epithelial cells as a potentially novel marker for colitis-associated neoplasia. Am J Pathol. 2011;179(3):1494-503.

329. Tang H, Sun Y, Shi Z, Huang H, Fang Z, Chen J, et al. YKL-40 induces IL-8 expression from bronchial epithelium via MAPK (JNK and ERK) and NF-kappaB

pathways, causing bronchial smooth muscle proliferation and migration. J Immunol. 2013;190(1):438-46.

330. Low D, Subramaniam R, Lin L, Aomatsu T, Mizoguchi A, Ng A, et al. Chitinase 3-like 1 induces survival and proliferation of intestinal epithelial cells during chronic inflammation and colitis-associated cancer by regulating S100A9. Oncotarget. 2015;6(34):36535-50.

331. Choi JY, Yeo IJ, Kim KC, Choi WR, Jung JK, Han SB, et al. K284-6111 prevents the amyloid beta-induced neuroinflammation and impairment of recognition memory through inhibition of NF-kappaB-mediated CHI3L1 expression. J Neuroinflammation. 2018;15(1):224.

332. Renkema GH, Boot RG, Au FL, Donker-Koopman WE, Strijland A, Muijsers AO, et al. Chitotriosidase, a chitinase, and the 39-kDa human cartilage glycoprotein, a chitin-binding lectin, are homologues of family 18 glycosyl hydrolases secreted by human macrophages. Eur J Biochem. 1998;251(1-2):504-9.

333. Bonneh-Barkay D, Wang G, Starkey A, Hamilton RL, Wiley CA. In vivo CHI3L1 (YKL-40) expression in astrocytes in acute and chronic neurological diseases. J Neuroinflammation. 2010;7:34.

334. Pinteac R, Montalban X, Comabella M. Chitinases and chitinase-like proteins as biomarkers in neurologic disorders. Neurol Neuroimmunol Neuroinflamm. 2021;8(1).

335. Yeo IJ, Lee CK, Han SB, Yun J, Hong JT. Roles of chitinase 3-like 1 in the development of cancer, neurodegenerative diseases, and inflammatory diseases. Pharmacol Ther. 2019;203:107394.

336. Bonneh-Barkay D, Bissel SJ, Kofler J, Starkey A, Wang G, Wiley CA. Astrocyte and macrophage regulation of YKL-40 expression and cellular response in neuroinflammation. Brain Pathol. 2012;22(4):530-46.

337. Hyvarinen T, Hagman S, Ristola M, Sukki L, Veijula K, Kreutzer J, et al. Co-stimulation with IL-1beta and TNF-alpha induces an inflammatory reactive astrocyte phenotype with neurosupportive characteristics in a human pluripotent stem cell model system. Sci Rep. 2019;9(1):16944.

338. Kim DH, Park HJ, Lim S, Koo JH, Lee HG, Choi JO, et al. Regulation of chitinase-3-like-1 in T cell elicits Th1 and cytotoxic responses to inhibit lung metastasis. Nat Commun. 2018;9(1):503.

339. Chen Y, Zhang S, Wang Q, Zhang X. Tumor-recruited M2 macrophages promote gastric and breast cancer metastasis via M2 macrophage-secreted CHI3L1 protein. J Hematol Oncol. 2017;10(1):36.

Annexes

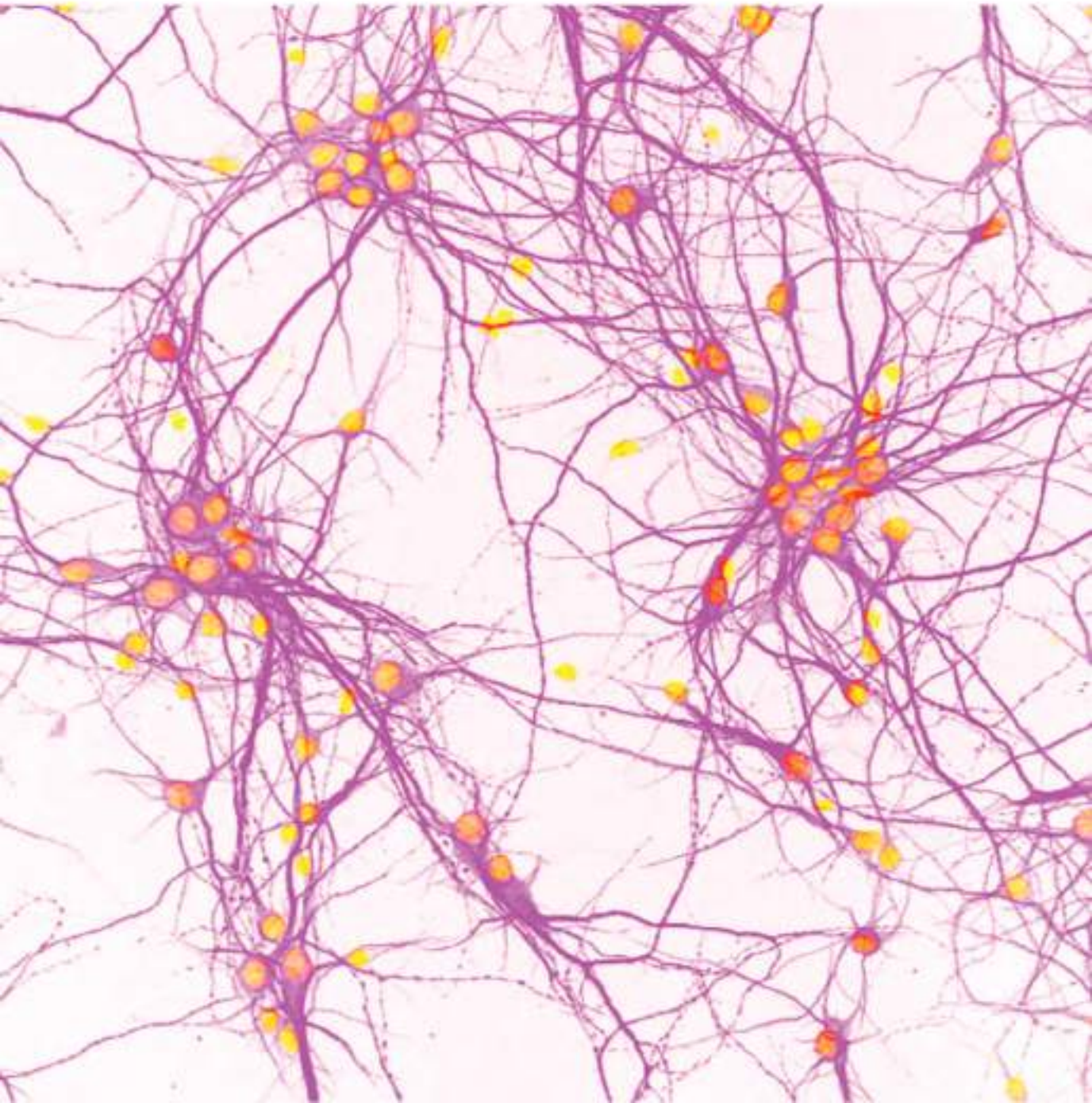

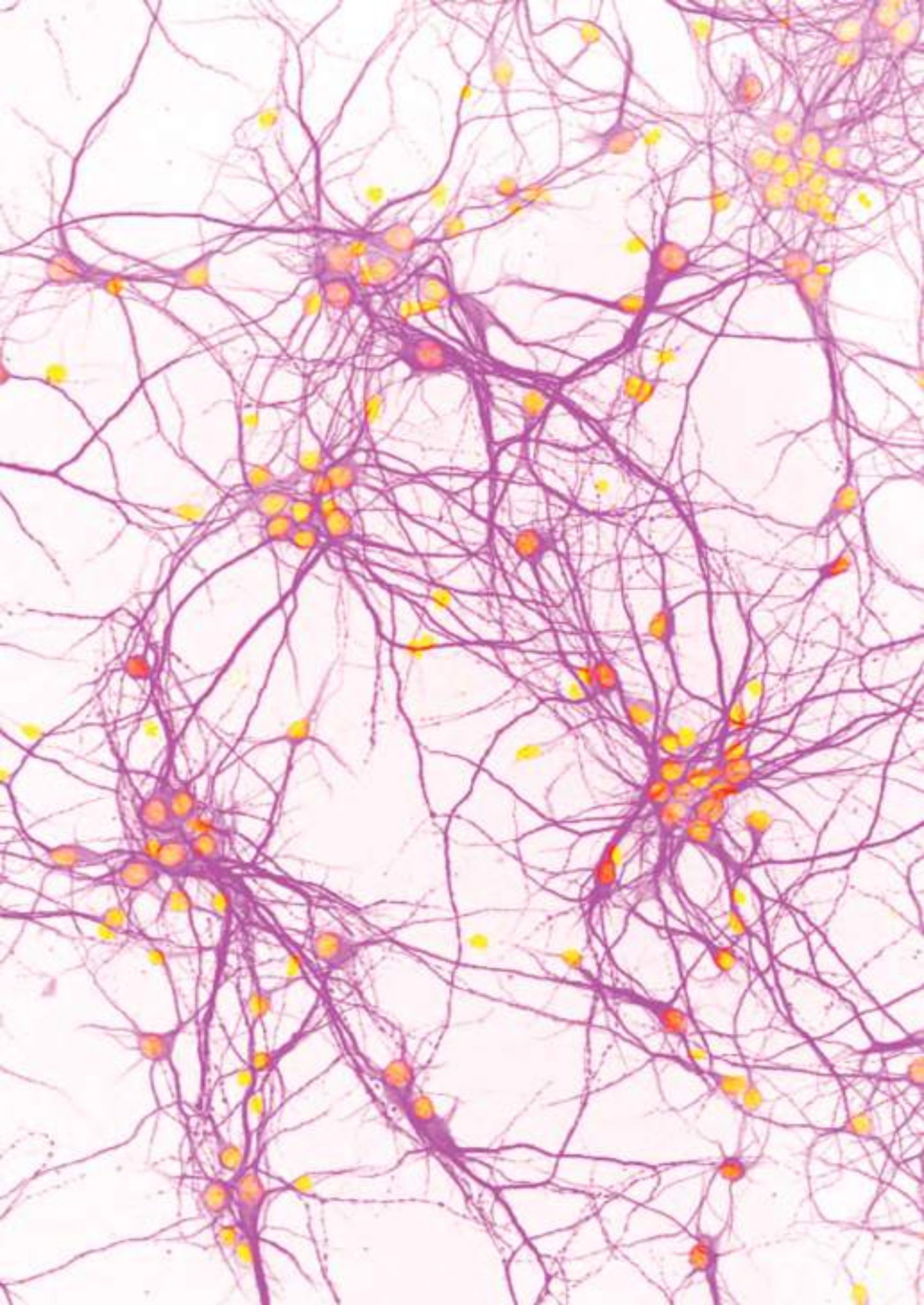

Annex 1. Funding

This study was funded by the Instituto de Salud Carlos III (Fondo de Investigación Sanitaria) under the grant PI15/01111. It was also supported by the Red Española de Esclerosis Múltiple (REEM) and by the Agència de Gestió d'Ajuts Universitaris i de Recerca (AGAUR), Generalitat de Catalunya, Spain.

Annex 2. Tables

Table A1. Antibody references used in immunofluorescence staining.

Antibody	Fluorochrome	Hot species	Reference	Manufacturer
Anti-GFAP	-	Rabbit, polyclonal	Z-0334	DAKO
Anti-GFAP	-	Mouse, monoclonal	G-3893	SIGMA
Anti-Iba1	-	Rabbit, polyclonal	019-19741	WAKO
Anti-NeuN	-	Mouse, monoclonal	MAB377	Merck-Millipore
Anti-MAP2	-	Mouse, monoclonal	M-1406	SIGMA
Anti-MAP2	-	Chicken, polyclonal	Ab5392	Abcam
Anti-GalC	-	Rabbit, polyclonal	AB142	Merck-Millipore
Anti-PSD-95	-	Mouse, monoclonal	Ab2723	Abcam
Anti-Synaptophysin	-	Rabbit, polyclonal	Ab32127	Abcam
Anti-mouse IgG (H+L)	568	Goat, polyclonal	A-11004	Invitrogen
Anti-rabbit IgG (H+L)	488	Goat, polyclonal	A-11008	Invitrogen
Anti-chicken IgY (H+L)	647	Goat, polyclonal	A-21449	Invitrogen

Abbreviations: GFAP: anti-glial fibrillary protein; Iba1: ionized calcium-binding adaptor molecule 1; NeuN: neuronal nuclear antigen; MAP2: microtubule-associated protein 2; GalC: galactocerebrosidase; PSD-95: post-synaptic density protein 95; Ig: immunoglobulin.